AD-A131 653 ACOUSTIC PULSE SCATTERING FROM IMPEDANCE COVERED CYLINDERS(U) PENNSYLVANIA STATE UNIV UNIVERSITY PARK APPLIED RESEARCH LAB A KHAVARAN AUG 83 1/2

UNCLASSIFIED ARL/PSU/TM-83-100 N00024-79-C-6043 F/G 20/1 NL

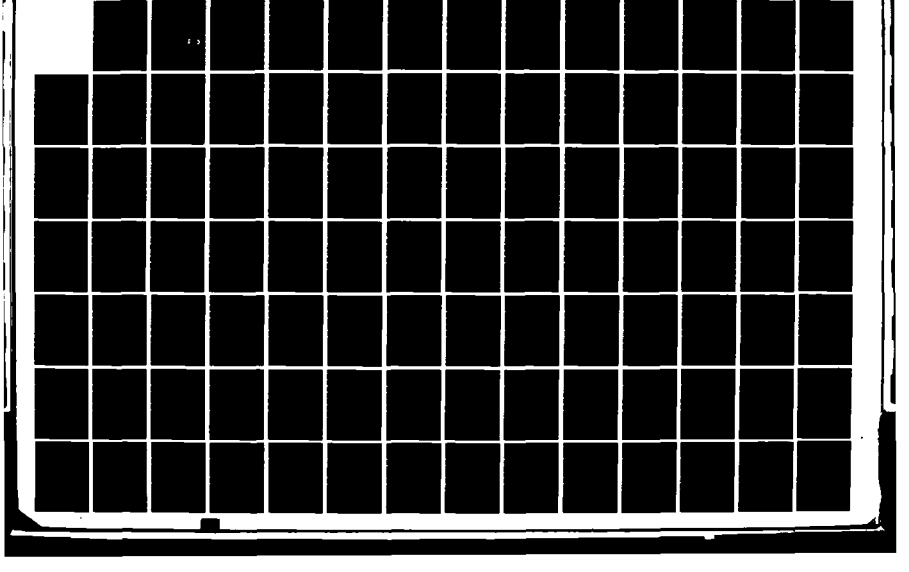

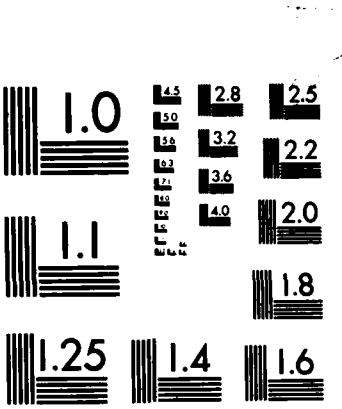

MICROCOPY RESOLUTION TEST CHART
NATIONAL BUREAU OF STANDARDS-1963-A

(6)

ACOUSTIC PULSE SCATTERING FROM IMPEDANCE COVERED CYLINDERS

Abbas Khavaran

Technical Memorandum
File No. TM 83-100
June 22, 1983
Contract No. N00024-79-C-6043

Copy No. 6

The Pennsylvania State University
Intercollege Research Programs and Facilities
APPLIED RESEARCH LABORATORY
Post Office Box 30
State College, PA 16801

NAVY DEPARTMENT

NAVAL SEA SYSTEMS COMMAND

UNCLASSIFIED
SECURITY CLASSIFICATION OF THIS PAGE (When Data Entered)

REPORT DOCUMENTATION PAGE	READ INSTRUCTIONS BEFORE COMPLETING FORM
1. REPORT NUMBER: 83-100	2. GOVT ACCESSION NO.: AD-A131 653
3. RECIPIENT'S CATALOG NUMBER	
4. TITLE (and Subtitle): ACOUSTIC PULSE SCATTERING FROM IMPEDANCE COVERED CYLINDERS	5. TYPE OF REPORT & PERIOD COVERED: Ph.D. Thesis, August 1983
	6. PERFORMING ORG. REPORT NUMBER: 83-100
7. AUTHOR(s): Abbas Khavaran	8. CONTRACT OR GRANT NUMBER(s): N00024-79-C-6043
9. PERFORMING ORGANIZATION NAME AND ADDRESS: The Pennsylvania State University, Applied Research Laboratory, P.O. Box 30, State College, PA 16801	10. PROGRAM ELEMENT, PROJECT, TASK AREA & WORK UNIT NUMBERS
11. CONTROLLING OFFICE NAME AND ADDRESS: Naval Sea Systems Command, Department of the Navy, Washington, DC 20362	12. REPORT DATE: June 22, 1983
	13. NUMBER OF PAGES: 136 pp.
14. MONITORING AGENCY NAME & ADDRESS (if different from Controlling Office)	15. SECURITY CLASS. (of this report): Unclassified, Unlimited
	15a. DECLASSIFICATION/DOWNGRADING SCHEDULE

16. DISTRIBUTION STATEMENT (of this Report)

Approved for public release, distribution unlimited, per NSSC (Naval Sea Systems Command), July 15, 1983

17. DISTRIBUTION STATEMENT (of the abstract entered in Block 20, if different from Report)

18. SUPPLEMENTARY NOTES

19. KEY WORDS (Continue on reverse side if necessary and identify by block number)

thesis, acoustic, pulse, scattering, impedance

20. ABSTRACT (Continue on reverse side if necessary and identify by block number)

An expression for the acoustic scattered pressure from an impedance covered cylinder due to an incident plane pulse is obtained analytically. The application of Fourier transform on time and subsequent Sommerfeld-Watson transformation results in separate expressions for geometrically reflected pressure and for creeping (or circumferential) waves. Using Cauchy contour integration theorem and saddle-point methods, the inverse Fourier transform is evaluated. The impulse response and convolution theorem have been utilized to obtain an

DD FORM 1 JAN 73 1473 EDITION OF 1 NOV 65 IS OBSOLETE UNCLASSIFIED

SECURITY CLASSIFICATION OF THIS PAGE (When Data Entered)

expression for the scattered pressure for incident harmonic pulse train and FM pulses. The first arrival of acoustic wave at an observer point in the far field is shown to be due to the geometrically reflected pressure. After the first arrival, creeping waves are shown to circumnavigate the cylinder surface for an indefinite number of times and radiate off tangentially at any angle.

These waves create the multiple echoes that return in the scattering of a single pulse. The circumferential waves are shown to decay exponentially as they encircle the cylinder surface.

ABSTRACT

An expression for the acoustic scattered pressure from an impedance covered cylinder due to an incident plane pulse is obtained analytically. The application of Fourier transform on time and subsequent Sommerfeld-Watson transformation results in separate expressions for geometrically reflected pressure and for creeping (or circumferential) waves. Using Cauchy contour integration theorem and saddle-point methods, the inverse Fourier transform is evaluated. The impulse response and convolution theorem have been utilized to obtain an expression for the scattered pressure for incident harmonic pulse train and FM pulses. The first arrival of acoustic wave at an observer point in the far field is shown to be due to the geometrically reflected pressure. After the first arrival, creeping waves are shown to circumnavigate the cylinder surface for an indefinite number of times and radiate off tangentially at any angle.

These waves create the multiple echoes that return in the scattering of a single pulse. The circumferential waves are shown to decay exponentially as they encircle the cylinder surface.

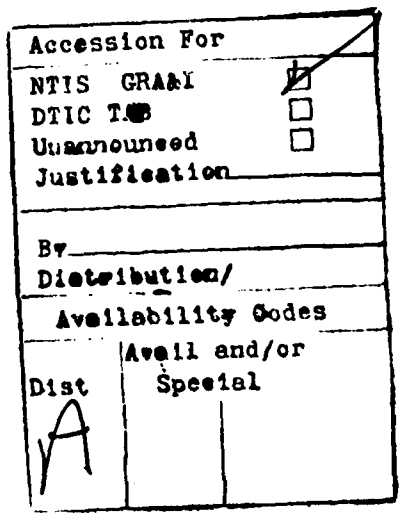

TABLE OF CONTENTS

LIST OF TABLES

LIST OF FIGURES

LIST OF MAJOR SYMBOLS

a	radius of the cylinder
a_1 and a_2	nondimensional parameters defined on page 14
$A(x)$	a function related to Airy's function
$Ai(x)$	Airy's function
$A_n(n)$	defined in Eq. (37)
b_1 and b_2	nondimensional parameters defined on page 14
$B_n(n)$	defined in Eq. (38)
c	sound velocity in the acoustic medium
$E_n(n)$	defined on page 44
F_1 and F_2	defined in Eq. (55)
$h(t)$	impulse response function
$H(t)$	Heaviside function
$H_\gamma^{(1),(2)}$	Hankel functions of first and second kind of order γ
J_γ	Bessel function of order γ
k	wave number
$\overline{k}$	stiffness
K_{γ_ℓ}	defined in Eq. (102)
M_i	defined on page 12
p_I^c	creeping waves on the surface of the cylinder
p_{II}^c	creeping waves in the far field
P_{inc}	incident acoustic pressure
P_{ref}	reflected acoustic pressure
P_o	amplitude of the incident wave
p^G	geometrically reflected pressure

$P_{\lambda s}$	defined in Eq. (127)
q	argument of the Airy's function defined in Eq. (91)
r	radius in cylindrical coordinates
$\overline{r}$	defined on page 50
s	defined on page 50
t	time variable, seconds
$t_{\lambda s}$	arrival time for creeping waves
T	time of duration of a pulse
u_{n0}	defined in Table 1
$u_{n\infty}$	defined in Table 1
u(t)	unit step function
$\overline{w}$	Wronskinan
X_i	defined on page 12
$\overline{Z}$	dimensionless impedance function
α	angle of reflection for geometrically reflected pressure
α_o	saddle point
β	a parameter related to frequency change of FM waves
ϕ	observation angle
$\delta(t)$	Dirac delta function
ξ	defined on page 38
γ	order of the cylindrical functions
ρ	mass density of the acoustic medium
ω	frequency of the incident plane wave
ω_o	resonance frequency of the impedance function
$\overline{\omega}$	dimensionless frequency ($\overline{\omega} = \omega/\omega_o$)
λ_o and $\overline{\lambda}$	defined on page 39

Ω	defined in Eq. (56)
χ	defined in Eq. (97)
δ	defined in Eq. (108)
τ_ℓ	defined in Eq. (109)
$(\eta_o)_{\ell,s,\lambda}$	saddle point defined on page 80

ACKNOWLEDGEMENTS

The author wishes to express his sincere appreciation to his thesis advisor, Professor Sabih I. Hayek, for his guidance and assistance throughout the entire study. Acknowledgements are also extended to Professor V.H. Neubert, L.W. Hu, J. Tichy and J. Kiusalaas for serving on the author's doctoral committee.

This research was supported by the Applied Research Laboratory of The Pennsylvania State University under contract with the U.S. Naval Sea Systems Command.

CHAPTER I

INTRODUCTION

1.1 Background

When an incident sound field encounters an obstacle, the acoustic energy is scattered in all directions. The scattered acoustic field depends on geometrical considerations such as curvature, size, discontinuities in slope (sharp edges) and in curvature as well as the impedance of the surface or its elasticity. If the incident acoustic field is harmonic in time, then the scattering field also depends on the wavelength vs. a typical length dimension and the scattered field generates a directivity that is fixed in time and is the result of interference between different parts of the scatterer. If the incident field is an acoustic pulse, then the scattered field is time dependent and the directivity is time dependent and is the result of distinct time signatures of each part of the scatterer. If the surface impedance is frequency dependent, then the scattered field is influenced by the interference between the frequency of the incident field and that of the impedance of the surface of the scatterer. However, the impedance of the scatterer would not have the same interference with an incident acoustic pulse. This difference between continuous and pulse acoustic scattering motivated this study.

1.2 Basic Approach

To investigate the influence of surface impedance on the reflection of an acoustic pulsed wave, a plane pulsed wave reflecting from an impedance covered plane is investigated. This geometry's

simplicity allows an extensive investigation of the pulse shape and time signature on the reflected pulse. For such a flat surface, the reflected field is primarily due to geometric-optics. To investigate the influence of curvature, the investigation is extended to include the pulse reflection from an impedance covered cylinder. Integral transforms on time and then use of eigenfunction expansions result in a series. This leads to the use of the Sommerfeld-Watson transformation which results in a double integral for the time signature of the reflected field. The resulting integral is then separated into two parts, i.e., the geometrically diffracted field and the creeping wave field. These are separately evaluated by asymptotic methods and by use of residue methods resulting in fastly convergent series. Those series are then integrated in a Duhamel-type integral to obtain the scattered field due to any type of incident pulse time signature.

1.3 Review of Previous Investigations

Studies of the scattering from objects have an extensive history in acoustics and optics. By far the greatest attention has been directed to objects with either rigid or pressure release surfaces. Acoustic scattering studies have mainly focused on scatterers which are simple, e.g., spherical, circular cylindrical, elliptical, etc., and for which the method of separation of variables can be brought to bear. In addition, there is a large literature of alternative methods that range from sophisticated function theoretic techniques to purely numerical ones in which integral equations for unknown surface distributions are approximated by sets of linear

equations and solved numerically. Keller and Levy[1] have analyzed the diffraction of time harmonic waves by smooth objects. Using the geometrical theory of diffraction, based on the postulate that fields propagate along rays, they solve the problem of scattering for simple shapes like spheres and cylinders. Keller formulates his solution for different types of boundary conditions, where he expands the solution asymptotically for large Ka. An important advantage of this method is that it does not depend on separation of variables or any such similar procedure. Therefore the shapes of the objects to which it can be applied are not restricted, but it can be expected to yield good results only when the wavelength is small compared to typical obstacle's dimensions and therefore cannot be applied in the case of a pulse.

Blank and Keller[2] discuss the diffraction and reflection of plane pulses by wedges and corners for the special case of rigid or pressure release boundary conditions. By following the propagation of the plane discontinuity in xyt-space, they obtain an explicit closed form expression in terms of elementary functions. But their technique, known as the method of conical flow, cannot be applied to the more general case of impedance boundary condition. Friedman and Shaw[3] have studied the diffraction of pulses by cylindrical obstacles of arbitrary cross-section. They discuss the two-dimensional problem of the diffraction of a plane acoustic shock wave in terms of a characteristic boundary value problem in four-dimensional (x,y,z,t) to which Green's identity may be applied, instead of an initial boundary value problem. An integral equation for the surface values of the pressure is formulated and approximated by a set of

successive, non-simultaneous algebraic equations which can be solved for a given geometry. For the case of a square box with rigid boundary conditions, the surface values of pressure are solved in this manner for a period of one transition time.

Hickling and Means[4,5] have investigated the scattering of FM pulses by spherical elastic shells in water. They discuss the problem in two areas of practical interest, (a) linear frequency-modulated (FM) pulses, and (b) higher frequencies where the wavelength is much smaller than the exterior radius of the shell. Adopting a statistical approach based on signal processing, they compute a cross-correlation function of each echo with its incident pulse. They show that there is a time delay between the first, second, third, and later peaks in the cross-correlation function and reach the conclusion that the first pulse in the echo corresponds to a reflection from outer surface of the shell closest to the source and the remaining pulses are due primarily to the elastic response of the sphere.

Shaw[6] studied the diffraction of arbitrary plane acoustic pulses by obstacles whose boundary offers inertial but no elastic resistance. The boundary condition is expressed in terms of the familiar Robin-type ($\phi + K\, \partial\phi/\partial n = 0$), where ϕ is tne velocity potential. A large value of K implies a heavy scattering surface (rigid) and a small value corresponds to an almost free surface. The method of solution is very much the same as that used in Ref. 3. Through some numerical approximation he solves the integral equation for a square box and finds the surface values of pressure for large K and surface values of velocity for small K.

Uberall[7] investigates the multiple echoes that are returned in the scattering of a single pulse and analyzes the presence of creeping waves or circumferential waves in the diffraction process. For the special case of an infinitely long, acoustically soft circular cylinder, he describes the creeping waves using Sommerfeld-Watson transformation method of Franz[8] and assumes that the initial plane sound wave possesses an arbitrary pulse shape. The expressions for the creeping pulses obtained on the surface of the scatterer includes, but go beyond previous results of Friedlander[9], found by a different method.

Doolittle, Uberall and Uguncius[10] discuss the problem of scattering of a simple harmonic plane wave by an infinite elastic cylinder. They apply the Sommerfeld-Watson transformation on the normal mode series. The complex velocities of the ensuing circumferential waves are found by numerical search for the zeros of a 3x3 determinant in the complex plane. Two distinct types of zeros are found: (a) "Franz-type" zeros, similar to those appearing in the scattering from rigid cylinders. These waves, propagating with speeds below the sound speed in the surrounding medium, are heavily attenuated and penetrate and exit the cylinder's surface tangentially, and (b) "Rayleigh-type" zeros, also found earlier by Goodman and Grace[11] and Franz and Beckmann for cylinders of finite conductivity[12]. The waves are weakly attenuated and have speeds approaching elastic velocities.

Ugincius and Uberall[13] investigate the steady-state scattering of a plane harmonic wave from an infinite elastic circular cylindrical shell, as treated by the creeping wave method. This work is basically

an extension of their previous study of sound scattering from elastic cylinders, but new interesting results were obtained in the limit of a thin shell. The resulting residue series is generated by poles that are the complex zeros of a 6x6 determinant. These zeros are found numerically by an extension of the Newton-Raphson method for complex functions. Finally it was found that besides the infinity of the well known rigid zeros, there exists a set of additional zeros that give rise to generalized Rayleigh and Stoneley waves. The behavior of these zeros has been studied as a function of the wave number and also of the shell thickness.

In most cases, the scattering problem was solved for objects with constant impedance or elastic boundary conditions. A combination of non-harmonic incident wave and frequency dependent impedance covering will create new complications in the numerical computation of the scattering problem which will be discussed later.

CHAPTER II

REFLECTION OF A PLANE WAVE PULSE FROM AN IMPEDANCE COVERED PLANE

2.1 Statement of the Problem

Consider an infinite flat surface in the x-y plane which bounds a semi-infinite acoustic medium $z \geq 0$. In this chapter a solution is sought for the reflected acoustic field due to a plane pulse incident on an infinite plane boundary. The boundary is covered with a material possessing a locally reacting impedance, which is frequency dependent and may have one or multiresonant character.

An incident plane pulse is propagating in (-z) direction, normal to the boundary. If t = 0 correspond to the time of arrival of the pulse at the boundary, then the incident wave can be expressed as:

$$P_{inc}(t) = \delta(t)$$

Applying the Fourier transform to $P_{inc}(t)$ one obtains

$$\phi(\omega) = \int_{-\infty}^{+\infty} P_{inc}(t)\, e^{-i\omega t}\, dt = \int_{-\infty}^{+\infty} \delta(t)\, e^{-i\omega t}\, dt = 1 \qquad (1)$$

Application of Fourier inverse transform on $\phi(\omega)$ would lead to reconstruction of the incident wave

$$\delta(t) = \frac{1}{2\pi} \int_{-\infty}^{+\infty} \phi(\omega)\, e^{i\omega t}\, d\omega = \frac{1}{2\pi} \int_{-\infty}^{+\infty} e^{i\omega t}\, dt \qquad (2)$$

The integrand in Eq. (2), corresponding to a definite value of ω, $f(\omega) = \phi(\omega)\, e^{i\omega t}$, represents a plane harmonic wave. Multiplying $f(\omega)$ by the reflection coefficient of the boundary one obtains the contribution to the reflected field arising from an individual harmonic wave. Finally applying the superposition principle, the reflected field due to an incident pulse can be written as follows:

$$h(t) = \frac{1}{2\pi} \int_{-\infty}^{+\infty} R(\omega)\, e^{i\omega t}\, d\omega \qquad (3)$$

The reflection coefficient $R(\omega)$, for normal incidence is expressed as:

$$R(\omega) = \frac{\frac{Z(\omega)}{\rho c} - 1}{\frac{Z(\omega)}{\rho c} + 1} = 1 - \frac{2}{\frac{Z(\omega)}{\rho c} + 1} \qquad (4)$$

where $Z(\omega)$ represents the impedance of the surface, and ρ and c represents respectively the mass density and sound speed of the medium. Considering a simple oscillator excited by a time harmonic force $F = f_o e^{i\omega t}$, the impedance can be expressed as the ratio of driving force to velocity

$$Z(\omega) = \frac{F}{\dot{X}} = c_o + im\omega_o\left(\frac{\omega}{\omega_o} - \frac{\omega_o}{\omega}\right) ,$$

and

$$\omega_o = \sqrt{k/m} \quad ,$$

where ω_o, k and m represents the natural frequency, the stiffness and the mass of the oscillator. Dividing $Z(\omega)$ by ρc and introducing the dimensionless constants a_1 and b_1 we have a model for the impedance of the surface:

$$\frac{Z(\omega)}{\rho c} = b_1 + ia_1\left(\frac{\omega}{\omega_o} - \frac{\omega_o}{\omega}\right) \qquad (5)$$

where

$$b_1 = \frac{c_o}{\rho c} \quad , \quad \text{and} \quad a_1 = \frac{\sqrt{km}}{\rho c} \quad .$$

Finally substituting Eqs. (4) and (5) in (3) one obtains:

$$h(t) = \frac{1}{2\pi}\int_{-\infty}^{+\infty} e^{i\omega t}\, d\omega - \frac{1}{2\pi}\int_{-\infty}^{+\infty} \frac{2e^{i\omega t}}{(b_1+1)+ia_1(\frac{\omega}{\omega_o}-\frac{\omega_o}{\omega})}\, d\omega$$

or

$$h(t) = \delta(t) - \frac{\omega_o}{\pi}\int_{-\infty}^{+\infty} \frac{\eta e^{i\omega_o t\eta}}{(b_1+1)\eta+ia_1(\eta^2-1)}\, d\eta \qquad (6)$$

The integral in Eq. (6) can be computed by using the Residue Theorem and closing the contour of integration along a semi-circle in upper half η-plane. The poles of the integrand are the roots of

$$(b_1+1)\eta + ia_1(\eta^2-1) = 0. \qquad (7)$$

It could be shown that both roots of Eq. (7) fall in the upper half of η-plane. For $(b_1+1) < 2a$, they would be symmetric with respect to imaginary axis and for $(b_1+1) > 2a_1$, both roots would be purely imaginary. For the special case of $(b_1+1) = 2a_1$, the roots coincide and hence the pole would be of second order. Let $\eta_n (n=1,2)$ be the roots of Eq. (7) and q_n be the corresponding residues

$$q_n = \frac{\eta_n}{(b_1+1) + 2ia_1\eta_n} \quad n = 1,2 \qquad (8)$$

Finally Eq. (6) can be written as:

$$h(t) = \delta(t) - \frac{\omega_o}{\pi}(2\pi i)\sum_{n=1,2} q_n\, e^{i\omega_o t\eta_n} \qquad (9)$$

It should be observed that the right hand side of Eq. (9) is thus necessarily a real quantity as is expected. The pulse response expressed by Eq. (9) could be substituted in Duhamel's integral to

obtain the reflected pressure due to any given incident plane pulse. It is also clear that the first term in Eq. (9) represents the reflected field due to rigid boundary condition and therefore the second term should correspond to the correction from a rigid boundary condition.

Assuming that the incident pressure is a harmonic pulse train, in the time interval [0,T],

$$P_{inc}(t) = \cos\omega t[H(t) - H(t-T)] \tag{10}$$

where H(t) is the step function, the reflected pressure due to normal incidence could be expressed as:

$$P_{ref}(t) = \int_0^t P_{inc}(\tau)\, h(t-\tau)d\tau. \tag{11}$$

Substituting Eqs. (9) and (10) into (11) one obtains:

for $t < T$

$$P_{ref}(t) = \int_0^t \cos\omega\tau[\delta(t-\tau) - 2i\omega_o \sum_n q_n\, e^{i\omega_o(t-\tau)\eta_n}]d\tau$$

or:

$$P_{ref}(t) = \cos\omega t - 2i \sum_n \frac{q_n e^{i\omega_o t\eta_n}}{(\frac{\omega}{\omega_o})^2 - \eta_n^2}\left[e^{-i\omega_o t\eta_n}(-i\eta_n\cos\omega t + \frac{\omega}{\omega_o}\sin\omega t) + i\eta_n\right] \tag{12}$$

and for $t > T$

$$P_{ref}(t) = -2i \sum_n \frac{q_n e^{i\omega_o t\eta_n}}{(\frac{\omega}{\omega_o})^2 - \eta_n^2}\left[e^{-i\omega_o T\eta_n}(-i\eta_n\cos\omega T + \frac{\omega}{\omega_o}\sin\omega T) + i\eta_n\right] \tag{13}$$

The factor $e^{i\omega_o t\eta_n}$ in Eq. (13) represents an exponential decay with time.

A different type of reflection that will be considered in this study is due to an incident FM pulse. Let

$$P_{inc}(t) = \cos[\omega t(1+r\omega_o t)][H(t)-H(t-T)] \tag{14}$$

In terms of non-dimensional quantities, $P_{inc}(t)$ can be expressed as

$$P_{inc}(t) = \cos[\omega t(1+\beta \frac{\omega t}{T})][H(t)-H(t-T)] \tag{15}$$

where $r = \beta \frac{\bar{\omega}}{T}$ and $\bar{\omega} = \frac{\omega}{\omega_o}$.

The frequency of the FM pulse as expressed by Eq. (15) is changing from ω to $(1+\beta)\omega$ as time changes from 0 to T. Substituting Eqs. (15) and (9) into (11), the reflected pulse can be expressed as:

for $t < T$

$$P_{ref}(t) = P_{inc}(t) - 2i\omega_o \sum_n q_n e^{i\omega_o t\eta_n} \int_o^t \cos[\omega\tau(1+r\omega_o\tau)]e^{-i\omega_o\eta\tau} \, d\tau$$

or

$$P_{ref}(t) = P_{inc}(t) - 2i \sum_n q_n e^{i\omega_o t\eta_n}(\frac{1+i}{4}) \sqrt{\frac{\pi}{2r\bar{\omega}}} \{e^{-i\frac{(\bar{\omega}-\eta_n)^2}{r\bar{\omega}}} \cdot \operatorname{erf}[\frac{1-i}{\sqrt{2r\bar{\omega}}}$$

$$(r\bar{\omega}\alpha + \bar{\omega} - \eta_n)] - i \operatorname{erf}[\frac{-1-i}{\sqrt{2r\bar{\omega}}} (-r\bar{\omega}\alpha - \bar{\omega} - \eta_n)]\}_{\alpha=0}^{\alpha=\omega_o t} \tag{16}$$

and for $t > T$

$$P_{ref}(t) = -2i \sum_n q_n e^{-i\omega_o t \eta_n} \left(\frac{1+i}{4}\right) \sqrt{\frac{\pi}{2r\bar{\omega}}} \left\{ e^{-i\frac{(\bar{\omega}-\eta_n)^2}{r\bar{\omega}}} \cdot \operatorname{erf}\left[\frac{1-i}{\sqrt{2r\bar{\omega}}}\right.\right.$$

$$\left.\left.(r\bar{\omega}\alpha + \bar{\omega} - \eta_n)\right] - i \operatorname{erf}\left[\frac{-1-i}{\sqrt{2r\bar{\omega}}}(-r\bar{\omega}\alpha - \bar{\omega} - \eta_n)\right]\right\}_{\alpha=0}^{\alpha=\omega_o T} \qquad (17)$$

2.2 Higher Order Impedance Functions

In general a multi-degree of freedom oscillator could be suggested as a model for the impedance function. Consider a two degrees of freedom system, with displacements, masses, stiffnesses and damping coefficients given by X_i, M_i, $\bar{k}_i$ and c_i, $i = 1,2$, respectively. If an external time harmonic force $F = f_o e^{i\omega t}$ is applied to mass m_2, the impedance function can be expressed as

$$Z(\omega) = \frac{F}{\dot{X}_2} \quad .$$

Force balance equations for masses m_1 and m_2 are given by

$$\begin{aligned} &\ddot{m}_2 X_2 + (X_2 - X_1)\bar{k}_2 + (\dot{X}_2 - \dot{X}_1)c_2 = F \\ &\ddot{m}_1 X_1 + c_1 \dot{X}_1 + \bar{k}_i X_1 = (X_2 - X_1)\bar{k}_2 + (\dot{X}_2 - \dot{X}_1)c_2 \end{aligned} \qquad (18\text{-a})$$

Substituting $X_1 = x_1 e^{i\omega t}$ and $X_2 = x_2 e^{i\omega t}$ one obtains

$$\dot{X}_2 = \frac{F}{D}\left(m_1 i\omega + c_1 + c_2 + \frac{\bar{k}_1 + \bar{k}_2}{i\omega}\right) \qquad (18\text{-b})$$

where D is the determinant of Eqs. (18-a)

$$D = \begin{vmatrix} (m_2 i\omega + c_2 + \frac{\bar{k}_2}{i\omega}) & -(\frac{\bar{k}_2}{i\omega} + c_2) \\ -(c_2 + \frac{\bar{k}_2}{i\omega}) & (m_1 i\omega + c_1 + c_2 + \frac{\bar{k}_1+\bar{k}_2}{i\omega}) \end{vmatrix} \tag{19}$$

The impedance function $Z(\omega)$ can then be expressed as:

$$Z(\omega) = \frac{F}{\dot{X}_2} = \frac{D}{m_1 i\omega + c_1 + c_2 + \frac{1}{i\omega}(\bar{k}_1+\bar{k}_2)}$$

Expanding the determinant D and dividing $Z(\omega)$ by ρc, one finally obtains:

$$\frac{Z(\omega)}{\rho c} = \frac{P(\omega)}{Q(\omega)} \tag{20}$$

where

$$P(\omega) = a_1 a_2 (\frac{\bar{\omega}_1}{\bar{\omega}_2} + \frac{\bar{\omega}_2}{\bar{\omega}_1}) - \frac{1}{\bar{\omega}_1\bar{\omega}_2} - \omega_1\omega_2 + a_2^2 + b_1 b_2 + i[a_2\bar{\omega}_2(b_1+b_2) + a_1\bar{\omega}_1 b_2 - (\frac{a_1 b_2}{\bar{\omega}_1} + \frac{a_2 b_1}{\bar{\omega}_2})]$$

$$Q(\omega) = (b_1+b_2) + i[a_1\bar{\omega}_1 - (\frac{a_1}{\bar{\omega}_1} + \frac{a_2}{\bar{\omega}_2})]$$

and

$$\omega_1^o = \sqrt{\frac{\bar{k}_1}{m_1}} \ , \ \omega_2^o = \sqrt{\frac{\bar{k}_2}{m_2}} \ , \ \bar{\omega}_1 = \frac{\omega}{\omega_1^o} \ , \ \bar{\omega}_2 = \frac{\omega}{\omega_2^o} \ , \ \alpha = \omega_2^o/\omega_1^o$$

$$a_1 = \sqrt{\bar{k}_1 m_1}\ /\rho c \ , \ a_2 = \sqrt{\bar{k}_2 m_2}\ /\rho c \ , \ b_1 = c_1/\rho c \ , \ b_2 = \frac{c_2}{\rho c} \ .$$

Parameters a_1, a_2, b_1, and b_2 are dimensionless positive numbers. In terms of the new variables, the two natural frequencies of the undamped oscillating system would be the positive roots of the following equation:

$$\Omega^4 - (\omega_1^{o\,2} + \omega_2^{o\,2} + \frac{a_2}{a_1}\omega_1^o\ \omega_2^o)\Omega^2 + (\omega_1^o\omega_2^o)^2 = 0 \qquad (20a)$$

Obviously the shape of the function $|R(\omega)|$ would depend on the values of the above-mentioned dimensionless numbers. As it can be seen later, by proper selection of these numbers, we can arrange for $|R(\omega)|$ to fall below an optional level in the frequency range of $\Omega_1 < \omega < \Omega_2$. Substituting the new impedance function in Eqs. (3) and (4), the reflected pressure due to an incident plane pulse can be expressed as:

$$h(t) = \delta(t) + \frac{1}{2\pi}\int_{-\infty}^{+\infty} \frac{-2e^{i\omega t}}{\frac{Z(\omega)}{\rho c} + 1}\ d\omega$$

$$= \delta(t) - \frac{\omega_1^o}{\pi}\int_{-\infty}^{+\infty} \frac{e^{i\omega_1^o t\eta}}{\frac{Z(\eta)}{\rho c} + 1}\ d\eta \qquad (21)$$

where

$$\frac{1}{\frac{Z(\eta)}{\rho c} + 1} = \frac{(b_1+b_2)\eta^2 + i[a_1\eta^3 - \eta(a_1+\alpha a_2)]}{u_1\eta^4 + u_2\eta^3 + u_3\eta^2 + u_4\eta + u_5} = \frac{A(\eta)}{B(\eta)} \qquad (22)$$

and

$$u_1 = -\frac{a_1 a_2}{\alpha}$$

$$u_2 = i[a_1(1+b_2)+\frac{a_2}{\alpha}(b_1+b_2)]$$

$$u_3 = (\alpha + \frac{1}{\alpha})a_1 a_2 + a_2^2 + b_1 b_2 + b_1 + b_2$$

$$u_4 = -i[a_1(1+b_2) + \alpha a_2(1+b_2)]$$

$$u_5 = -\alpha a_1 a_2$$

The denominator of Eq. (22) is a fourth degree polynomial with complex coefficients u_2 and u_4. Let η_n be the complex roots of this equation in the upper half of the complex η-plane.

$$u_1\eta^4 + u_2\eta^3 + u_3\eta^2 + u_4\eta + u_5 = 0 \tag{23}$$

Substituting Eq. (22) into Eq. (21), using the Residue Theorem and closing the path of integration along a semi-circle in the upper half of the complex plane, h(t) can be expressed as:

$$h(t) = \delta(t) - (\frac{\omega_1^o}{\pi})(2\pi i) \sum_n q_n e^{i\omega_1^o t\eta_n} \tag{24}$$

The residue q_n can be expressed as:

$$q_n = \frac{A(\eta_n)}{B'(\eta_n)} \tag{25}$$

and summation index n, as mentioned before, applies only to those poles located in the upper half of the complex plane. The complex roots of Eq. (23) can be shown to be either purely imaginary or pairs symmetric with respect to the imaginary axis and as a result the right hand side of Eq. (24) represents a real function. It can be

observed that with the exception of the summation index n, Eq. (24) looks exactly the same as Eq. (9) which was discussed before for the case of single degree of freedom oscillator. So we can state that Eqs. (12), (13), (16) and (17) would again represent the reflected pressure due to harmonic pulse train or to an FM pulse ,respectively, knowing that q_n is computed from Eqs. (25) and (23).

2.3 Discussion of the Results

2.3.1 Single degree of freedom impedance model

The impedance function $Z(\omega)$ in this case depends on two parameters a_1 and b_1 expressed by Eq. (5). The absolute value of the reflection coefficient $R(\omega)$ is plotted in Figure 1 for a fixed value of b_1 and three different values of the parameter a_1. The minimum value of the bell-shaped function $|R(\omega)|$ depends on the parameter b_1 only, occuring at the tuned frequency $\omega = \omega_o$ and its value can be expressed as:

$$|R(\omega_o)| = \left(\frac{b_1-1}{b_1+1} \right)$$

On the other hand an increase in the value of a_1 would result in a sharper bell-shaped curve as demonstrated in Figure 1. To show how the function $R(\omega)$ influences the reflected pressure, let's look at the following incident pulse:

$$P_{inc}(t) = \cos\omega t[H(t) - H(t-T)] \ , \ \frac{\omega T}{2\pi} = 4$$

For a fixed $R(\omega)$, ($a_1 = 1.5$, $b_1 = 1.1$), the reflected pressure is plotted for different ratios of ω/ω_o . Figure 2 demonstrates the special case when the frequency of the incident pulse train is equal

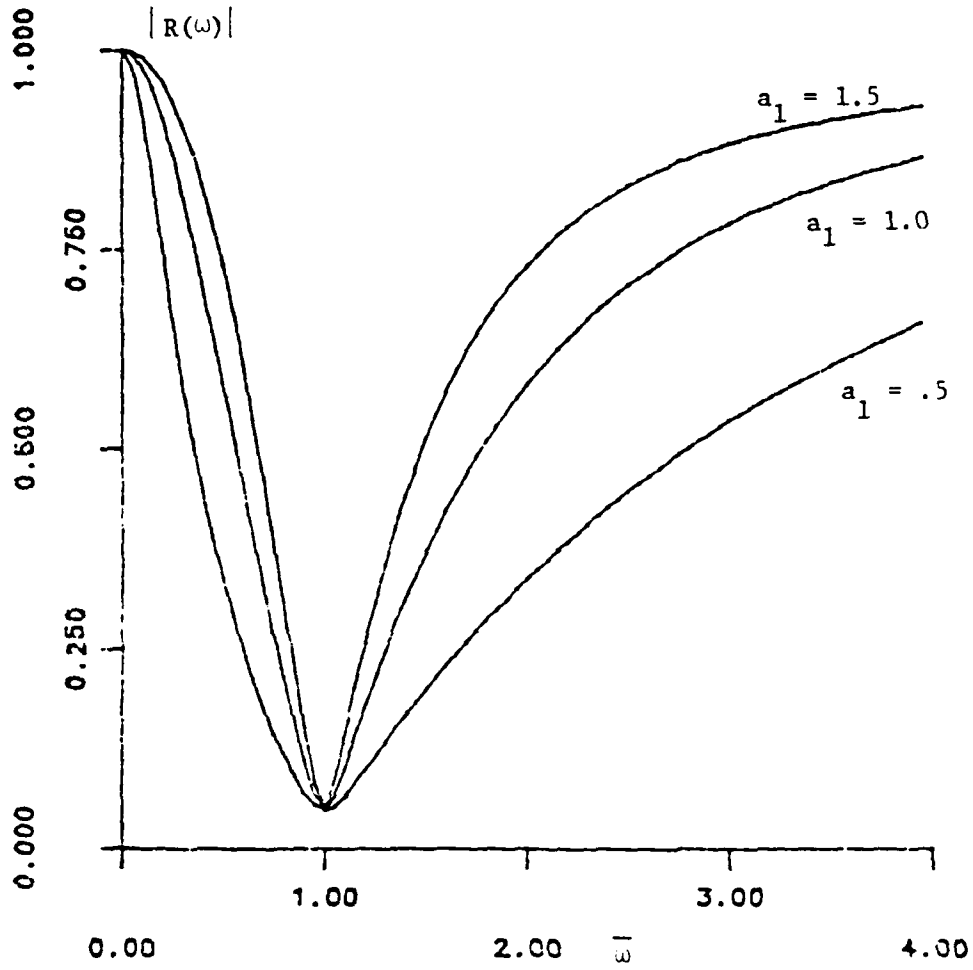

Figure 1. Plot of the Absolute Value of the Reflection Coefficient for a Single Degree of Freedom Impedance Model with $b_1 = 1.1$.

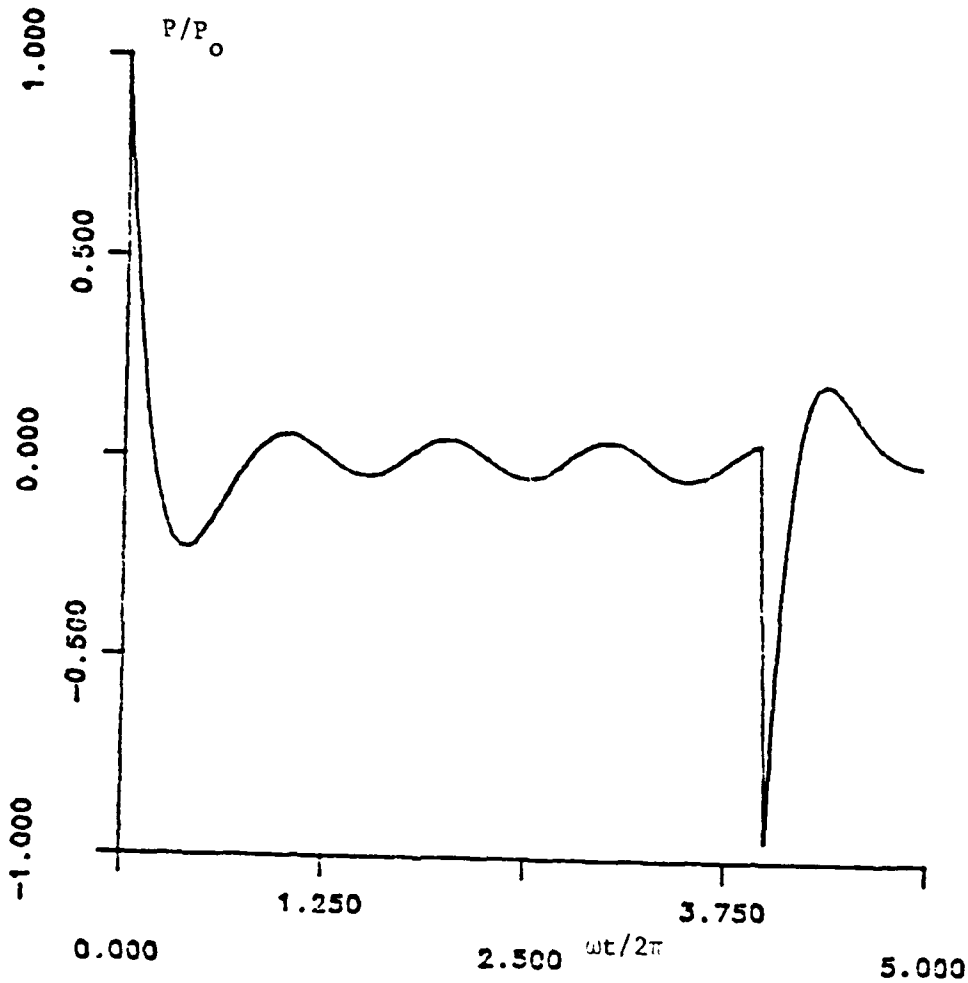

Figure 2. Reflection of a Time Harmonic Pulse Train with $a_1 = 1.5$, $b_1 = 1.1$ and $\omega = 1.0$.

to the natural frequency of the impedance boundary. Figures 3 and 4 correspond to the case when $\omega/\omega_0 = .8$ and 1.2 respectively. It is observed that the amplitude of the reflected pressure could be reduced to almost 8% of that of the incident wave for $\omega/\omega_0 = 1$. Any increase or decrease in the ratio of ω/ω_0 would lead to a higher reflection amplitude as demonstrated by Figures 3 and 4.

On the other hand for a fixed value of ω/ω_0, reducing the parameter a_1, which corresponds to shifting to a flatter bell-shaped curve, would result in a smaller reflection amplitude as expected. In all cases, the residual part of the reflected pulse, corresponding to time $\omega t/2\pi > 4.0$, decays exponentially as expressed in Eq. (13).

Next let's look at FM incident plane pulse.

In Eq. (15) let $\beta = 1$, $\omega = 0.8$ and $\omega t/2\pi = 4.0$. This represents an FM pulse train, with a frequency range of $.8 \leq \omega/\omega_0 \leq 1.6$ for the duration of the pulse. The reflected pressure, as demonstrated in Fig. 5, shows a gradual build-up in the amplitude with increasing frequency. Figure 6 represents the reflected pressure for the same incident wave but corresponding to a different value of parameter a_1. Once again it is observed that a smoother reflection coefficient function would result in a smaller reflection. For a fixed reflection coefficient function, any increase in the frequency range of the FM wave would result in a higher reflection as demonstrated by Figures 6 and 7.

2.3.2 Two degrees of Freedom Impedance model

The reflection coefficient as expressed by Eqs. (4) and (20) is plotted vs. frequency in Figure 8 for the set of parameters

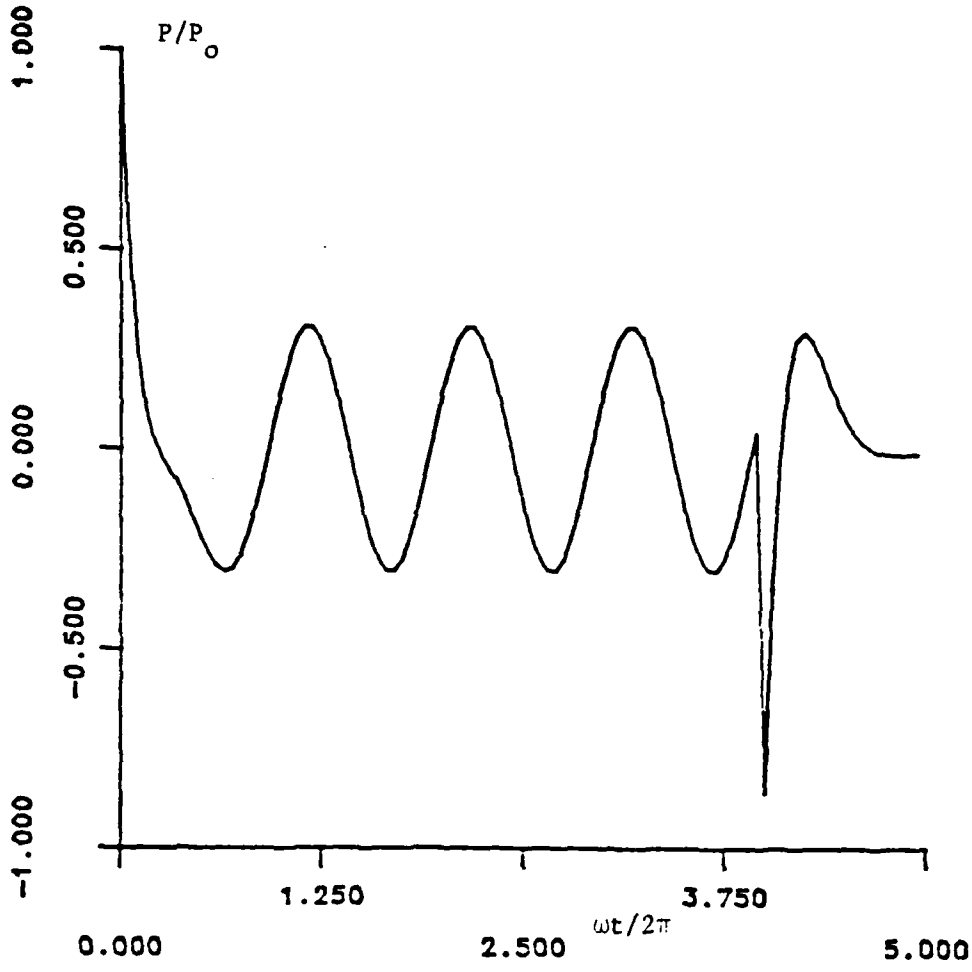

Figure 3. Reflection of a Time Harmonic Pulse Train with $a_1 = 1.5$, $b_1 = 1.1$ and $\zeta = .8$.

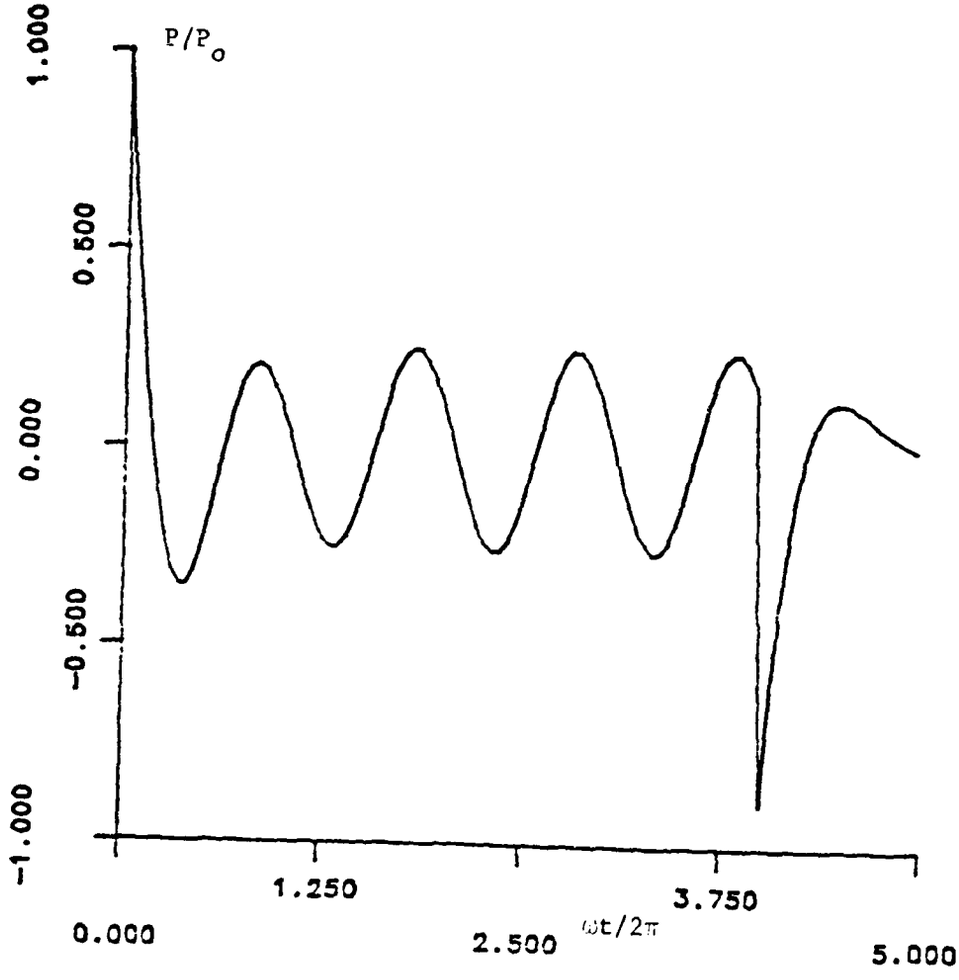

Figure 4. Reflection of a Time Harmonic Pulse Train with $a_1 = 1.5$, $b_1 = 1.1$ and $\underline{\ } = 1.2$.

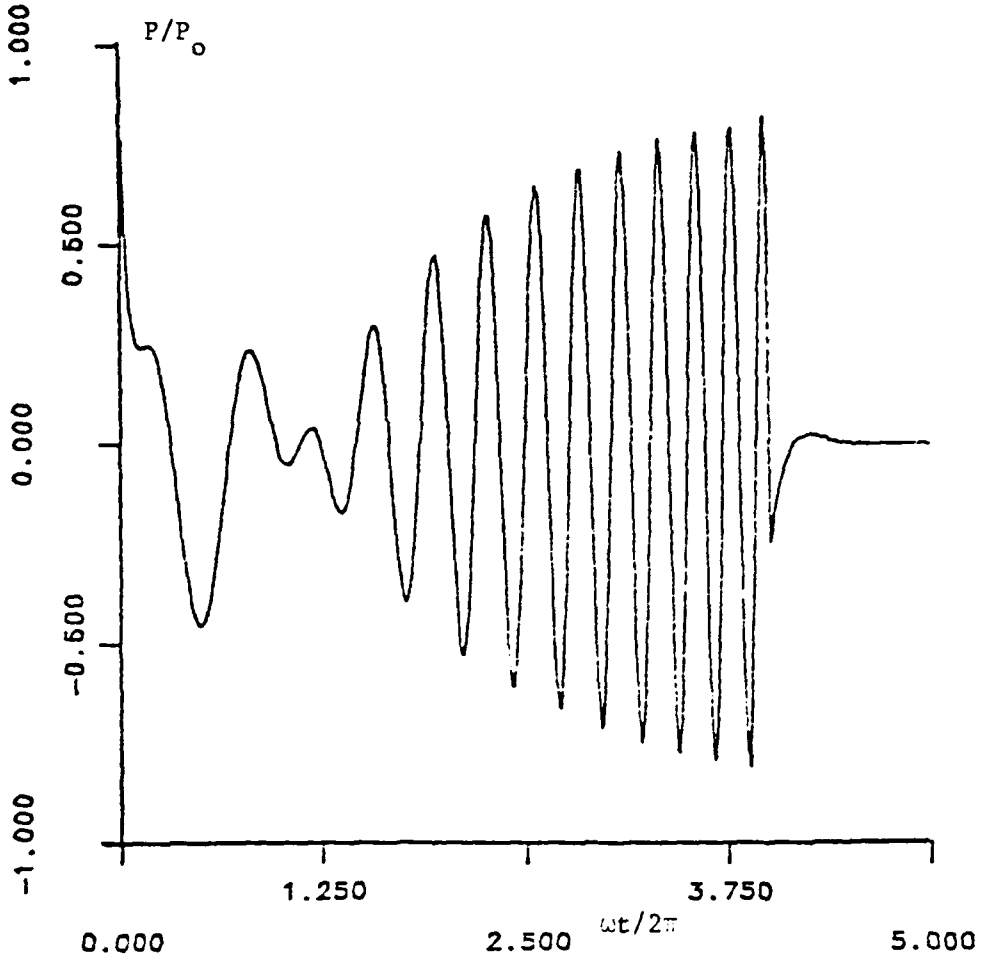

Figure 5. Reflected Pressure for an Incident FM Plane Pulse with $a_1 = 1.5$, $b_1 = 1.1$, $\beta = 1$ and $\bar{\omega} = .8$.

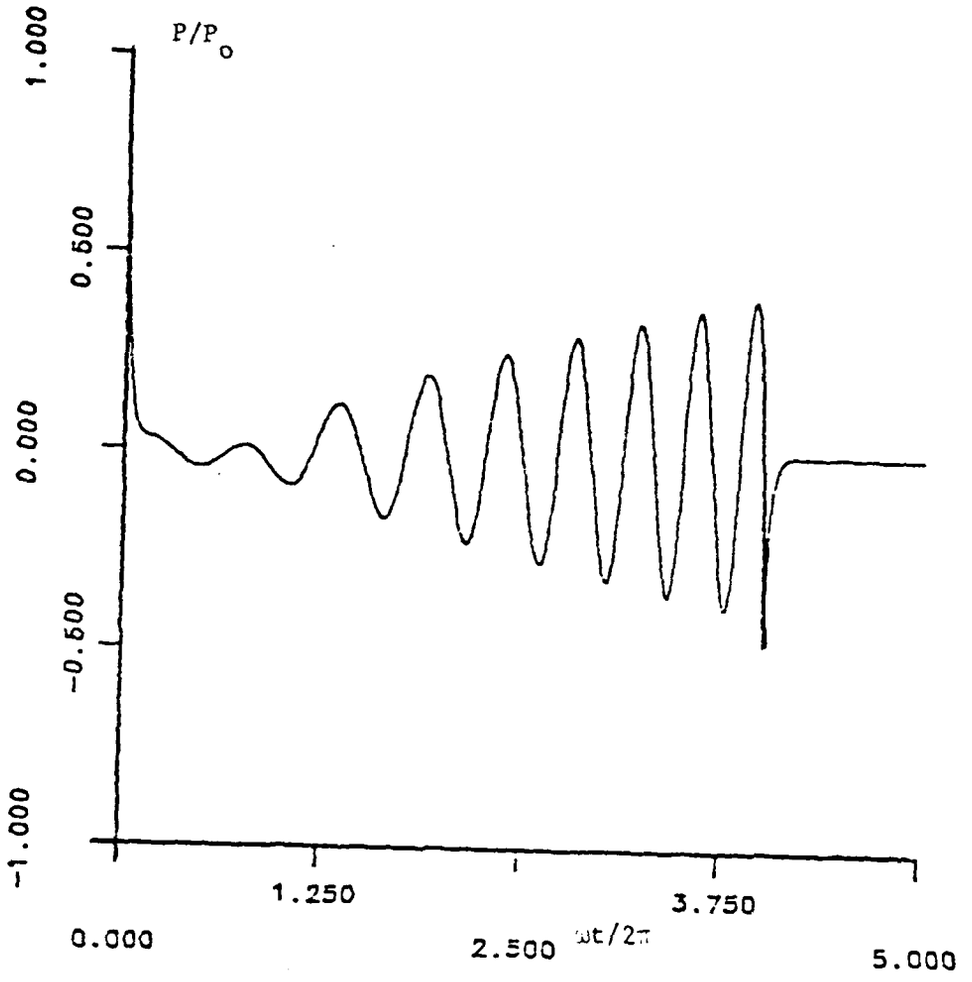

Figure 6. Reflected Pressure for an Incident FM Plane Pulse with $a_1 = 0.5$, $b_1 = 1.1$, $\varepsilon = 1$ and $\bar{\omega} = .8$.

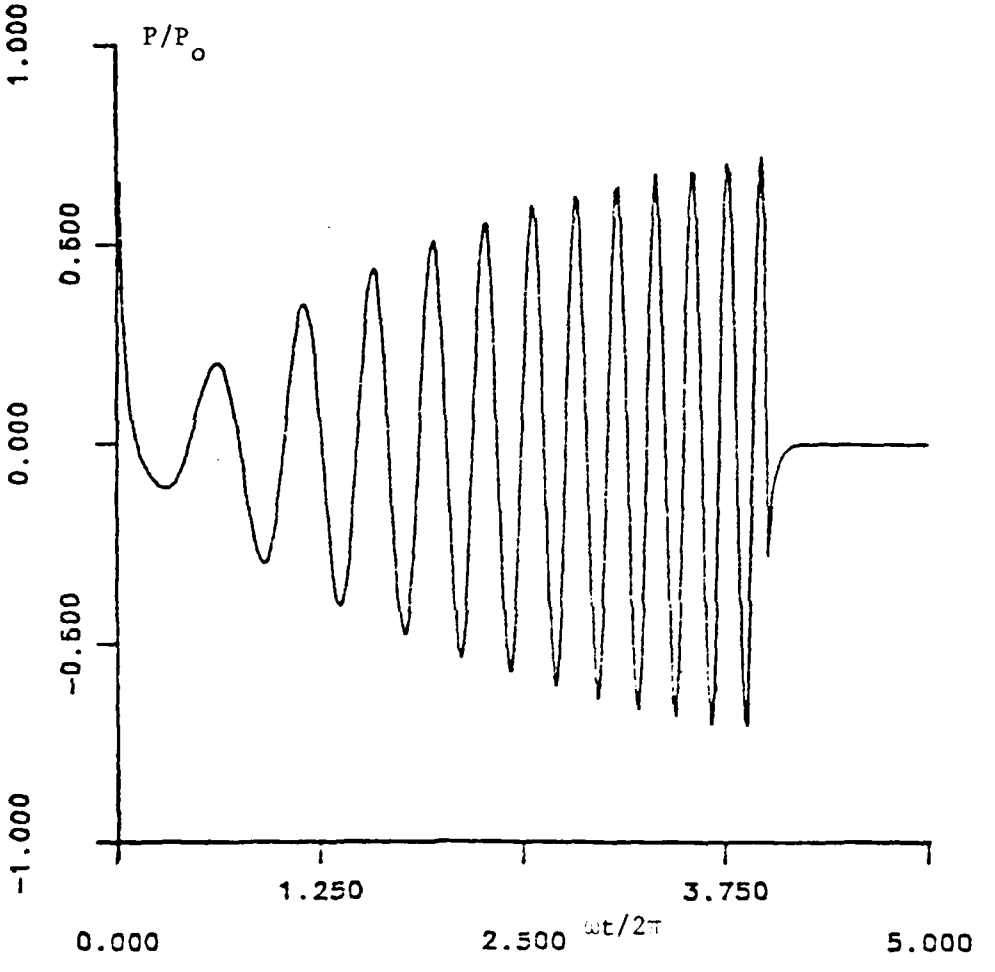

Figure 7. Reflected Pressure for an Incident FM Plane Pulse with $a_1 = .5$, $b_1 = 1.1$, $\beta = 2$ and $\bar{\omega} = 1.0$.

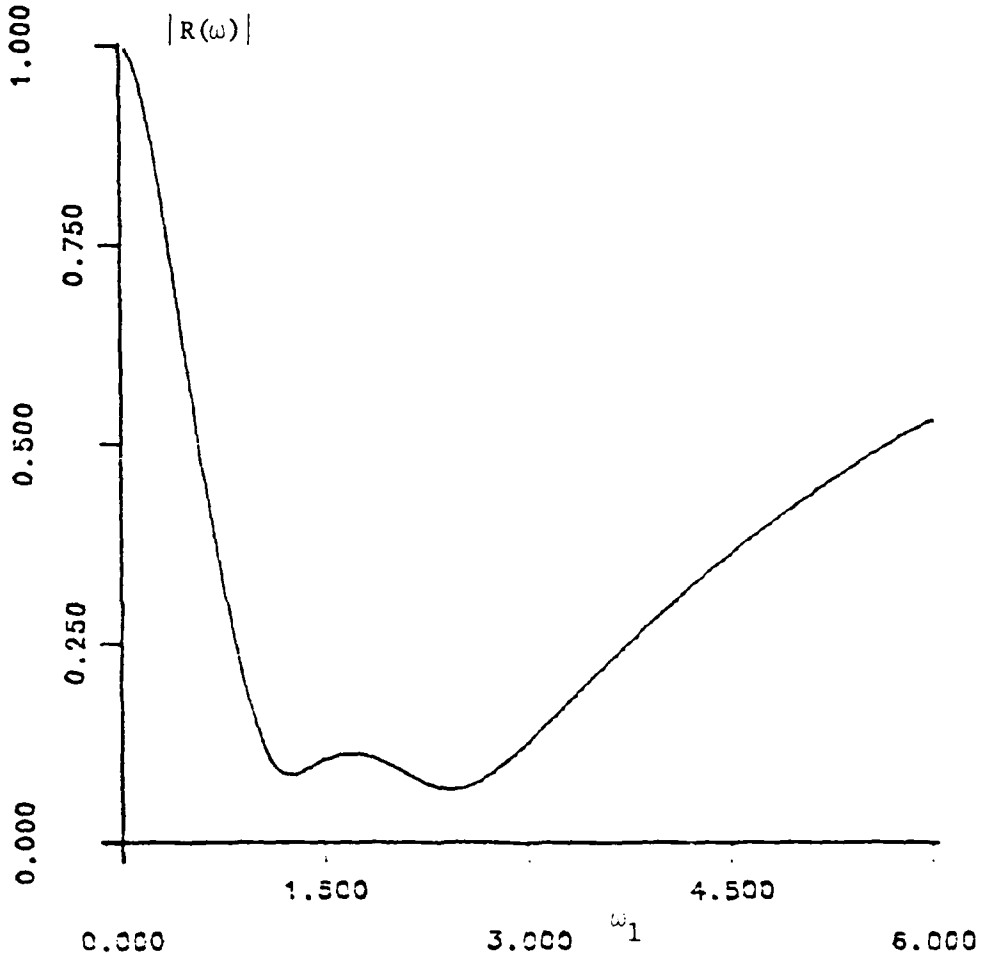

Figure 8. Plot of Absolute Value of the Reflection Coefficient for a Two Degree of Freedom Impedance Model with a_1 = 1.0, a_2 = .65, b_1 = 1.0 and b_2 = .7.

$$\alpha = \frac{\omega_2^o}{\omega_1^o} = 3,\ a_1 = 1.0,\ a_2 = .65,\ b_1 = 1.0,\ \text{and}\ b_2 = 0.7$$

The natural frequencies of the undamped oscillator obtained by solving Eq. (20a) would be

$$\frac{\Omega_1}{\omega_1^o} = .898 \quad \text{and} \quad \frac{\Omega_2}{\omega_1^o} = 3.338.$$

For the above set of numbers, the absolute value of the reflection coefficient function would fall below 0.2 in the frequency range $\Omega_1 < \omega < \Omega_2$ as shown in Figure 8. The complex poles of Eq. (21) are

$\eta_1 = (0.0, .5808)$

$\eta_2 = (.9869, 1.168)$

$\eta_3 = (-.9869, 1.168)$

$\eta_4 = (0.0, 6.630)$

An FM incident pulse represented by

$$P_{inc}(t) = \cos\omega t\left(1+ \frac{\beta}{8\pi}\ \omega t\right)[H(t) - H(t-8\pi)]$$

with $\beta = 1$ and $\omega/\omega_o = 1.2$ corresponds to an FM wave of constant amplitude and a frequency variation of $1.2 < \omega_o/\omega_1 < 2.4$ corresponding to the duration of the pulse. It can be seen from Figure 8, the magnitude of the reflection coefficient function is less than 11% for this frequency range. In Figure 9, the reflected pressure has an amplitude of less than 20% for almost the whole duration of the pulse. A comparison of Figures 5 and 9 shows that a multi-degree of freedom impedance function would minimize the reflection amplitude of an FM wave in the frequency range corresponding to the natural frequencies of the imepedance model.

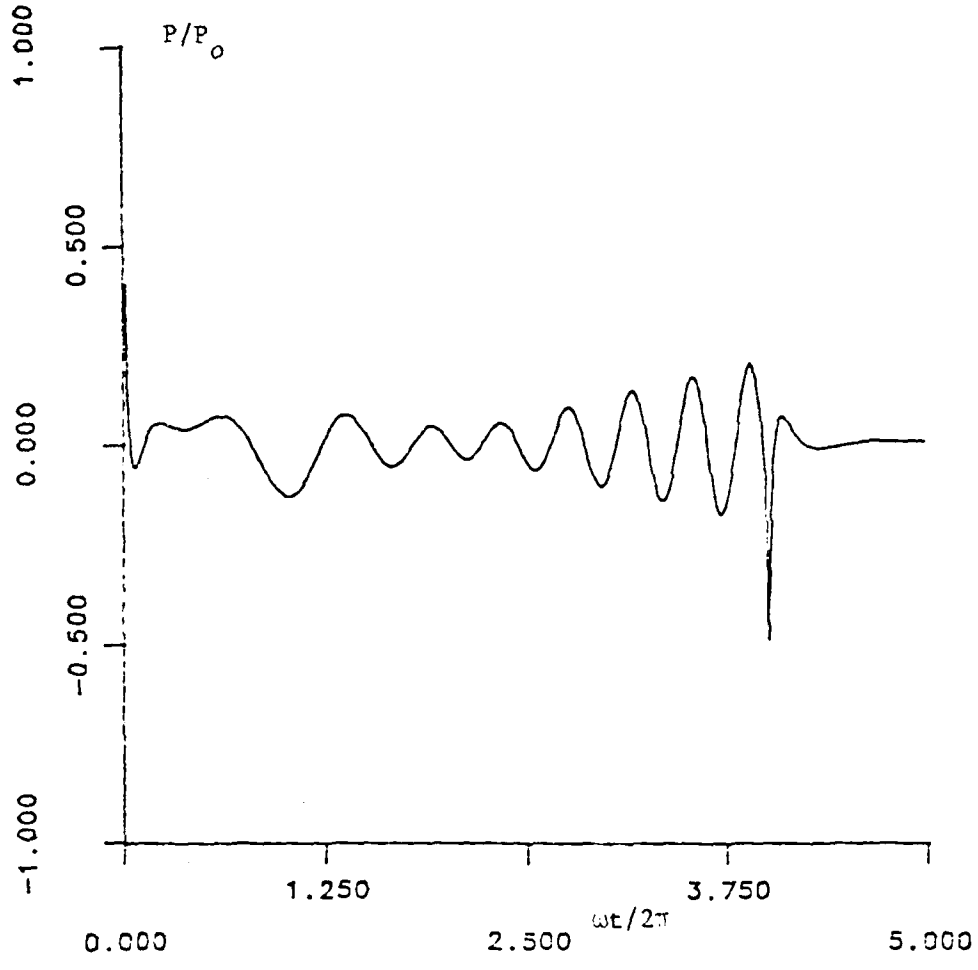

Figure 9. Reflected Pressure for an incident FM Plane Pulse with $\bar{\omega}_1 = 1.2$ and $\bar{\epsilon} = 1$.

Figure 10 shows the reflection for a frequency variation of $1 < \omega/\omega_0 < 3$ which represents a gradual build up in amplitude to almost 45% around $\omega t = 8\pi$. Figures 11 through 15 demonstrate the reflection for cases when the amplitude of the incident FM pulse is not constant. Two types of amplitude variations have been considered, linear and parabolic. The frequency range of the incident wave is still $1 < \omega/\omega_0 < 3$ for all these cases. The reflection has been computed by numerical integration of Eq. (11) after substitution of the residues from Eqs. (24) and (25).

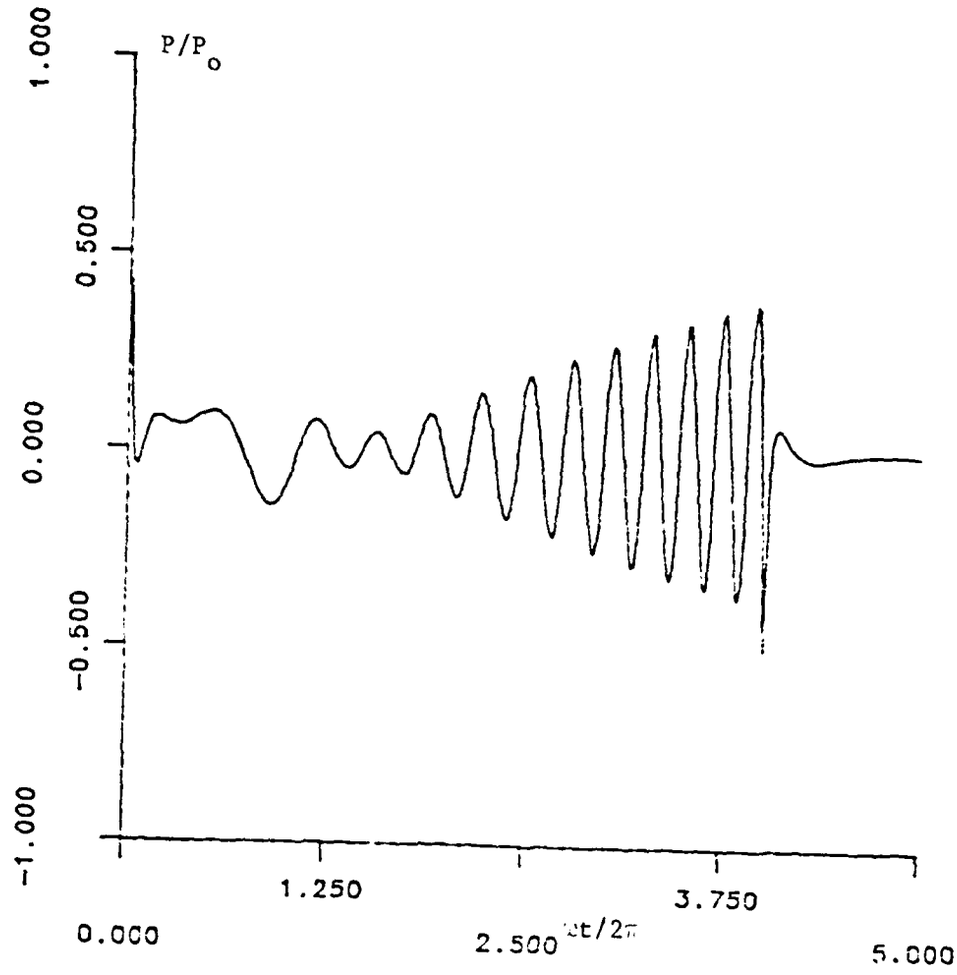

Figure 10. Reflected Pressure for an Incident FM Plane Pulse with τ_1 = 1.0 and β = 2.

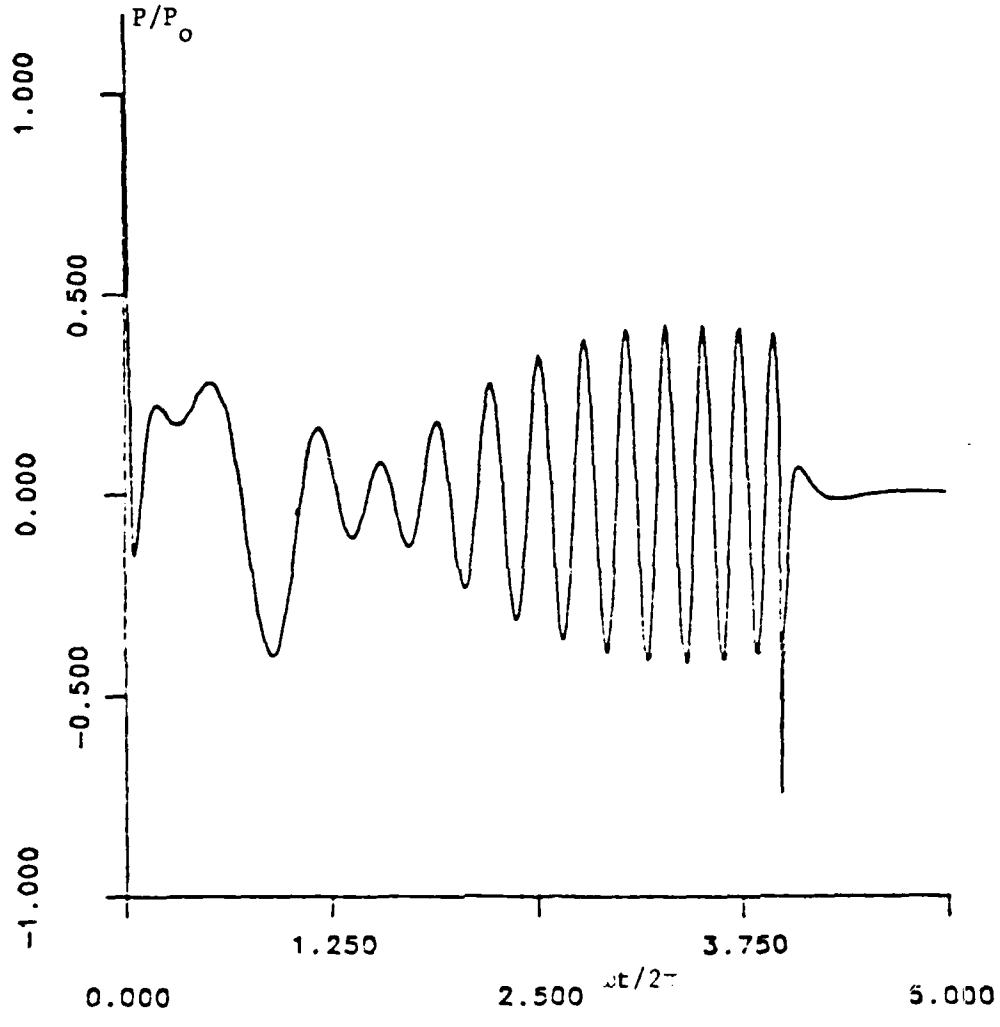

Figure 11. Reflected Pressure for $P_{inc} = \gamma\cos\omega t[1 + \frac{\beta}{8\pi} \omega t]$ $[H(t)-H(t-T)]$ with $\gamma = \gamma_o - (\frac{\gamma_o-1}{\beta})\omega t$, $\gamma_o = 3$, $\bar{\omega}_1 = 1$ and $\beta = 2$.

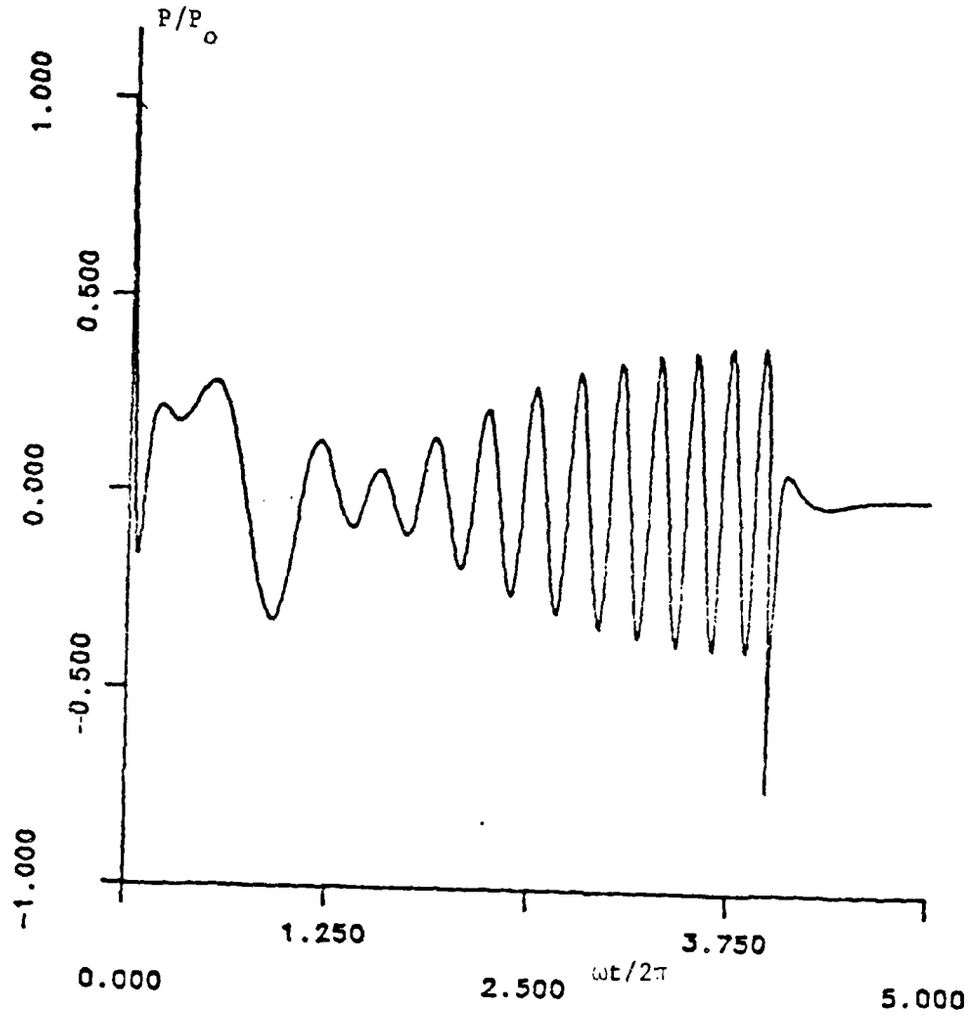

Figure 12. Reflected Pressure for $P_{inc} = y\cos\omega t[1 + \frac{\beta}{8\pi}\omega t]$ $[H(t)-H(t-T)]$ with $y = y_o + (1-y_o)\sqrt{\omega t/8\pi}$, $y_o = 3$, $\bar{\omega}_1 = 1$ and $\beta = 2$.

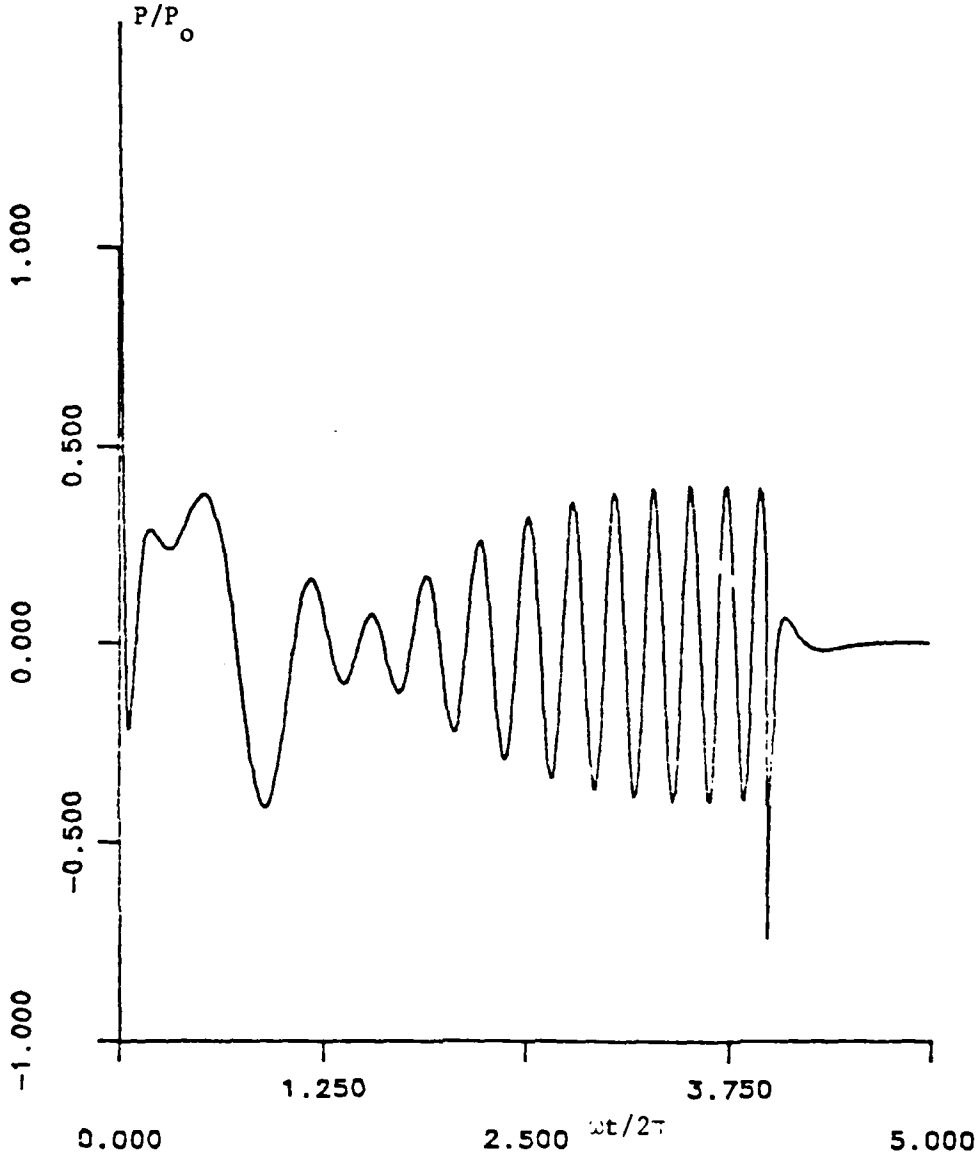

Figure 13. Reflected Pressure for $P_{inc} = y\cos\omega t[1 + \frac{\beta}{8\pi}\omega t]$ $[H(t)-H(t-T)]$ with $y = y_o + (1-y_o)\sqrt{\omega t/8\pi}$, $y_o = 4$, $\bar{\omega}_1 = 1$ and $\beta = 2$.

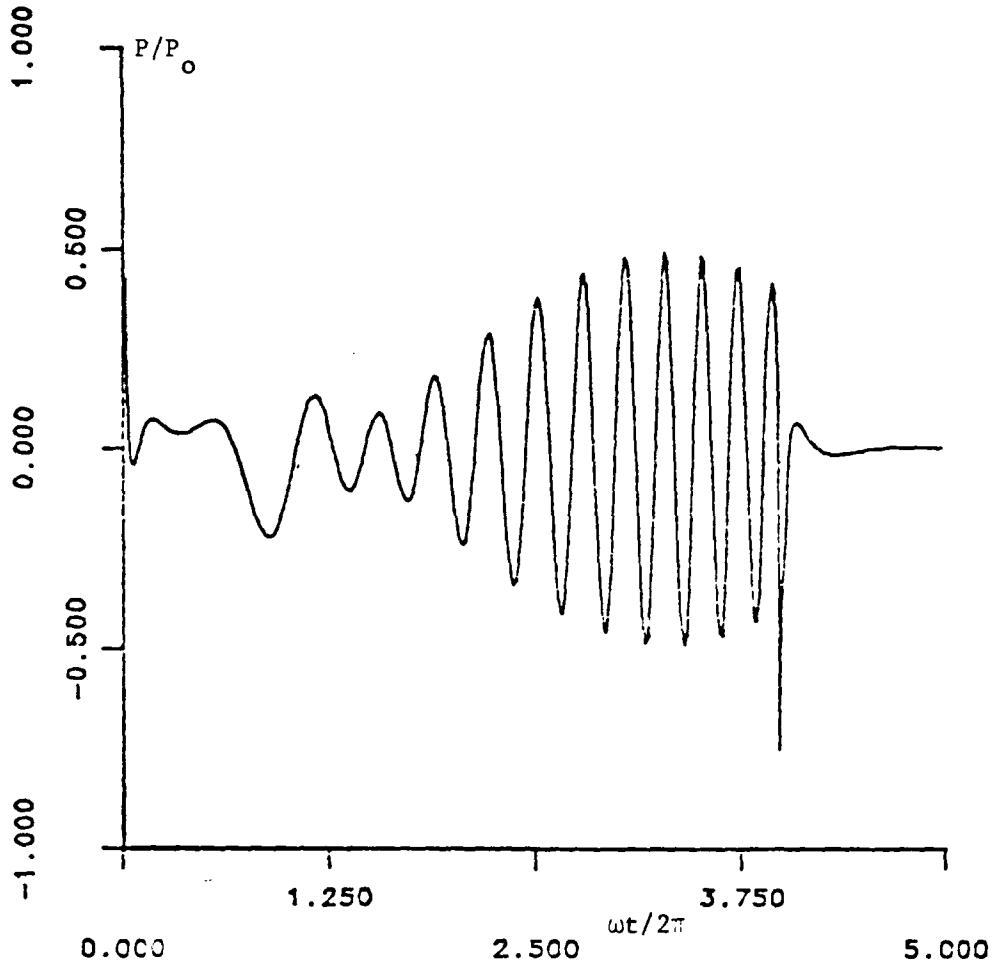

Figure 14. Reflected Pressure for $P_{inc} = y\cos\omega t[1 + \frac{\beta}{8\pi}\omega t]$ $[H(t)-H(t-T)]$ with $y = -(\omega t/4\pi)^2 + \omega t/2\pi + 1$, $\overline{\omega}_1 = 1$ and $\beta = 2$.

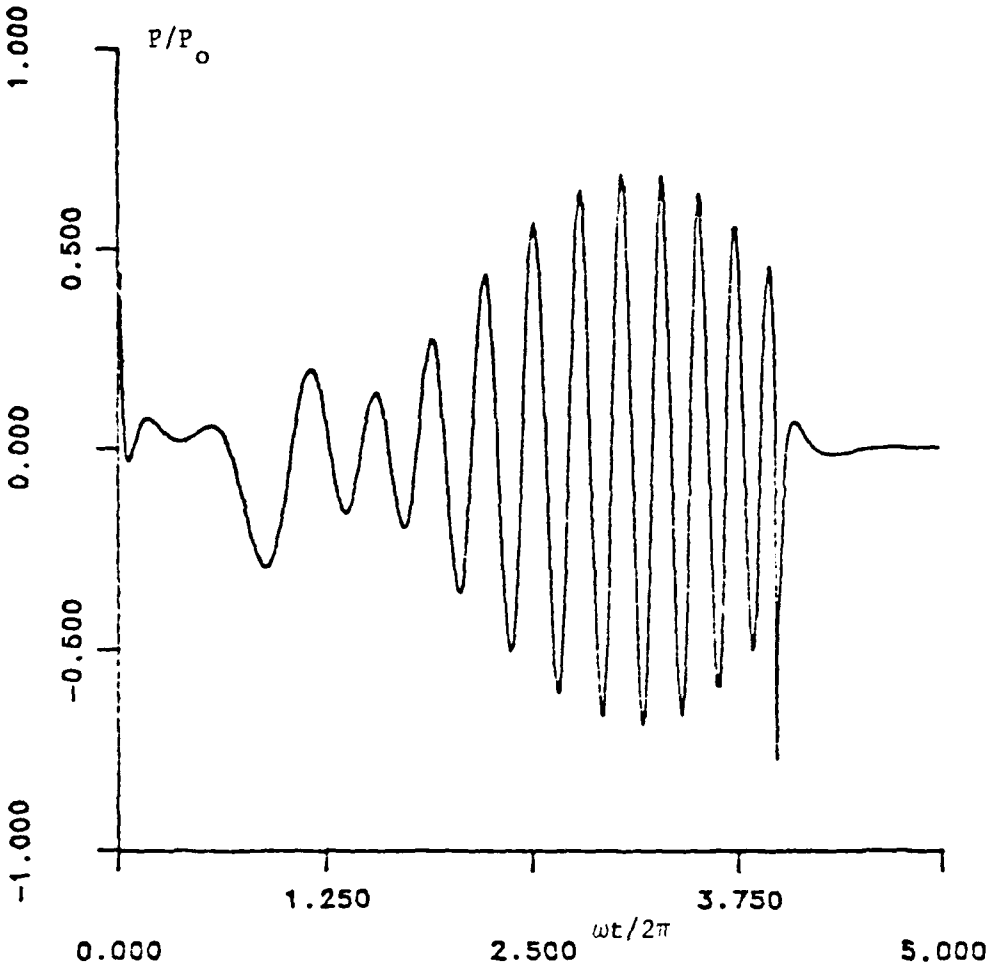

Figure 15. Reflected Pressure for $P_{inc} = y\cos\omega t[1 + \frac{\beta}{8\pi}\omega t]$ $[H(t)-H(t-T)]$ with $y = -2(\omega t/4\pi)^2 + \omega t/\pi + 1$, $\overline{\omega}_1 = 1$ and $\beta = 2$.

CHAPTER III

PULSE SCATTERING FROM IMPEDANCE COVERED CYLINDERS

3.1 Statement of the Problem

In this chapter, the problem of a pulsed plane wave scattered by an infinite cylinder will be solved. The cylinder is infinite in extent and the incident plane wave is parallel to its axis. The cylinder is assumed to have a cover that possesses a locally reacting impedance as the case in Chapter II.

Consider a plane pulse traveling with speed c in the x-direction perpendicular to the cylinder's axis (see Figure 16).

$$P_{inc} = P_o \delta(\frac{x}{c} - t) \tag{26}$$

Applying complex Fourier transform on P_{inc}, one obtains:

$$P_{i\omega} = \int_{-\infty}^{+\infty} P_{inc}\, e^{i\omega t}\, dt = \int_{-\infty}^{+\infty} P_o\, \delta(\frac{x}{c} - t) e^{i\omega t}\, dt = P_o\, e^{ikx} \tag{27}$$

where $k = \omega/c$ is the wave number. The incident wave can be reconstructed by applying inverse Fourier transform:

$$P_{inc} = \frac{1}{2\pi} \int_{-\infty}^{+\infty} P_{i\omega}\, e^{-i\omega t} d\omega = \frac{P_o}{2\pi} \int_{-\infty}^{+\infty} e^{i\omega(\frac{x}{c} - t)} d\omega = P_o \delta(\frac{x}{c} - t) \tag{28}$$

The integrand of Eq. (28) $P_{i\omega}\, e^{-i\omega t}$ represents a time harmonic component of the incident wave. Since the scattered field due to this component of the incident wave would have the same time dependency, factor $e^{-i\omega t}$ for convenience will be suppressed. $P_{i\omega}$ can be expanded in terms of cylindrical functions [17] as:

$$P_{i\omega} = P_o\, e^{ikr\cos\phi} = P_o \sum_{n=0}^{\infty} \varepsilon_n\, i^n\, J_n(kr)\cos n\phi \tag{29}$$

where

$$\varepsilon_o = 1 \text{ and } \varepsilon_n = 2 \text{ for } n \neq 0$$

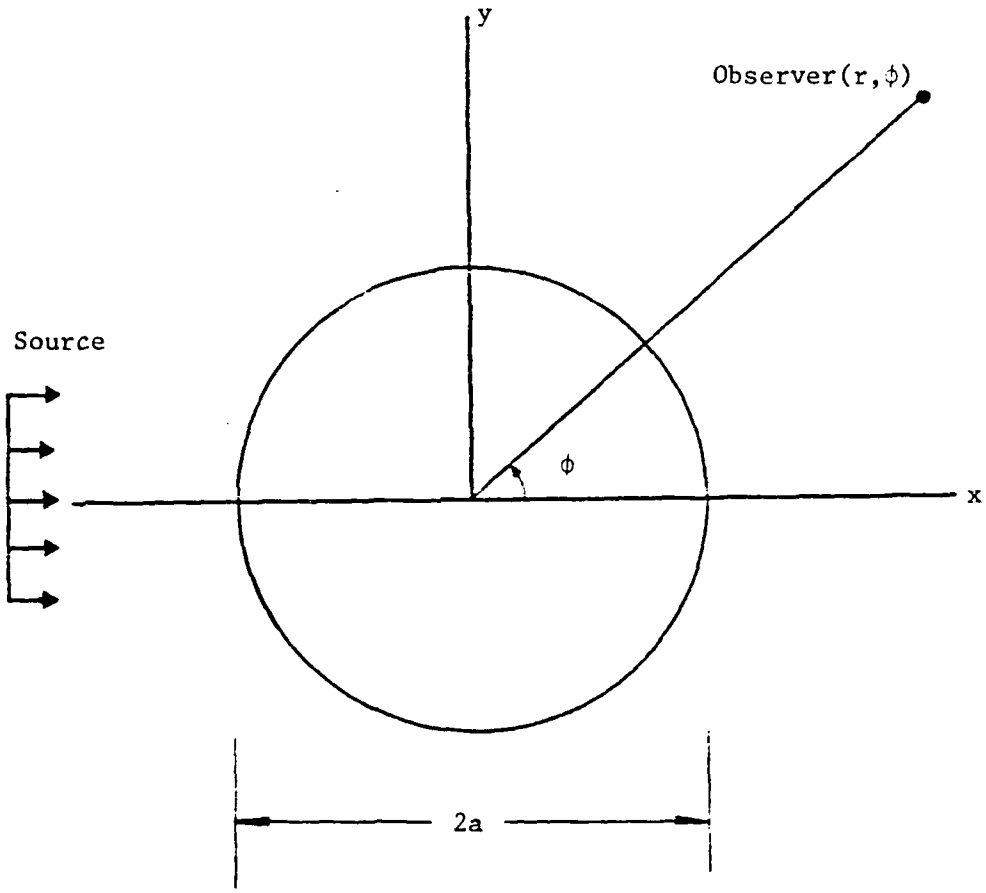

Figure 16. Geometry of the Impedance Covered Cylinder.

The scattered field $P_{s\omega}$ corresponding to an incident pressure $P_{i\omega}$ can be expressed as

$$P_{s\omega} = P_o \sum_{n=0}^{\infty} A_n \varepsilon_n i^n H_n^{(1)}(kr)\cos n\phi \tag{30}$$

the Fourier coefficients A_n are obtained by applying the boundary condition

$$\frac{P_{i\omega} + P_{s\omega}}{u_{i\omega} + u_{s\omega}} = Z(\omega) \quad \text{at} \quad r = a \tag{31}$$

where $u_{i\omega}$ and $u_{s\omega}$ represent the incident and scattered components of velocity in the radial direction and $Z(\omega)$ is the impedance of the boundary, which is a function of the frequency.

$u_{i\omega}$ and $u_{s\omega}$ can be expressed as follows:

$$u_{i\omega} = \frac{1}{i\omega\rho}\frac{\partial P_{i\omega}}{\partial r} = \frac{P_o}{2\rho c}\sum_{n=0}^{\infty} \varepsilon_n i^{n+1}[J_{n+1}(kr)-J_{n-1}(kr)]\cos n\phi$$

$$u_{s\omega} = \frac{1}{i\omega\rho}\frac{\partial P_{s\omega}}{\partial r} = -\frac{P_o}{2\rho c}\sum_{n=0}^{\infty} A_n \varepsilon_n i^{n+1}[H_{n-1}^{(1)}(kr) - H_{n+1}^{(1)}(kr)]\cos n\phi \tag{32}$$

where ρ is the mass density of the acoustic medium surrounding the cylinder. Substituting $P_{i\omega}$, $P_{s\omega}$, $u_{i\omega}$ and $u_{s\omega}$ in Eq. (31) and solving for the constant A_n, one obtains:

$$A_n(ka) = -\frac{J_n(ka) + \frac{iZ(\omega)}{\rho c} J_n'(ka)}{H_n^{(1)}(ka) + \frac{iZ(\omega)}{\rho c} H_n'^{(1)}(ka)} \qquad n = 0, 1, 2 \ldots \tag{33}$$

where the prime stands for differentiation with respect to the argument of the cylindrical functions. Finally the scattered pressure due to an incident plane pulse on the cylinder can be expressed as:

$$P_s(r,t,\phi) = \frac{1}{2\pi}\int_{-\infty}^{+\infty} P_{s\omega}\, e^{-i\omega t}\, d\omega,$$

or
$$P_s(r,t,\phi) = \frac{P_o}{2\pi}\sum_{n=0}^{\infty} \varepsilon_n i^n \cos n\phi \int_{-\infty}^{+\infty} A_n(ka) H_n^{(1)}(kr) e^{-i\omega t} d\omega. \tag{34}$$

Letting $\eta = ka$ and $\xi = c/a$, then Eq. (34) can be written as:

$$P_s(r,t,\phi) = \frac{P_o \xi}{2\pi}\sum_{n=0}^{\infty} \varepsilon_n i^n \cos n\phi \int_{-\infty}^{+\infty} A_n(\eta) H_n^{(1)}(\eta \frac{r}{a}) e^{-i\eta\xi t} d\eta \tag{35}$$

3.2 Impedance Function

Consider the simple oscillator as a model for the impedance of the surface expressed as:

$$Z = c_o - im\omega_o(\frac{\omega}{\omega_o} - \frac{\omega_o}{\omega}) \quad , \quad \omega_o^2 = \frac{k}{m}$$

Dividing Z by ρc and introducing the constants

$$b_1 = \frac{c_o}{\rho c} \quad \text{and} \quad a_1 = \sqrt{km/\rho c}$$

then

$$\frac{Z}{\rho c} = b_1 - ia_1(\frac{\omega}{\omega_o} - \frac{\omega_o}{\omega})$$

To express the impedance in non-dimensional variables, the following variables are introduced:

$$\lambda_o = \frac{2\pi c}{\omega_o} \quad , \quad \bar{\lambda} = \frac{\lambda_o}{2\pi a} = \frac{\xi}{\omega_o} \quad .$$

Then the variable η can be written as

$$\eta = ka = \left(\frac{\omega}{\omega_o}\right)\left(\frac{1}{\bar{\lambda}}\right)$$

or $$\left(\frac{\omega}{\omega_o}\right) = \eta\bar{\lambda}$$

Finally let $\bar{Z}(\eta) = \frac{Z}{\rho c}$

$$\bar{Z}(\eta) = b_1 - ia_1\left(\bar{\lambda}\eta - \frac{1}{\bar{\lambda}\eta}\right) \tag{36}$$

The impedance function, as expressed by Eq. (36), is expressed as a function of the radius of the cylinder as well as the characteristics of the oscillator. Finally the reflection amplitude coefficients are given by:

$$A_n(\eta) = -\frac{J_n(\eta) + i\bar{Z}(\eta)J_n'(\eta)}{H_n^{(1)}(\eta) + i\bar{Z}(\eta)H_n'^{(1)}(\eta)} \qquad n = 0, 1, 2, \ldots \tag{37}$$

Using the identify $J_n(\eta) = 1/2\ [H_n^{(1)}(\eta) + H_n^{(2)}(\eta)]$, $A_n(\eta)$ can be rewritten as:

$$A_n(\eta) = -\frac{1}{2}\left[1 + \frac{H_n^{(2)}(\eta) + i\bar{Z}(\eta)H_n'^{(2)}(\eta)}{H_n^{(1)}(\eta) + i\bar{Z}(\eta)H_n'^{(1)}(\eta)}\right] = -\frac{1}{2}\left[1 + B_n(\eta)\right] \tag{38}$$

Substituting Eq. (38) into Eq. (35) one obtains:

$$P_s(r,t,\phi) = \frac{-P_o\xi}{4\pi} \sum_{n=0}^{\infty} \varepsilon_n i^n \cos n\phi \int_{-\infty}^{+\infty} H_n^{(1)}(n\frac{r}{a}) e^{-in\xi t} dn$$

$$- \frac{P_o\xi}{4\pi} \sum_{n=0}^{\infty} \varepsilon_n i^n \cos n\phi \int_{-\infty}^{+\infty} B_n(n) H_n^{(1)}(n\frac{r}{a}) e^{-in\xi t} dn \quad (39)$$

It can be shown that the first integral on the right hand side of Eq. (39) has no contribution to the scattered pressure.

Let

$$Q = \sum_{n=0}^{\infty} \varepsilon_n i^n \cos n\phi \int_{-\infty}^{+\infty} H_n^{(1)}(n\frac{r}{a}) e^{-in\frac{ct}{a}} dn$$

first let's consider the case when $r/a \gg 1$. Using the asymptotic expression for $H_n^{(1)}(nr/a)$ one obtains:

$$Q = \sum_{n=0}^{\infty} \varepsilon_n i^n \cos n\phi \left(\sqrt{\frac{2}{\pi r/a}}\right) e^{-i(n\pi/2 + \pi/4)} \int_{-\infty}^{+\infty} \frac{1}{\sqrt{n}} e^{-in\frac{ct-r}{a}} dn$$

or

$$Q = \sqrt{\frac{2}{\pi r/a}} e^{-i\pi/4} \int_{-\infty}^{+\infty} \frac{1}{\sqrt{n}} e^{-in\frac{ct-r}{a}} dn \left\{ \sum_{n=0}^{\infty} \varepsilon_n \cos n\phi \, i^n e^{-in\pi/2} \right\}$$

but

$$\sum_{n=0}^{\infty} \varepsilon_n \cos n\phi i^n e^{-in\pi/2} = \sum_{n=0}^{\infty} \varepsilon_n \cos n\phi = 2\{\frac{1}{2} + \cos\phi + \cos 2\phi + \ldots\}$$

$$= 2(\frac{1}{2} - \frac{1}{2}) = 0$$

hence $Q = 0$. Furthermore, one can consider the integral

$$I_n = \int_{-\infty}^{+\infty} H_n^{(1)}(n) e^{-i\alpha n} dn \quad (\alpha = ct/r > 1)$$

This integral is obtained by a change of variable in the expression for Q

$$Q = \frac{1}{r/a} \sum_{n=0}^{\infty} \varepsilon_n i^n \cos n\phi (I_n)$$

it can be proven that Q is a pure imaginary number and hence would not have any real contributions to the scattered pressure. Let's consider the following contour integration

$$\int_C H_n^{(1)}(\eta)\, e^{-i\alpha\eta} d\eta,$$

where C is the closed contour shown in Figure 17. The function $H_n^{(1)}(\eta)$ does not have any pole inside the closed contour. Furthermore, on Γ the integrand is

$$H_n^{(1)}(\eta)\, e^{i\alpha\eta} = \sqrt{2/\pi\eta}\, e^{+i(\eta - \frac{n\pi}{2} - \frac{\pi}{4})}\, e^{-i\alpha\eta}$$

$$= \sqrt{2/\pi\eta}\, e^{-i(\frac{n\pi}{2} - \frac{\pi}{4})}\, e^{-i\eta(\alpha-1)}$$

since $(\alpha-1) > 0$ then $e^{-i\eta(\alpha-1)}$ vanishes on Γ . On the small contour c_ε, $|\eta| << 1$. The asymptotic expressions for the Hankel function for small argument [18] are given by:

$$H_o^{(1)}(\eta) \sim \frac{2i}{\pi} \ln\eta$$

and $$H_n^{(1)}(\eta) \sim -\frac{i}{\pi} \frac{(n-1)!}{\eta^n} 2^n \quad \text{for} \quad n \geq 1$$

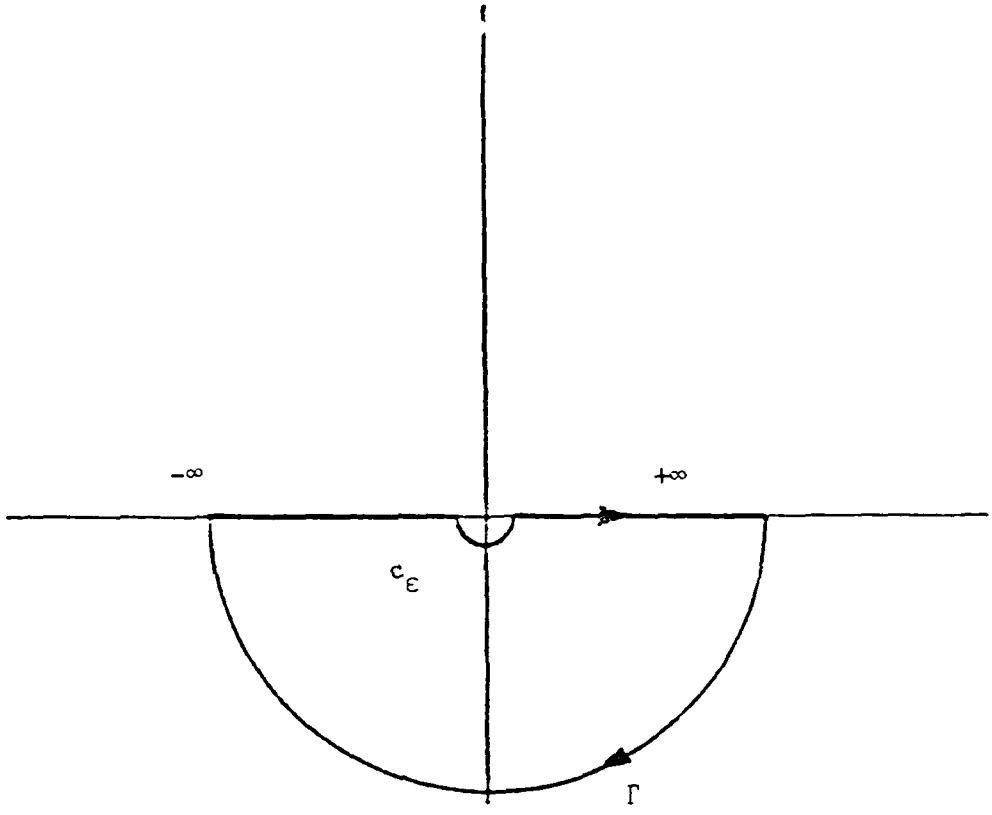

Figure 17. Contour 'C' in the Complex η-plane.

Consider the n = 0 term, letting $\eta = \varepsilon e^{\vartheta}$, then

$$I_o = \int_{-\infty}^{+\infty} H_o^{(1)}(\eta)e^{-i\alpha\eta}d\eta = -\int_{C_\varepsilon} H_o^{(1)}(\eta)e^{-i\alpha\eta}d\eta$$

$$= -\int_{-\infty}^{+\infty} \frac{2i}{\pi} \ell n(\varepsilon e^{i\theta})\, e^{-i\alpha\varepsilon e^{i\theta}} (i\varepsilon e^{i\vartheta})d\theta = \frac{2\varepsilon}{\pi}\int_{-\pi}^{0} (i\theta + \ell n\varepsilon)e^{i\theta}d\theta$$

$$= -\frac{4i}{\pi}\varepsilon\ell n\varepsilon - 2\varepsilon = 0 \text{ as } \varepsilon \to 0 \ .$$

for n > 1 the integral is given by:

$$I_n = \int_{-\infty}^{+\infty} H_n^{(1)}(\eta)e^{-i\alpha\eta}d\eta = -\int_{C_\varepsilon} [H_n^{(1)}(\eta)e^{-i\alpha\eta}]d\eta$$

$$= -\frac{i}{\pi}(2^n)\frac{(n-1)!}{(n-1)}\varepsilon^{1-n}[1 + (-1)^n] = \begin{cases} 0 & n = \text{odd} \\ -(\frac{i}{\pi})2^{n+1}(n-2)!\ \varepsilon^{1-n} & n = \text{even} \end{cases}$$

Summing up all these contributions, then

$$Q = \frac{a}{r}\sum_{n=0}^{\infty} \varepsilon_n\, i^n \cos n\phi\ I_n = (\frac{a}{r})(\frac{i}{\pi})\sum_n (\text{real fun.})$$

is purely an imaginary number.

3.3 Watson Transformation

The scattered pressure due to an incident plane pulse on the cylinder can thus be expressed as:

$$P_s(r,t,\phi) = \frac{-P_o\xi}{4\pi}\sum_{n=0}^{\infty} \varepsilon_n i^n \cos n\phi \int_{-\infty}^{+\infty} B_n(\eta)H_n^{(1)}(\eta\,\frac{r}{a})e^{-i\eta ct/a}\,d\eta$$

where

$$B_n(\eta) = \frac{H_n^{(2)}(\eta) + i\bar{Z}(\eta)\, H_n'^{(2)}(\eta)}{H_n^{(1)}(\eta) + i\bar{Z}(\eta)\, H_n'^{(1)}(\eta)} \quad . \tag{40}$$

Let $E_n(\eta) = B_n(\eta)\, H_n^{(1)}(\eta \frac{r}{a})$

Using the following properties of the cylindrical functions

$$H_{-\gamma}^{(1)}(\eta) = e^{\gamma\pi i}\, H_\gamma^{(1)}(\eta) \ ,$$

$$H_\gamma^{(2)}(\eta) = e^{-\gamma\pi i}\, H_\gamma^{(2)}(\eta),$$

it is easy to show that $E_{-\gamma}(\eta) = e^{-\gamma\pi i}\, E_\gamma(\eta)$. For the special case that γ is an integer one obtains:

$$E_{-n}(\eta) = (-1)^n\, E_n(\eta) \tag{41}$$

Eq. (41) would lead to the following identity

$$\sum_{n=0}^{\infty} \varepsilon_n\, i^n \cos n\phi\, E_n(\eta) = \sum_{n=-\infty}^{+\infty} i^n \cos n\phi\, E_n(\eta) \tag{42}$$

Using Sommerfeld-Watson transformations, the right hand side of Eq. (42) can be expressed as:

$$\sum_{n=-\infty}^{\infty} i^n \cos n\phi\, E_n(\eta) = \frac{i}{2} \int_C \frac{e^{-\gamma\pi i/2} \cos\gamma\phi\, E_\gamma(\eta)}{\sin\gamma\pi}\, d\gamma \tag{43}$$

where

$$\left(\frac{d\ \sin\gamma\pi}{d\gamma}\right)_{\gamma\ =\ \pi} = (-1)^{n}\pi$$

with the contour C shown in Figure 18. It can be shown that the value of the integral on the lower half of the contour 'C' is the same as that for the upper half. Letting

$$I = \int_C \frac{e^{-\gamma\pi i}\cos\gamma\phi\ E_\gamma(n)}{\sin\gamma\pi}\,d\gamma = \int_{-\infty}^{+\infty}(\quad)d\gamma + \int_{+\infty}^{-\infty}(\quad)d\gamma \qquad (44)$$

and making a change of variable ($\gamma \rightarrow -\gamma$), one obtains an expression for I as:

$$I = \int_{-\infty}^{+\infty}(\quad)d\gamma + \int_{-\infty}^{+\infty} e^{\gamma\pi i/2}\cos\gamma\phi\ E_{-\gamma}(n)\,\frac{d\gamma}{\sin\gamma\pi}$$

which, upon substitution of $E_{-\gamma}(n) = e^{-\gamma\pi i}\,E_\gamma(n)$ becomes:

$$I = 2\int_{-\infty}^{+\infty} e^{\frac{-\gamma\pi i}{2}}\cos\gamma\pi\ E_\gamma(n)\ \frac{d\gamma}{\sin\gamma\pi} \qquad (45)$$

Incorporating the above transformations into Eq. (40), the scattered pressure field could be written as:

$$P_s(r,t,\phi) = -i\,\frac{P_o\xi}{4\pi}\int_{-\infty}^{+\infty}\int_{-\infty}^{+\infty}\frac{e^{-\gamma\pi i/2}\cos\gamma\phi\ B_\gamma(n)}{\sin\gamma\pi}\,H_\gamma^{(1)}(n\tfrac{r}{a})e^{-inct/a}d\gamma dn \qquad (46)$$

where

$$B_\gamma(n) = \frac{H_\gamma^{(2)}(n) + i\bar{Z}(n)\,H_\gamma'^{(2)}(n)}{H_\gamma^{(1)}(n) + i\bar{Z}(n)\,H_\gamma'^{(1)}(n)} \qquad (47)$$

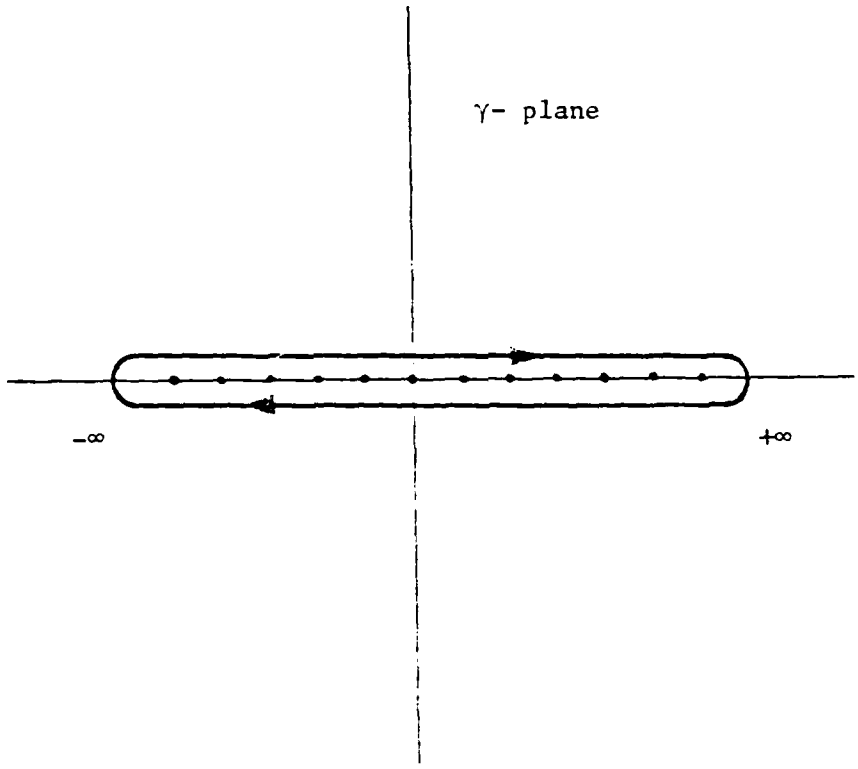

Figure 18. Contour of Sommerfeld-Watson Transformation.

Following Uberall [7], the scattered pressure as expressed by Eq. (46) could be split into two parts:

1) A geometrically reflected field

2) Creeping or circumferential waves that encircle the cylinder any number of times and propagate to the observer.

The presence of circumferential waves has been confirmed experimentally by measuring the multiple echoes that return in the scattering of a single pulse. This can be demonstrated mathematically by expanding

$$\cos\gamma\phi = e^{i\gamma\pi}\cos[(\pi - \phi)\gamma] - i\, e^{i\gamma(\pi - \phi)}\sin\gamma\pi$$

$$\frac{1}{\sin\gamma\pi} = -2i\, e^{i\gamma\pi} \sum_{s=0}^{\infty} e^{2is\gamma\pi}$$

The product

$$e^{-\gamma\pi i/2}\cos\gamma\phi/\sin\gamma\pi$$

can thus be expressed in either of the following forms:

$$\frac{e^{\frac{-\gamma\pi i}{2}}\cos\gamma\phi}{\sin\gamma\pi} = \left[-i \sum_{\lambda=\pm} \sum_{s=0}^{\infty} e^{i\gamma(\phi_\lambda' + 2\pi s)}\right] - i\, e^{i\gamma(\frac{\pi}{2} - \phi)} \qquad (48\text{-a})$$

where $$\phi_-' = -\frac{\pi}{2} + (\pi - \varphi) + 2\pi = \frac{5\pi}{2} - \varphi \ ,$$

and $$\varphi_+' = -\frac{\pi}{2} - (\pi - \varphi) + 2\pi = \frac{\pi}{2} + \varphi \ ,$$

or in the form:

$$\frac{e^{\frac{-\gamma\pi i}{2}}\cos\gamma\phi}{\sin\gamma\pi} = \left[-i\, e^{\frac{i\gamma\pi}{2}} \sum_{\lambda = \pm} \sum_{s=0}^{\infty} e^{i\gamma(\phi_\lambda'' + 2\pi s)}\right] - ie^{i\gamma(\frac{\pi}{2} - \phi)} \tag{48-b}$$

where $\phi_-'' = 2\pi - \phi$,

and $\phi_+'' = \phi$.

Substituting Eq. (48) into (46) one obtains:

$$P_s(r,t,\phi) = -\frac{P_o\xi}{4\pi}\ (p_I^c + p^G) \tag{49}$$

where

$$p_I^c(r,t,\phi) = \sum_{\lambda= \pm} \sum_{s=0}^{\infty} \int_{-\infty}^{+\infty}\int_{-\infty}^{+\infty} e^{i\gamma(\phi_\lambda' + 2\pi s)} B_\gamma(n) H_\gamma^{(1)}(n\,\frac{r}{a}) e^{-inct/a}\, d\gamma dn, \tag{50}$$

and

$$p^G(r,t,\phi) = \int_{-\infty}^{+\infty}\int_{-\infty}^{+\infty} e^{i\gamma(\frac{\pi}{2} - \phi)} B_\gamma(n) H_\gamma^{(1)}(n\,\frac{r}{a}) e^{-inct/a}\, d\gamma dn\ . \tag{51}$$

In Eq. (49), p^G corresponds to geometric optic reflection and p_I^c corresponds to creeping waves on the surface or close to the surface of the cylinder. The angle ϕ_+' represents the waves that encircle the cylinder in c.c.w direction and the angle ϕ_-' corresponds to c.w creeping wave (see Fig. 19). These waves could be observed both in the insonified and shadow boundary of the cylinder.

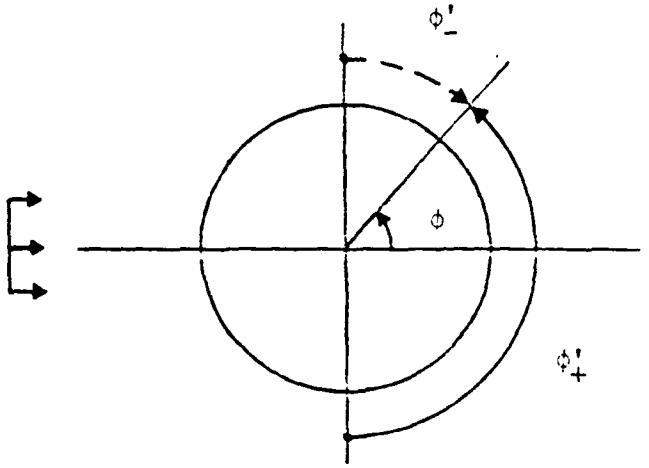

Figure 19a. Circumferential Waves on the Shadow Surface of the Cylinder.

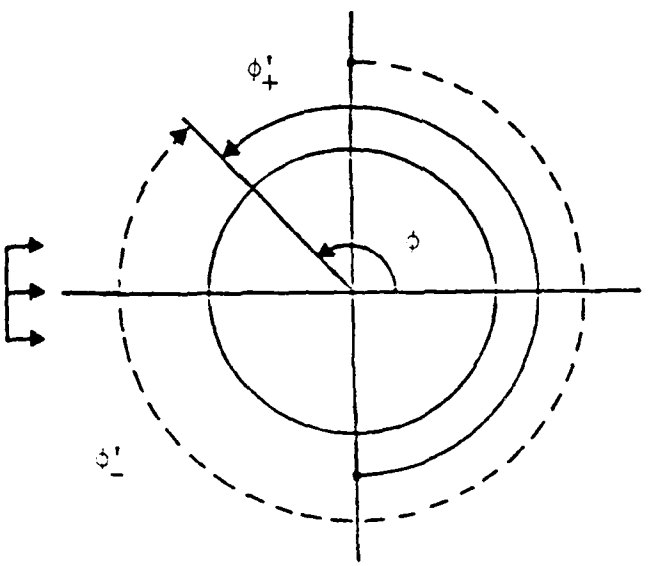

Figure 19b. Circumferential Waves in the Insonified Zone.

The summation on s indicates the presence of creeping waves that encircle the cylinder more than 2π radians in the positive or the negative sense.

On the other hand, substituting Eq. (48) into (46), the scattered pressure can be written in a different form which would be valid for an observer in the far field:

$$P_s(r,t,\phi) = -\frac{P_o\xi}{4\pi}\,(p^c_{II} + p^G) \tag{52}$$

where

$$p^c_{II} = \sum_{\lambda=\pm}\ \sum_{s=0}^{\infty}\ \int_{-\infty}^{+\infty}\int_{-\infty}^{+\infty} e^{\frac{i\gamma\pi}{2}}\, e^{i\gamma(\phi''_\lambda + 2\pi s)} B_\gamma(n) H^{(1)}_\gamma(n\,\frac{r}{a}) e^{-inct/a}\, d\gamma\, dn \tag{53}$$

and p^G is again given by Eq. (51). In Eq. (53), p^c_{II} represents circumferential waves travelling to an observer in the farfield in either the insonified or the shadow region (see Fig. 20).

If t = 0 corresponds to the arrival of the wave at the shadow boundary then the arrival time for an abserver at r/a >> 1 and angle ϕ (see Fig. 21) could be expressed as:

$$\bar{r} = \sqrt{a^2 + r^2 - 2a\cos\alpha}$$

$$\alpha = \frac{\pi - \phi}{2}$$

$$\bar{r} = r\sqrt{1 + (\frac{a}{r})^2 - \frac{2a}{r}\sin\frac{\phi}{2}} \approx r - a\sin\frac{\phi}{2}$$

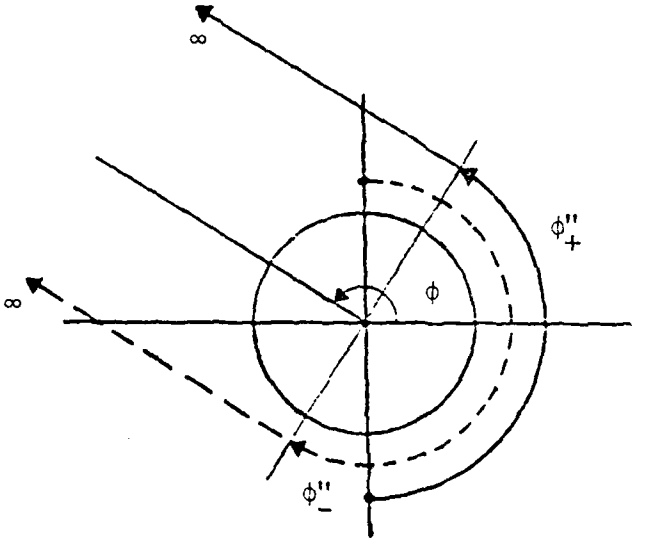

Figure 20a. Circumferential Waves Traveling to a Far Distant Observer in $|\phi| > \pi/2$ Region.

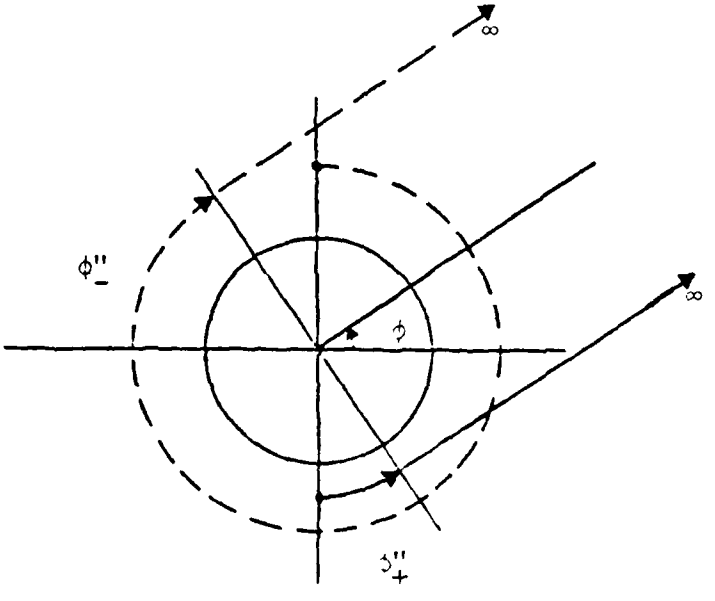

Figure 20b. Circumferential Waves Traveling to a Far Distant Observer in $|\phi| < \pi/2$ Region.

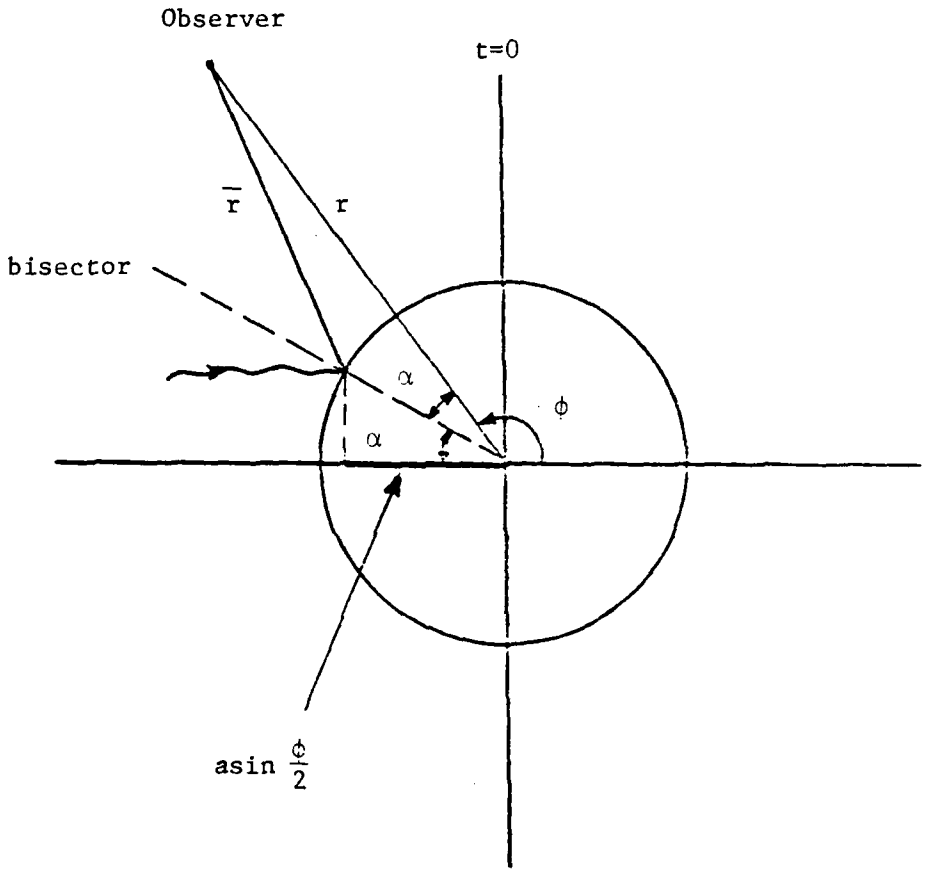

Figure 21. Plot of the Geometrically Reflected Pressure for an Observer in the Far Field.

Then the arrival time for the reflected pulse can be expressed as

$$\delta(ct - \bar{r} + a \sin\frac{\phi}{2}) = \delta(ct - r + 2a \sin\frac{\phi}{2})$$

For $\alpha > 45°$, the geometrically reflected wave reaches into the $\phi \leq 90°$ region.

3.4 Geometrically Reflected Pressure ($r/a \gg 1$, $0 \leq \phi \leq \pi$)

Since the reflected pressure is symmetric with respect to the x-axis, angle ϕ could be limited to $0 \leq \phi \leq \pi$. Dropping the factor $-P_o\xi/4\pi$ for the time being, the geometrically reflected pressure is given by

$$p^G(r,t,\phi) = \int_{-\infty}^{+\infty} \int_{-\infty}^{+\infty} e^{i\gamma(\frac{\pi}{2} - \phi)} B_\gamma(\eta) H_\gamma^{(1)}(\eta \frac{r}{a}) e^{-i\eta\frac{ct}{a}} d\gamma d\eta \qquad (54)$$

where $B_\gamma(\eta)$ is expressed by Eq. (47). Letting $\eta = \gamma \sec\alpha$, then the cylindrical functions $H_\gamma^{(1)}(\eta)$ and $H_\gamma^{(2)}(\eta)$ can be expressed in the following generalized form:

$$H_\gamma^{(1)}(\gamma\sec\alpha) = F_1(\gamma,\alpha)e^{i\psi(\gamma,\alpha)}$$

and

$$H_\gamma'^{(1)}(\gamma\sec\alpha) = F_2(\gamma,\alpha)\, e^{i\psi(\gamma,\alpha)} \qquad (55)$$

where

$$\psi(\gamma,\alpha) = \gamma(\tan\alpha - \alpha) - \frac{\pi}{4} .$$

For the case when $|\gamma| \gg 1$, $F_1(\gamma,\alpha)$ and $F_2(\gamma,\alpha)$ can be expressed as [18]:

$$F_1(\gamma,\alpha) = \sqrt{2/\pi\gamma\tan\alpha}\ \ [L(\gamma,\alpha) - iM(\gamma,\alpha)]$$

$$F_2(\gamma,\alpha) = \sqrt{\sin 2\alpha/\pi\gamma}\ \ [iN(\gamma,\alpha) - O(\gamma,\alpha)]$$

where L, M, N and O are expressed in terms of the following convergent series:

$$L(\gamma,\alpha) \simeq \sum_{k=0}^{\infty} \frac{u_{2k}(i\cot\alpha)}{\gamma^{2k}}$$

$$M(\gamma,\alpha) \simeq -i \sum_{k=0}^{\infty} \frac{u_{2k+1}(i\cot\alpha)}{\gamma^{2k+1}}$$

$$N(\gamma,\alpha) \simeq \sum_{k=0}^{\infty} \frac{V_{2k}(i\cot\alpha)}{\gamma^{2k}}$$

$$O(\gamma,\alpha) \simeq i \sum_{k=0}^{\infty} \frac{V_{2k+1}(i\cot\alpha)}{\gamma^{2k+1}}$$

and $u_o(t) = 1$

$$u_{k+1}(t) = \frac{1}{2} t^2(1 - t^2)u_k'(t) + \frac{1}{8} \int_o^t (1-5t^2)u_k(t)dt \qquad k=0,1,2,\ldots$$

$$V_o(t) = 1$$

$$V_k(t) = u_k(t) + t^2(t^2-1)\{ \frac{1}{2} u_{k-1}(t) + tu_{k-1}'(t)\} \ , \ k=1,2,\ldots$$

Substituting for γ in terms of the variable α and η ($\gamma=\eta\cos\alpha$) one obtains:

$$B_{\eta\cos\alpha}(\eta) = \frac{H_\gamma^{(2)}(\eta) + i\bar{Z}(\eta)H_\gamma'^{(2)}(\eta)}{H_\gamma^{(1)}(\eta) + i\bar{Z}(\eta)H_\gamma'^{(1)}(\eta)} \Bigg|_{\gamma = \eta\cos\alpha}$$

$$= \frac{\bar{F}_1(\eta\cos\alpha,\alpha) + i\bar{Z}(\eta)\bar{F}_2(\eta\cos\alpha,\alpha)}{F_1(\eta\cos\alpha,\alpha) + i\bar{Z}(\eta)F_2(\eta\cos\alpha,\alpha)} \ e^{-2i\psi(\eta\cos\alpha,\alpha)}$$

$$= G(\alpha,\eta)e^{-2i\psi} \qquad (55)$$

where $\psi(\eta\cos\alpha,\alpha) = \eta(\sin\alpha - \alpha\cos\alpha) - \pi/4$.

For an observer in the farfield ($r/a \gg 1$)

$$H_\gamma^{(1)}(\eta \frac{r}{a}) \sim \sqrt{\frac{2}{\pi r/a}} \ e^{\,i(\eta r/a - \frac{\gamma\pi}{2} - \frac{\pi}{4})}$$

Eq. (54) can now be expressed in terms of the new variable as:

$$p^G(r,t,\phi) = \int_{\eta=-\infty}^{+\infty} \int_{C_\alpha} G(\alpha,\eta) e^{-2i\psi} \cdot e^{i\eta\cos\alpha(\frac{\pi}{2}-\phi)} \cdot \sqrt{\frac{2}{\pi\eta r/a}} \cdot$$

$$\cdot e^{i(\eta\frac{r}{a} - \frac{\pi}{2}\eta\cos\alpha - \frac{\pi}{4})} \cdot e^{-i\eta\frac{ct}{a}} \cdot (-\eta\sin\alpha d\alpha)\, d\eta$$

or

$$p^G(r,t,\phi) = -\sqrt{\frac{2}{\pi\frac{r}{a}}}\, e^{i\pi/4} \int_{\eta=-\infty}^{+\infty} \sqrt{\eta}\, e^{-i\eta\Omega} d\eta \int_{C_\alpha} G(\alpha,\eta)\sin\alpha e^{-ing(\alpha)} d\alpha \tag{56}$$

where $\Omega = \frac{ct-r}{a}$,

$$g(\alpha) = 2\sin\alpha + (\phi - 2\alpha)\cos\alpha \ , \tag{57}$$

and C_α describes the path of integration in complex α-plane (see Fig. 22). Changing the direction of integration Eq. (56) can be rewritten as:

$$p^G(r,t,\phi) = \sqrt{\frac{2}{\pi r/a}}\, e^{\frac{i\pi}{4}} \int_{-\infty}^{+\infty} \sqrt{\eta}\, I(\eta)\, e^{-i\eta\Omega} d\eta \tag{58}$$

where $I(\eta) = \int_{C_\alpha} G(\alpha,\eta)\sin\alpha\, e^{-ing(\alpha)} d\alpha$ (59)

Eq. (59) can be approximated by integration along the path of the steepest descent.

3.5 Method of the Steepest Descent

The saddle point for the integral in Eq. (59) is located at $\alpha = \alpha_0$ where

$$g'(\alpha_0) = 0$$

or $\frac{\partial g}{\partial \alpha} = (2\alpha - \phi)\sin\alpha = 0,\ \alpha_0 = \frac{\pi}{2}$

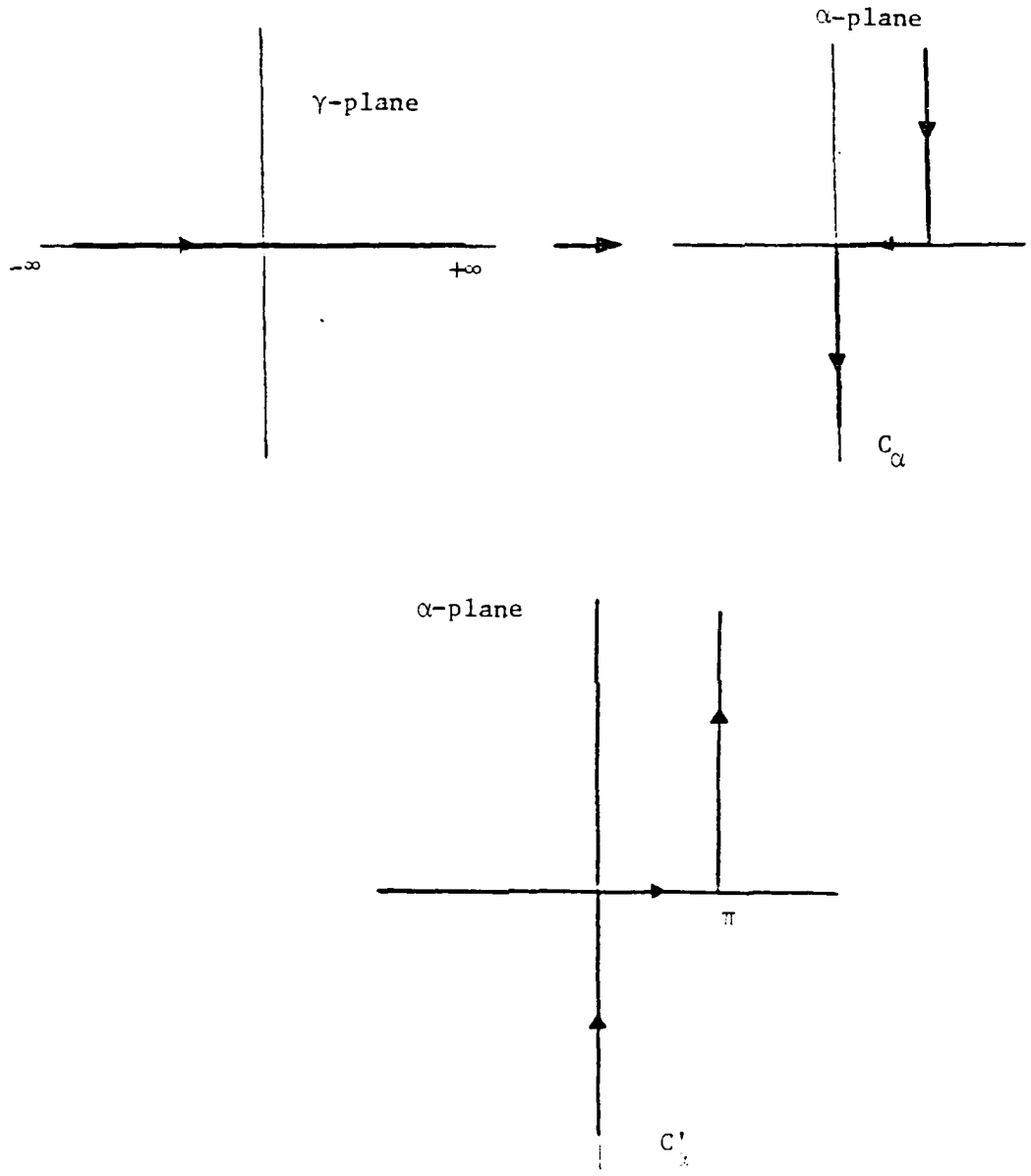

Figure 22. Transformation from γ-plane to α-plane.

The equation of the steepest descent path (Fig. 23) is expressed by:

$$\mathrm{Im}[g(\alpha)] = \text{const} = \mathrm{Im}[g(\alpha_o)] = \mathrm{Im}[2\sin\tfrac{\phi}{2}] = 0$$

Substituting $\alpha = \alpha_r + i\alpha_i$,then the equation becomes:

$$(1 - \alpha_i \coth\alpha_i) = (\tfrac{\phi}{2} - \alpha_r)\tan\alpha_r \qquad (60)$$

The asymptotes of the steepest descent path given by Eq. (60) are

$$\alpha_i \to \pm\infty \quad \text{at} \quad \alpha_r = \pi/2.$$

The slope of the steepest descent path at $\alpha = \alpha_o$ is given by:

$$\frac{d\alpha_i}{d\alpha_r} = \frac{-\tan\alpha_r + (\frac{\phi}{2} - \alpha_r)\sec^2\alpha_r}{-\coth\alpha_i + \alpha_i/\sinh^2\alpha_i}$$

$$\left(\frac{d\alpha_i}{d\alpha_r}\right)_{\alpha = \alpha_o} = \frac{-\tan\alpha/2}{-0} = \infty$$

It can also be shown that the integrand in Eq. (59) vanishes on Γ_1 and Γ_2. Thus, the integral in Eq. (59) is seen to be equivalent to:

$$I(\eta) = \int_{SDP} G(\alpha,\eta)\sin\alpha\, e^{-in g(\alpha)} d\alpha \qquad (61)$$

Letting $W^2 = g(\alpha_o) - g(\alpha)$,

or $W^2 = 2\sin\alpha_o - 2\sin\alpha + 2(\alpha - \alpha_o)\cos\alpha$,

then $2W \frac{dW}{d\alpha} = -2\cos\alpha + 2\cos\alpha - 2(\alpha - \alpha_o)\sin\alpha = -2(\alpha - \alpha_o)\sin\alpha$,

and $\frac{d\alpha}{dW} = -\frac{W}{(\alpha-\alpha_o)\sin\alpha}$.

Substituting for α in terms of W, Eq. (61) could be expressed as:

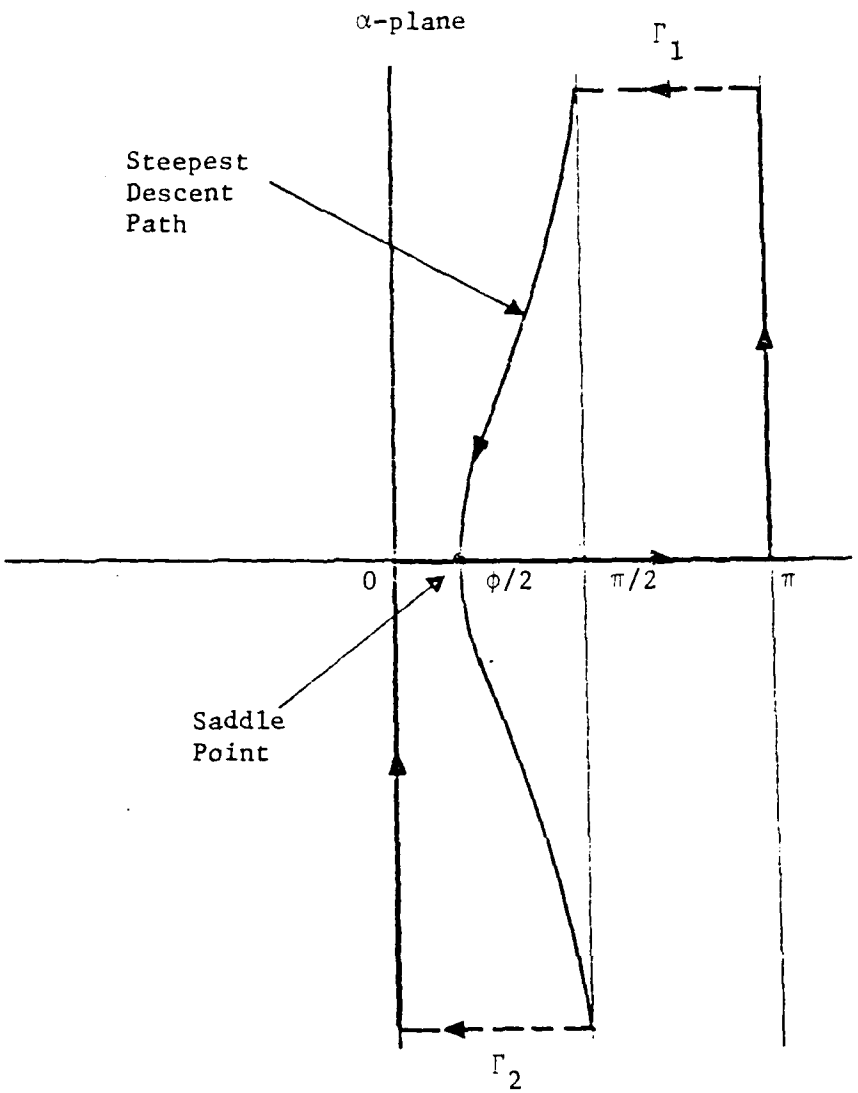

Figure 23. Steepest Descent Path for the Far Field Pressure.

$$I(\alpha) = -2 \int_{W=0}^{\infty} \left[\frac{G(\alpha,\eta)W(\alpha)}{\alpha - \alpha_o}\right]_{\alpha=\alpha(W)} e^{-i\eta[g(\alpha_o)-W^2]}\, dW$$

$$= 2e^{-2i\eta\sin\alpha_o} \int_{W=0}^{\infty} \left[\frac{G(\alpha,\eta)W(\alpha)}{\alpha - \alpha_o}\right]_{\alpha=\alpha(W)} e^{i\eta W^2} dW \qquad (62)$$

Letting $F(W,\eta) = \left[\frac{G(\alpha,\eta)W(\alpha)}{\alpha - \alpha_o}\right]_{\alpha=\alpha(W)}$,

then $F(W,\eta)$ could be expanded in a Taylor's series about $W = 0(\alpha=\alpha o)$ as follows:

$$F(W,\eta) = F(0,\eta) + \left[\frac{d}{dW} F(W,\eta)\right]_{W=0} W + \left[\frac{d^2}{dW^2} F(W,\eta)\right]_{W=0} \frac{W^2}{2!} + \cdots$$

with $\frac{d}{dW} F(W,\eta) = \frac{d}{d\alpha}\left[\frac{G(\alpha,\eta)W(\alpha)}{\alpha - \alpha o}\right] \frac{d\alpha}{dW}$

$$= \{G'(\alpha,\eta)\frac{W(\alpha)}{\alpha-\alpha o} + G(\alpha,\eta) \frac{d}{d\alpha}\left[\frac{W(\alpha)}{\alpha-\alpha_o}\right]\} \frac{d\alpha}{dW} \quad .$$

On the other hand expanding $g(\alpha)$ in a Taylor's series

$$W^2 = g(\alpha_o) - g(\alpha)$$

$$= g(\alpha_o) - [g(\alpha_o) + (\alpha-\alpha_o)g'(\alpha_o) + \frac{(\alpha-\alpha_o)^2}{2!} g''(\alpha_o) + \cdots]$$

$$= (\alpha-\alpha_o)^2 \left[-\frac{1}{2!}g''(\alpha_o) - \frac{1}{3!}g'''(\alpha_o)(\alpha-\alpha_o)\cdots\right]$$

or $$\left(\frac{W}{\alpha-\alpha_o}\right) = \left[-\frac{2}{2!} g''(\alpha_o) - \frac{1}{3!} g'''(\alpha_o)(\alpha-\alpha_o)\cdots\right]^{1/2} \qquad (63)$$

which is approximated in the limit when $W \to 0$ $(\alpha \to \alpha_o)$ by:

$$\lim_{\alpha \to \alpha_o}\left(\frac{W}{\alpha-\alpha_o}\right) = \left[-\frac{2}{2!} g''(\alpha_o)\right]^{1/2} = \left[-\frac{2\sin\alpha_o}{2}\right]^{1/2} = \sqrt{-\sin\alpha_o}$$

Differentiating Eq. (63) with respect to α one obtains:

$$\frac{d}{d\alpha}\left(\frac{W(\alpha)}{\alpha-\alpha_o}\right) = \frac{1}{2}\left[-\frac{1}{3!}g''(\alpha_o) - \frac{2}{4!}(\alpha-\alpha_o)g^{IV}(\alpha_o) + \ldots\right]\left[-\frac{1}{2!}g''(\alpha_o)\right.$$

$$\left. - \frac{1}{3!}(\alpha-\alpha_o)g'''(\alpha_o) + \ldots\right]^{-1/2} \qquad (64)$$

$$\text{or} \quad \lim_{\alpha \to \alpha_o} \frac{d}{d\alpha}\left(\frac{W(\alpha)}{\alpha-\alpha_o}\right) = \frac{1}{2}\left[-\frac{1}{6}g'''(\alpha_o)\right]\left[-\frac{1}{2}g''(\alpha_o)\right] = -\frac{\cos\alpha_o}{3\sqrt{-\sin\alpha_o}}$$

Differentiating Eq. (63) once more, then

$$\lim_{\alpha \to \alpha_o} \frac{d^2}{d\alpha^2}\left(\frac{W}{\alpha-\alpha_o}\right) = \frac{\sin\alpha_o}{\sqrt{-\sin\alpha_o}}\left(\frac{1}{4} + \frac{1}{9}\cot^2\alpha_o\right)$$

Finally an expression for first derivatives of F is given by:

$$\left[\frac{d}{dW}F(W,\eta)\right]_{W=0} = \left[G'(\alpha_o,\eta)\sqrt{-\sin\alpha_o} + G(\alpha_o,\eta)\frac{-\cos\alpha_o}{3\sqrt{-\sin\alpha_o}}\left(\frac{-1}{\sin\alpha_o}\right)\sqrt{-\sin\alpha_o}\right.$$

$$= G'(\alpha_o,\eta) + \frac{1}{3}\cot\alpha_o\, G(\alpha_o,\eta) \qquad (65)$$

Similarly

$$\frac{d^2}{dW^2}F(W,\eta) = \frac{d}{d\alpha}\left\{\left[G'(\alpha,\eta)\frac{W(\alpha)}{\alpha-\alpha_o} + G(\alpha,\eta)\frac{d}{d\alpha}\left(\frac{W(\alpha)}{\alpha-\alpha_o}\right)\right]\left(\frac{d\alpha}{dW}\right)\right\}\frac{d\alpha}{dW}$$

$$= \left\{\left[G''(\alpha,\eta)\frac{W(\alpha)}{\alpha-\alpha_o} + G'(\alpha,\eta)\frac{d}{d\alpha}\left(\frac{W}{\alpha-\alpha o}\right) + G'(\alpha,\eta)\frac{d}{d\alpha}\left(\frac{W}{\alpha-\alpha_o}\right)\right.\right.$$

$$\left.\left. + G(\alpha,\eta)\frac{d^2}{d\alpha^2}\left(\frac{W(\alpha)}{\alpha-\alpha_o}\right)\right]\frac{d\alpha}{dW} + \left(\frac{\frac{d}{dW}F(W,\eta)}{\frac{d\alpha}{dW}}\right)\frac{d}{d\alpha}\left(\frac{d\alpha}{dW}\right)\right\}\frac{d\alpha}{dW}$$

and

$$\frac{d}{d\alpha}\left(\frac{d\alpha}{dW}\right) = \frac{d}{d\alpha}\left[-\frac{W(\alpha)}{(\alpha-\alpha_o)\sin\alpha}\right] = -\frac{d}{d\alpha}\left[\frac{W(\alpha)}{\alpha-\alpha_o}\right]\frac{1}{\sin\alpha} + \frac{W(\alpha)}{\alpha-\alpha_o}\frac{\cos\alpha}{\sin^2\alpha}$$

$$\text{or } \left[\frac{d^2}{dW^2}F(W,\eta)\right]_{W=0} = \{G''(\alpha_o,\eta)\sqrt{-\sin\alpha_o} + 2G'(\alpha_o,\eta)\frac{-\cos\alpha}{3\sqrt{-\sin\alpha_o}}$$

$$+ G(\alpha_o,\eta)\left[-\frac{\sin\alpha_o}{\sqrt{-\sin\alpha_o}}\left(\frac{1}{4}+\frac{1}{9}\cot^2\alpha_o\right)\right]\}\left(-\frac{\sqrt{-\sin\alpha_o}}{\sin\alpha_o}\right)^2$$

$$+ \left[G'(\alpha_o,\eta) + \frac{1}{3}\cot\alpha_o\, G(\alpha_o,\eta)\right]\left[\frac{\cos\alpha_o}{3\sqrt{-\sin\alpha_o}}\left(\frac{1}{\sin\alpha_o}\right) + \sqrt{-\sin\alpha_o}\frac{\cos\alpha_o}{\sin^2\alpha_o}\right]$$

Finally

$$\left[\frac{d^2}{dW^2}F(W,\eta)\right]_{W=0} = \{G''(\alpha_o,\eta) - \left(\frac{1}{4}+\frac{1}{3}\cot^2\alpha_o\right)G(\alpha_o,\eta)\}\left(\frac{-1}{\sqrt{-\sin\alpha_o}}\right) \quad (66)$$

The Taylor's expansion of $F(W,\eta)$ about $W = 0$ could be written as:

$$F(W,\eta) = G(\alpha_o,\eta)\sqrt{-\sin\alpha_o} + \left[G'(\alpha_o,\eta) + \frac{\cot\alpha_o}{3}G(\alpha_o,\eta)\right]W$$

$$+ \left[G''(\alpha_o,\eta) - \left(\frac{1}{4}+\frac{1}{3}\cot^2\alpha_o\right)G(\alpha_o,\eta)\right]\left(\frac{-1}{\sqrt{-\sin\alpha_o}}\right)\frac{W^2}{2!} + \cdots \quad (67)$$

using the relationship

$$\int_{-\infty}^{+\infty} e^{-\frac{1}{2}\rho y^2} y^{2n}\, dy = \sqrt{2\pi/\rho}\,\frac{(2n)!}{\rho^n \Gamma(n+1)}$$

the integral over the steepest descent path becomes:

$$I(\alpha) \sim -e^{-2in\sin\alpha_o} \int_{-\infty}^{+\infty} F(W,n)\, e^{inW^2}\, dW$$

$$= -e^{-2in\sin\alpha_o} \{G(\alpha_o,n)\sqrt{-\sin\alpha_o}\,(\sqrt{\pi i/n}) + [G''(\alpha_o,n) -$$

$$(\tfrac{1}{4} + \tfrac{1}{3}\cot^2\alpha_o)G(\alpha_o,n)](-\frac{1}{\sqrt{-\sin\alpha_o}})(i/n\sqrt{\pi i/n}) + \ldots \qquad (68)$$

The first term of the asymptotic series in Eq. (68) represents the major contribution to the geometrically reflected field

$$I(\alpha) \sim -G(\alpha_o,n)\sqrt{\sin\alpha_o}\sqrt{\pi/n}\, e^{-i(\pi/4 + 2n\sin\alpha_o)} \qquad (69)$$

Substituting Eq. (69) into Eq. (58), then the geometric-optic reflected pulse is given by:

$$p^G(r,t,\phi) = -\sqrt{\frac{2\sin\alpha_o}{r/a}} \int_{-\infty}^{+\infty} G(\alpha_o,n)e^{-in(\Omega + 2\sin\alpha_o)}dn \qquad (70)$$

The function $G(\alpha_o,n)$ is of the order $O(n)$. In order to apply the reside theorem to the integral in Eq. (70), it is necessary to write $G(\alpha_o,n)$ as:

$$G(\alpha_o,n) = -1 + H(\alpha_o,n) \qquad (71)$$

where the function $H(\alpha_o,n)$ is of order $O(1/n)$ for $|n| \gg 1$. From Eq. (55)

$$H(\alpha_o,n) = \frac{(F_1 + \bar{F}_1) + i\bar{Z}(n)(F_2 + \bar{F}_2)}{F_1 + i\bar{Z}(n)\, F_2} \qquad (72)$$

and for the special case $|\gamma|>>1$, it can be seen that

$$H(\alpha_o,\eta) = 2\,\frac{L(\alpha_o,\eta) - i\bar{Z}(\eta)O(\alpha_o,\eta)\sin\alpha_o}{[L(\alpha_o,\eta) - iM(\alpha_o,\eta)] + i\bar{Z}(\eta)[iN(\alpha_o,\eta) - O(\alpha_o,\eta)]\sin\alpha_o} \tag{73}$$

Substituting the expressions for L,M,N and O in the above equation and letting $\gamma = \eta\cos\alpha_o$, it can easily be seen that $H(\alpha_o,\eta)$ is of $1/\eta$. Pulling out the factor (-1) from $G(\alpha_o,\eta)$ corresponds to separating the major contribution due to rigid boundary condition because:

$$e^{-2i\psi}\cdot G(\alpha_o,\eta) = \left[\frac{H_\gamma^{(2)}(\eta) + i\bar{Z}(\eta)H_\gamma'^{(2)}(\eta)}{H_\gamma^{(1)}(\eta) + i\bar{Z}(\eta)H_\gamma'^{(1)}(\eta)} - \frac{H_\gamma'^{(2)}(\eta)}{H_\gamma'^{(1)}(\eta)}\right] + \frac{H_\gamma'^{(2)}(\eta)}{H_\gamma'^{(1)}(\eta)}$$

$$= \frac{-\bar{W}[H_\gamma^{(1)}(\eta),H_\gamma^{(2)}(\eta)]}{[H_\gamma^{(1)}(\eta) + i\bar{Z}(\eta)H_\gamma'^{(1)}(\eta)]H_\gamma'^{(1)}(\eta)} + \frac{H_\gamma'^{(2)}(\eta)}{H_\gamma'^{(1)}(\eta)}$$

$$= \frac{4i/\pi\eta}{[H_\gamma^{(1)}(\eta) + i\bar{Z}(\eta)H_\gamma'^{(1)}(\eta)]H_\gamma'^{(1)}(\eta)} + \frac{H_\gamma'^{(2)}(\eta)}{H_\gamma'^{(1)}(\eta)}$$

where $\bar{W}$ is the Wronskian and $\gamma = \eta\cos\alpha_o$. The first term on the right is of order $1/\eta^2$ for $|\eta|>>1$. The second term corresponds to reflection from rigid cylinder and can be rewritten as:

$$\frac{H_\gamma'^{(2)}(\eta)}{H_\gamma'^{(1)}(\eta)} \sim \frac{O(\alpha_o,\eta) + iN(\alpha_o,\eta)}{O(\alpha_o,\eta) - iN(\alpha_o,\eta)} \; e^{-2i\psi(\alpha_o,\eta)}$$

$$= [-1 + 2 \frac{O(\alpha_o,\eta)}{O(\alpha_o,\eta) - iN(\alpha_o,\eta)}] \; e^{-2i\psi(\alpha_o,\eta)}$$

The second term in the bracket can be recognized to be of the order $(1/\eta)$ and hence the term (-1) represents the major contribution to the reflected pressure due to a rigid cylinder. Finally from Eqs. (70) and (71) one can write an expression for the geometric optic terms as:

$$p^G(r,t,\phi) \sim -\sqrt{\frac{2\sin\alpha_o}{r/a}} \int_{-\infty}^{+\infty} [-1 + H(\alpha_o,\eta)] e^{-i\eta(\Omega + 2\sin\alpha_o)} \, d\eta$$

$$= \sqrt{\frac{2\sin\alpha_o}{r/a}} \left\{ \int_{-\infty}^{+\infty} e^{-i\eta(\frac{ct-r}{a} + 2\sin\alpha_o)} \, d\eta - \int_{-\infty}^{+\infty} H(\alpha_o,\eta) \right.$$

$$\left. e^{-i\eta(\Omega + 2\sin\alpha_o)} \, d\eta \right. \qquad (74)$$

The first integral can be recognized as a delta Dirac function. The second integral can be computed for $(\Omega + 2\sin\alpha_o) > 0$ by closing the path of integration along a semi-circle of radius infinity in the lower half of the complex η-plane. The poles of the integrand are the roots of the denominator in Eq. (72) which are the same as the roots of transcendental equation:

$$H_\gamma^{(1)}(\eta) + i\bar{Z}(\eta)H_\gamma'^{(1)}(\eta) = 0, \quad \text{for } \gamma = \eta\cos\alpha_o \tag{75}$$

Let η_n be the complex roots of Eq. (75) in the lower half plane. Then Eq. (74) can be written as:

$$p^G(r,t,\phi) \sim \sqrt{\frac{2\sin\phi/2}{r/a}}\{a\delta(2a\sin\tfrac{\phi}{2} + ct-r) + 2\pi i \sum_n \ell_n e^{\frac{-i\eta_n}{a}(2\sin\phi/2+ct-r)} \cdot u(\frac{ct-r}{a} + 2\sin\phi/2)] \tag{76}$$

where u(t) is a unit step function and ℓ_n are defined by

$$\ell_n = \frac{(F_1 + \bar{F}_1) + i\bar{Z}(\eta)(F_2 + \bar{F}_2)}{\frac{d}{d\eta}\ [F_1 + i\bar{Z}(\eta)F_2]} \qquad \text{at } \eta = \eta_n \tag{77}$$

To express the residue ℓ_n in terms of cylindrical functions one may write

$$F_1 + \bar{F}_1 = (J_\gamma + iY_\gamma)e^{-i\psi} + (J_\gamma - iY_\gamma)e^{i\psi} ,$$

$$= 2(J_\gamma\cos\psi + Y_\gamma\sin\psi) ,$$

$$F_2 + \bar{F}_2 = (J_\gamma' + iY_\gamma')e^{-i\psi} + (J_\gamma' - iY_\gamma')e^{i\psi} ,$$

$$= 2(J_\gamma'\cos\psi + Y_\gamma'\sin\psi) ,$$

and

$$R = \frac{d}{d\eta}\ [F_1 + i\bar{Z}F_2]_{\eta_n} = \frac{d}{d\eta}\ \{[H_\gamma^{(1)}(\eta) + i\bar{Z}(\eta)H_\gamma'^{(1)}(\eta)]e^{-i\psi(\alpha_o,\eta)}\}_{\gamma = \eta\cos\alpha_o \quad \eta_n} ,$$

$$= \frac{d}{d\eta}\ \{[H_\gamma^{(1)}(\eta) + i\bar{Z}(\eta)H_\gamma'^{(1)}(\eta)]\}_{\eta = \eta_n} e^{-i\psi(\alpha_o,\eta_n)} .$$

$$\gamma = \eta\cos\alpha_o$$

Since the order of the Hankel function is dependent on η, then the differentiation should be applied to both the argument and the order. Let a prime represents diffrentiation with respect to the argument and a dot stands for differentiation with respect to the order. Using the chain rule of differentiation, then:

$$R = \{H_\gamma^{'(1)} + i\bar{Z}' H_\gamma^{'(1)} + i\bar{Z}\, H_\gamma^{''(1)} + (H_\gamma^{\cdot(1)} + \bar{i}Z\, H_\gamma^{\cdot'(1)})\frac{d\gamma}{d\eta}\}e^{-i\psi(\alpha_o,\eta_n)}_{\eta = \eta_n}$$

$$= \{(1 + i\bar{Z}')H_\gamma^{'(1)} + i\bar{Z}\, H_\gamma^{''(1)} + (H_\gamma^{\cdot(1)} + i\bar{Z}\, H_\gamma^{\cdot'(1)})\cos\alpha_o\}\, e^{-i\psi(\alpha_o,\eta_n)}_{\eta = \eta_n}$$

Using the identities:

$$H_\gamma^{''(1)}(\eta) = -\frac{1}{\eta}H_\gamma^{'(1)}(\eta) + (\frac{\gamma^2}{\eta^2} - 1)H_\gamma^{(1)}(\eta) = -\frac{1}{\eta}\, H_\gamma^{'(1)}(\eta) - \sin^2\alpha_o H_\gamma^{(1)}(\eta)$$

$$H_\gamma^{'(1)}(\eta) = H_{\gamma-1}^{(1)}(\eta) - \frac{\gamma}{\eta}\, H^{(1)}(\eta)$$

or:

$$H_\gamma^{\cdot'(1)}(\eta) = H_{\gamma-1}^{\cdot(1)}(\eta) - \frac{1}{\eta}\, H_\gamma^{(1)}(\eta) - \frac{\gamma}{\eta}\, H_\gamma^{\cdot(1)}(\eta)$$

then R becomes:

$$R = \{(1 + i\bar{Z}' - \frac{i\bar{Z}}{\eta})H_\gamma^{'(1)} - i\bar{Z}\sin^2\alpha_o H_\gamma^{(1)} + \cos\alpha_o\, [(1 - \frac{\gamma}{\eta} \cdot i\bar{Z}(\eta))H_\gamma^{\cdot(1)}$$

$$+ i\bar{Z}(\eta)(H_{\gamma-1}^{\cdot(1)} - \frac{1}{\eta}\, H_\gamma^{(1)})]\}\, e^{-i\psi(\alpha_o,\eta_n)}_{\eta = \eta_n}$$

Substituting for $H_\gamma^{'(1)}(\eta_n) = -\frac{1}{i\bar{Z}(\eta_n)} H_\gamma^{(1)}(\eta_n)$ for $\gamma = \eta_n\cos\alpha_o$ then R can be expressed by:

$$R = \{[\frac{i}{\bar{Z}(\eta_n)} - \frac{\bar{Z}'}{\bar{Z}} + \frac{1}{\eta_n} - i\bar{Z}(\sin^2\alpha_o + \frac{\cos\alpha_o}{\eta_n})]H_\gamma^{(1)}(\eta_n) + \cos\alpha_o(1-i\cos\alpha_o\bar{Z})$$

$$\cdot H_\gamma^{\cdot(1)}(\eta_n) + i\bar{Z}(\eta_n)\cos\alpha_o\, H_{\gamma-1}^{\cdot(1)}\} \quad e^{-i\psi(\alpha_o,\eta_n)}$$

or

$$R = \{T(\alpha_o,\eta_n)H_\gamma^{(1)}(\eta_n) + [1-i\bar{Z}(\eta_n)\cos\alpha_o]\cos\alpha_o\, H_\gamma^{\cdot(1)}(\eta_n)$$

$$+ i\bar{Z}(\eta_n)\cos\alpha_o\, H_{\gamma-1}^{\cdot(1)}(\eta_n)\} \cdot e^{-i\psi(\alpha_o,\eta_n)} \qquad (78)$$

$$\gamma = \eta\cos\alpha_o$$

where

$$T(\alpha_o,\eta_n) = \frac{1}{\bar{Z}(\eta_n)}[i - \bar{Z}'(\eta_o) - i\bar{Z}(\eta_n)[\sin^2\alpha_o + \frac{\cos\alpha_o}{\eta_n}] + \frac{1}{\eta_n} \quad .$$

From Eq. (77), the residue ℓ_n can be expressed as:

$$\ell_n = \frac{2}{R(\alpha_o,\eta_n)} \{[J_\gamma(\eta)\cos\psi + Y_\gamma(\eta)\sin\psi] + i\bar{Z}(\eta)[J_\gamma'(\eta)\cos\psi + Y'(\eta)\sin\psi]\}_{\eta=\eta_n} \qquad (79)$$

The derivative of the Hankel function with respect to its order which is needed in computation of Eq. (78) can be obtained from:

$$\frac{\partial}{\partial\gamma} H_\gamma^{(1)}(x) = H_\gamma^{\cdot(1)}(x) = \left[(1+\cot\pi\gamma)\ell n(\frac{x}{2}) - \frac{\pi}{\sin^2\pi\gamma}\right] J_\gamma(x)$$

$$+ \frac{1}{\sin\gamma\pi}\left[\ell n(\frac{x}{2}) + \pi\cot\gamma\pi\right] J_{-\gamma}(x)$$

$$- (1+\cot\gamma\pi)(\frac{x}{2}) \sum_{k=0}^{\infty} (-1)^k \frac{\bar{\psi}(\gamma + k + 1)}{\Gamma(\gamma + k + 1)} \frac{(\frac{x^2}{4})^k}{k!}$$

$$- \operatorname{cosc}\gamma\pi(\frac{x}{2})^{-\gamma} \sum_{k=0}^{\infty} (-1)^k \frac{\bar{\psi}(-\gamma + k + 1)}{\Gamma(-\gamma + k + 1)} \frac{(\frac{x^2}{4})^k}{k!} \qquad (80)$$

The functions $\bar{\psi}$ in Eq. (80) could be obtained from its asymptotic representation [18]:

$$\bar{\psi}(Z) = (\ell nZ - \frac{1}{2Z}) - \sum_{n=1}^{\infty} \frac{B_{2n}}{2nZ^{2n}} \qquad (81)$$

where B_n are Bernouli's numbers [18]. The following asymptotic series for $\bar{\psi}(Z)$ can be used for large values of $|Z|$:

$$\bar{\psi}(Z) = (\ell nZ - \frac{1}{2Z}) - \left(\frac{1}{12Z^2} - \frac{1}{120Z^4} + \frac{1}{252Z^6} - \frac{1}{240Z^8} + \ldots\right)$$

The following relations could then be used to compute $\bar{\psi}(Z)$ for any values of Z

$$\bar{\psi}(Z-1) = \bar{\psi}(Z) - \frac{1}{Z-1}$$

$$\bar{\psi}(-Z) = \bar{\psi}(Z) + \frac{1}{Z} + \pi\cot\pi Z$$

Finally, multiplying p^G by the factor $-P_o\xi/4\pi$, which was dropped out earlier, one obtains:

$$p^G(r,t,\phi) \simeq -\frac{P_o}{4\pi}\sqrt{\frac{2\sin\phi/2}{r/a}}\{c\delta(2a\sin\tfrac{\phi}{2} + ct-r) + 2\pi i(\tfrac{c}{a})\sum_n \ell_n e^{-i\frac{\eta_n}{a}(2a\sin\frac{\phi}{2} + ct-r)} u(\Omega + 2\sin\tfrac{\phi}{2})\}\ . \tag{82}$$

Given an incident plane wave $F_{in}(t)$, one may apply Duhamel's integral on Eq. (82) to compute the geometrically reflected field for any given incident plane pulse. For a cosine pulse

$$F_{inc}(t) = \cos\omega t[H(t) - H(t-T)]. \tag{83}$$

It should be noted that the time $t_1=(a/c)(r/a - 2\sin\phi/2)$ corresponds to arrival of the reflected pulse at the point (r,ϕ). Let $\bar{\omega} = \omega/\omega_o$ then for $t_1 < t < t_1 + T$

$$F^G(r,t,\phi) = \int_o^t p^G(\tau)h(t-\tau)d\tau \tag{84}$$

The first term of Eq. (82) when substituted in Eq. (84) gives:

$$I_1 = -\frac{P_o}{4\pi}\sqrt{\frac{2\sin\phi/2}{r/a}}\int_o^t c\cos\omega\tau\,\delta(2a\sin\tfrac{\phi}{2} + ct - c\tau - r)d\tau$$

$$= -\frac{P_o}{4\pi}\sqrt{\frac{2\sin\phi/2}{r/a}}\cos[(\tfrac{\bar{\omega}}{\bar{\lambda}})(2\sin\tfrac{\phi}{2} + \tfrac{ct-r}{a})]$$

This term would be equal to zero for $t > t_1 + T$. The 2nd term of Eq. (82) which is of the form $h(r,t,\phi)u(t-t_1)$ when substituted on Eq. (84) leads to:

$$I_2 = \int_o^t \cos\omega\tau h(r,t-\tau,\phi)[u(\tau)-u(\tau-T)]u(t-\tau-t_1)d\tau$$

$$= \int_o^{t-t_1} \cos\omega\tau h(r,t-\tau,\phi)d\tau = \int_{t_1}^{t} \cos\omega(t-\tau)h(r,\tau,\phi)d\tau$$

$$\underline{\text{if}}\ t \leq t_1 + T$$

$$= \int_o^{T} \cos\omega\tau h(r,t-\tau,\phi)d\tau = \int_{t-T}^{t} \cos\omega(t-\tau)h(r,\tau,\phi)d\tau$$

$$\underline{\text{if}}\ t > t_1 + T$$

Substituting for $h(r,t,\phi)$ one obtains expressions for I_2 during the time interval $t \leq t_1 + T$ as:

$$I_2 = -\frac{P_o}{4\pi}\sqrt{\frac{2\sin\phi/2}{r/a}}\ (2\pi i)\left(\frac{c}{a}\right)\ \sum_n \ell_n\, e^{-i\eta_n\left(\frac{ct-r}{a} + 2\sin\frac{\phi}{2}\right)}$$

$$\int_o^{\sigma} e^{i\eta_n\tau}\cos\left(\frac{\omega}{\lambda}\tau\right)\frac{d\tau}{\left(\frac{c}{a}\right)}$$

$$= -\frac{P_o}{4\pi}\sqrt{\frac{2\sin\phi/2}{r/a}}\ (2\pi i)\sum_n \frac{\ell_n}{\left(\frac{\omega}{\lambda}\right)^2 - \eta_n^2}\left\{i\eta_n\cos\left(\frac{\omega}{\lambda}\sigma\right) + \frac{\omega}{\lambda}\sin\left(\frac{\omega}{\lambda}\sigma\right)\right.$$

$$\left. -i\eta_n\, e^{-i\eta_n\sigma}\right\}$$

The geometrically reflected pulse can finally be expressed as:

$$F^G(r,t,\phi) = -\frac{P_o}{4\pi}\sqrt{\frac{2\sin\phi/2}{r/a}}\left\{\cos\left(\frac{\omega}{\lambda}\sigma\right) + 2\pi i\sum_n \ell_n\left(\frac{1}{\left(\frac{\omega}{\lambda}\right)^2 - \eta_n^2}\right)\left[i\eta_n\cos\left(\frac{\omega}{\lambda}\sigma\right)\right.\right.$$

$$\left.\left. + \left(\frac{\omega}{\lambda}\right)\sin\left(\frac{\omega}{\lambda}\sigma\right) - i\eta_n\, e^{-i\eta_n\sigma}\right]\right\}, \qquad (85)$$

where $\sigma = ct-r/a + 2\sin\phi/2$. It can be observed that in the case of $\bar{\omega}/\bar{\lambda} = \eta_n$, the corresponding term in the series summation would be indeterminate which nevertheless has a finite limit.

For $t > t_1 + T$, the reflected pressure can be obtained as:

$$F^G(r,t,\phi) = -\frac{P_o}{4\pi}\sqrt{\frac{2\sin\phi/2}{r/a}}\,(2\pi i)\sum_n \frac{\ell_n}{(\frac{\bar{\omega}}{\bar{\lambda}})^2 - \eta_n^2}\{i\eta_n\cos\bar{\omega}T + \frac{\bar{\omega}}{\bar{\lambda}}\sin\bar{\omega}T]$$

$$e^{i\eta_n cT/a} - i\eta_n\} e^{-i\eta_n\sigma} \qquad (86)$$

The factor $e^{-i\eta_n\sigma}$ represents an exponentially decaying function of time in this equation.

It should be observed that ℓ_n in the above equations is a function of both the radius of the cylinder (because of the factor $\bar{\lambda} = (c/a)/\omega_c$ in the expression of the impedance function) and the observation angle ($\gamma = \pi\cos\phi/2$). For any values of the dimensionless parameter $\bar{\lambda}$ and the observation angle ϕ, Eq. (75) should be solved numerically for the complex value of η_n in the lower half-plane. Eqs. (78)-(81) are then used to compute the corresponding values of ℓ_n which are then substituted in Eqs. (85) and (86) to compute the geometrically reflected pressure as a function of time and observation point coordinates. On the other hand, changing the parameter $\bar{\omega} = \omega/\omega_o$ in Eq. (85) will demonstrate the dependence of the scattered pressure on the characteristics of the impedance boundary as was discussed for the case of a plane boundary.

3.6 Creeping Waves

For an observer in the farfield, the creeping wave part of the scattered pressure was shown in Eq. (53) to be:

$$p^c(r,t,\phi)= \sum_{\lambda=\pm} \sum_{s=0}^{\infty} \int_{-\infty}^{+\infty}\int_{-\infty}^{+\infty} e^{i\gamma\pi/2}\, e^{i\gamma(\phi_\lambda'' +2\pi s)} H_\gamma^{(1)}(\eta\tfrac{r}{a}) B_\gamma(\eta) e^{-inct/a}\, d\gamma d\eta$$

where the II has been dropped from p^c_{II}, and

$$\phi_+'' = \phi \quad \text{and} \quad \phi_-'' = 2\pi - \phi \ .$$

The integration on γ can be carried out using the residue theorem and closing the contour of integration along a semi-circle of radius ∞, in the upper half of the complex γ-plane.

$$p^c(r,t,\phi) = \sum_{\lambda=\pm} \sum_{s=0}^{\infty} \sum_{\ell=0}^{\infty} \int_{\eta=-\infty}^{+\infty} e^{i\gamma_\ell\pi/2} \cdot e^{i\gamma_\ell(\phi_\lambda'' +2\pi s)} H_{\gamma_\ell}^{(1)}(\eta\tfrac{r}{a}) K_{\gamma_\ell}(\eta)\, e^{-inct/a}\, d\eta \qquad (87)$$

where γ_ℓ ($\ell = 0,1,2,\ldots$) are the roots of

$$H_\gamma^{(1)}(\eta) + i\bar{Z}(\eta) H_\gamma'^{(1)}(\eta) = 0 \qquad (88)$$

in the upper half of complex γ-plane and

$$K_{\gamma_\ell}(\eta) = \frac{H_\gamma^{(2)}(\eta) + i\bar{Z}(\eta) H_\gamma'^{(2)}(\eta)}{\frac{d}{d\gamma}\left[H_\gamma^{(1)}(\eta) + i\bar{Z}(\eta) H_\gamma'^{(1)}(\eta)\right]} \quad \text{at } \gamma = \gamma_\ell \qquad (89)$$

which can be written in the form:

$$K_{\gamma_\ell}(\eta) = \frac{R_\gamma(\eta)}{\frac{d}{d\gamma} Q_\gamma(\eta)} \quad \text{at } \gamma = \gamma_\ell \qquad (90)$$

One may express the Hankel function in terms of a function related to Airy's function as follows:

$$H_\gamma^{(1)}(\rho) \sim (\frac{2}{\pi})(\frac{6}{\rho})^{1/3} e^{-i\pi/3} A(q)$$

$$q = (\frac{6}{\rho})^{1/3} e^{-\frac{i\pi}{3}} (\gamma-\rho) \qquad (91)$$

$$|\rho| >> 1$$

where A(q) is related to the Airy's function and is defined by [18]:

$$A(q) = \frac{1}{2} \int_{-\infty}^{+\infty} e^{i(q\tau-\tau^3)} d\tau = \int_{-\infty}^{+\infty} \cos(q\tau-\tau^3) d\tau \ , \qquad (92)$$

and

$$A''(q) + \frac{q}{3} A(q) = 0. \qquad (93)$$

Differentiating Eq. (91) with respect to the argument one obtains:

$$\frac{d}{d\rho} H_\gamma^{(1)}(\rho) = H_\gamma'^{(1)}(\rho) \sim - (\frac{2}{\pi})(\frac{6}{\rho})^{2/3} e^{-\frac{2\pi i}{3}} A'(q) \qquad (94)$$

and differentiating Eq. (91) with respect to order one obtains:

$$\frac{d}{d\gamma} H_\gamma^{(1)}(\rho) \sim (\frac{2}{\pi})(\frac{6}{\rho})^{2/3} e^{-\frac{2\pi i}{3}} A'(q) = - H_\gamma'^{(1)}(\rho) \ . \qquad (95)$$

In addition, differentiating $H_\gamma'^{(1)}(\rho)$ in Eq. (94) with respect to γ one obtains:

$$\frac{d}{d\gamma} H_\gamma'^{(1)}(\rho) \sim (\frac{2}{\pi})(\frac{6}{\rho}) A''(q) \ .$$

Substituting Eqs. (91) through (95) into Eq. (90), expressions for the functions $R_\nu(\eta)$ and $Q_\nu(\eta)$ are obtained as follows:

$$\frac{dQ_{\gamma_\ell}(\eta)}{d\gamma_\ell} \sim \frac{d}{d\gamma}\left[H_\gamma^{(1)}(\eta) + i\bar{Z}(\eta)\, H_\gamma^{'(1)}(\eta)\right]_{\gamma=\gamma_\ell} ,$$

$$= \{(\frac{2}{\pi})(\frac{6}{\eta})^{2/3} e^{-\frac{2\pi i}{3}} A'(q) + i\bar{Z}(\eta)(\frac{2}{\pi})(\frac{6}{\eta})A''(q)\}_{\gamma=\gamma_\ell} ,$$

$$= (\frac{2}{\pi})(\frac{6}{\eta})A'(q_\ell)\{(\frac{6}{\eta})^{-1/3} e^{-\frac{2\pi i}{3}} + i\bar{Z}(\eta)(-\frac{q}{3})\frac{A(q)}{A'(q)}\}_{\gamma=\gamma_\ell} .$$

On the other hand using Eq. (88), one can simplify this expression further, i.e.,

$$(\frac{2}{\pi})(\frac{6}{\eta})^{1/3} e^{-\frac{i\pi}{3}} A(q_\ell) + i\bar{Z}(\eta)(-\frac{2}{\pi})(\frac{6}{\eta})^{2/3} e^{-\frac{2\pi i}{3}} A'(q_\ell) = 0$$

or $$\frac{A(q_\ell)}{A'(q_\ell)} = Z(\eta)(\frac{6}{\eta})^{1/3} e^{\pi i/6}$$

subsituting for $A(q_\ell)/A'(q_\ell)$ in the expression for $dQ_{\gamma_\ell}(\eta)/d\gamma_\ell$ results in:

$$\frac{dQ_{\gamma_\ell}(\eta)}{d\gamma_\ell} \sim (\frac{2}{\pi})(\frac{6}{\eta})A'(q_\ell)\,\chi(\eta) , \tag{96}$$

where $$\chi(\eta) = (\frac{6}{\eta})^{-1/3} e^{-\frac{2\pi i}{3}} - (\frac{q_\ell}{3})\bar{Z}(\eta)(\frac{6}{\eta})^{1/3} e^{\frac{2\pi i}{3}} , \tag{97}$$

and $$q_\ell = (\frac{6}{\eta})^{1/3}(\gamma_\ell - \eta)e^{-i\pi/3} . \tag{98}$$

Similarly the numerator of Eq. (90) can be written as:

$$R_{\gamma_\ell}(\eta) = [H_\gamma^{(2)}(\eta) + i\bar{Z}(\eta)\, H_\gamma'^{(2)}(\eta)]_{\gamma=\gamma_\ell} = H_\gamma^{(2)}(\eta)\{1 + i\bar{Z}(\eta)\frac{H_\gamma'^{(2)}(\eta)}{H_\gamma^{(2)}(\eta)}\}, \gamma=\gamma_\ell \tag{99}$$

Using the definition of the Wronskian

$$\bar{W}(H_\gamma^{(1)}(\eta), H_\gamma^{(2)}(\eta)) = -\frac{4i}{\pi\eta} \quad , \tag{100}$$

and combining Eqs. (88), (99) and (100) the denominator becomes:

$$R_{\gamma_\ell}(\eta) = \frac{4\bar{Z}(\eta)}{\pi\eta} \quad \frac{1}{H_{\gamma_\ell}^{(1)}(\eta)}$$

Substituting for $H_\gamma^{(1)}(\eta)$ in terms of Airy's function one gets:

$$R_{\gamma_\ell}(\eta) \sim \frac{4\bar{Z}(\eta)}{\pi\eta} \quad \frac{1}{(\frac{2}{\pi})(\frac{6}{\eta})^{1/3} e^{-\frac{i\pi}{3}} A(q_\ell)} \tag{101}$$

Replacing $R_{\gamma_\ell}(\eta)$ and $dQ_{\gamma_\ell}(\eta)/d\gamma_\ell$ in Eq. (96) and (101) into Eq. (90), then

$$K_{\gamma_\ell}(\eta) \sim \frac{\bar{Z}(\eta)\, e^{i\pi/3}}{(\frac{6}{\pi})(\frac{6}{\eta})^{1/3} A(q_\ell)A'(q_\ell)\chi(\eta)} \quad ,$$

which may be put in final form by substituting for $A'(q_\ell)$, resulting in an expression for K_{γ_ℓ} in terms of Airy function:

$$K_{\gamma_\ell}(\eta) \sim [\frac{\bar{Z}(\eta)}{A(q_\ell)}]^2 \quad \frac{e^{i\pi/2}}{(\frac{6}{\eta})\,\chi(\eta)} \tag{102}$$

Substituting the asymptotic approximation of Hankel function, valid in the farfield:

$$H^{(1)}_{\gamma_\ell}(\eta\frac{r}{a}) \sim \sqrt{\frac{2}{\pi\frac{r}{a}}}\; e^{i(\eta\frac{r}{a} - \gamma_\ell \frac{\pi}{2} - \frac{\pi}{4})} \qquad \frac{r}{a} >> 1$$

then Eq. (87) for the creeping wave part of the scattered pressure can be written as:

$$p^c(r,t,\phi) \sim \sum_{\lambda=\pm} \sum_{s=0}^{\infty} \sum_{\ell=0}^{\infty} \sqrt{\frac{2}{\pi r/a}}\; e^{-\frac{i\pi}{4}} \int_{-\infty}^{+\infty} \frac{K_{\gamma_\ell}(\eta)}{\sqrt{\eta}}\; e^{if(\eta)} d\eta \,, \tag{103}$$

where $f(\eta) = \gamma_\ell(\phi_\lambda'' + 2\pi s) - \Omega\eta, \quad \Omega = \frac{ct-r}{a}$. (104)

The integral in Eq. (103) can be computed by the stationary phase technique but first it is necessary to express γ_ℓ as a function of η. For that one can use the following approximate expression for Hankel function when $|\rho| >> 1$

$$H^{(1)}_{\gamma}(\rho) \sim \sqrt{\frac{2}{3}}\; \frac{e^{-i\pi/3}}{\rho^{1/2}}\, (\gamma-\rho)^{1/2}\, H^{(1)}_{1/3}\{\tfrac{1}{3}(-2\tau)^{3/2}\} \,, \tag{105}$$

where $\tau = \frac{\gamma-\rho}{\rho^{1/3}}$, $|\frac{\gamma-\rho}{\rho}| << 1$,

$$H^{(1)}_{1/3}(\eta) = 2i(\frac{\sqrt{3}}{\bar{\xi}^{1/3}})\, Ai(\xi\, e^{-\pi i/3}),$$

$$A(q) = \frac{\pi}{3^{1/3}}\, Ai(-\frac{q}{3^{1/3}}) \,, \quad \bar{\xi} = (\tfrac{3}{2}\eta)^{2/3} \,,$$

and Ai(x) is the Airy function [18]. The asymptotic expression for $H'^{(1)}_{\gamma}(\rho)$ can also be expressed as:

$$H'^{(1)}_{\gamma}(\rho) \sim \frac{2}{\sqrt{3}} \frac{e^{i\pi/3}}{\rho} (\gamma-\rho)\, e^{-i\pi/2}\, H^{(1)}_{2/3}\{-\tfrac{1}{3}(-2\tau)^{3/2}\} \qquad (106)$$

Substituting Eqs. (105) and (106) in Eq. (88) results in a transcendental equation on γ:

$$\frac{e^{-\frac{\pi i}{3}} H^{(1)}_{2/3}\{\frac{1}{3}(-2\tau_s)^{3/2}\}}{H^{(1)}_{1/3}\{\frac{1}{3}(-2\tau_s)^{3/2}\}} = -\frac{1}{\delta\sqrt{-2\tau_s}} \qquad (107)$$

where $\delta = \dfrac{\bar{Z}(\rho)}{i\rho^{1/3}}$ (108)

The roots of Eq. (107) can be expressed as [19]

$$\tau_\ell = \tau_{\ell o} - \delta - \frac{2}{3}\tau_{\ell o}\delta^3 + \frac{1}{2}\delta^4 - \frac{4}{5}\tau^2_{\ell o}\delta^5 + \ldots \quad \text{if } |\delta| \ll 1 \qquad (109)$$

and

$$\tau_\ell = \tau_{\ell\infty} - \frac{1}{2\tau_{\ell\infty}}\frac{1}{\delta} - \frac{1}{8\tau^3_{\ell\infty}}\frac{1}{\delta^2} + \ldots \quad \text{if } |\delta| \gg 1 \qquad (110)$$

where: $\tau_{\ell o} = \frac{1}{2}(3x_\ell)^{2/3} e^{i\pi/3}$

x_ℓ are the roots of $J_{1/3}(x) + J_{-1/3}(x) = 0$

and $\tau_{\ell\infty} = \frac{1}{2}(3x_\ell)^{2/3} e^{i\pi/3}$

x_ℓ are the roots of $J_{2/3}(x) - J_{-2/3}(x) = 0$

The values of the first few roots of the above equations are listed in Table 1.

Table 1

$\tau_{\ell 0} = u_{\ell 0}\, e^{i\pi/3}$	$\tau_{\ell \infty} = u_{\ell \infty}\, e^{i\pi/3}$
$u_{0,0} = 1.856$	$u_{0,\infty} = .808$
$u_{1,0} = 3.245$	$u_{1,\infty} = 2.577$
$u_{2,0} = 4.382$	$u_{2,\infty} = 3.824$
$u_{3,0} = 5.386$	$u_{3,\infty} = 4.892$
$u_{4,0} = 6.305$	$u_{4,\infty} = 5.851$
$u_{6,0} = 7.161$	$u_{6,\infty} = 6.737$

Another form of Eq. (107) in terms of Airy's function can be stated as:

$$\frac{\sqrt[3]{6}\; e^{-\pi i/3}\; A'(q)}{A(q)} = -\frac{1}{\delta} \quad . \tag{111}$$

The roots of this equation can be expressed in terms of τ_ℓ as $q_\ell = 6^{1/3}\, e^{-\pi i/3}\, \tau_\ell$ and τ_ℓ is given by Eq. (109) or Eq. (110) depending on the magnitude of the factor $\delta = \overline{Z}(\rho)/i\rho^{1/3}$.

Substituting the impedance function $\bar{Z}(\rho)$ into Eq. (108) it can be observed that for large value of ρ

$$|\delta| \sim a_1 \bar{\lambda}\rho^{2/3} >> 1$$

indicating that Eq. (110) is the proper relation describing the roots of Eq. (88). Finally substituting for τ_ℓ in the right hand-side of Eq. (110) one gets

$$\frac{\gamma-\rho}{\rho^{1/3}} = \tau_{\ell\infty} - \frac{1}{2\tau_{\ell\infty}} \frac{1}{\delta} + \ldots \tag{112}$$

Using only the first term of the above series, a relation between γ_ℓ and η can be written as

$$\gamma_\ell(\eta) \sim \eta + \eta^{1/3} \tau_{\ell,\infty} \qquad |\eta| >> 1 \tag{113}$$

which can be substituted in Eq. (104) resulting in an expression for the exponential term $f(\eta)$ as:

$$f(\eta) \sim (\eta + \eta^{1/3}\tau_{\ell,\infty})(\phi_\lambda'' + 2\pi s) - \Omega\eta \tag{114}$$

The saddle point is the zero of function $f'(\eta)$

$$f'(\eta) = (1 + \frac{1}{3}\eta^{-2/3}\tau_{\ell,\infty})(\phi_\lambda'' + 2\pi s) - \Omega$$

$$f'(\eta_0) = 0 \quad \text{or} \quad (\eta_0)_{\ell,s,\lambda} \sim e^{i\pi/2} \left(\frac{u_{\ell,\infty}}{3}\right)^{3/2} \frac{(\phi_\lambda'' + 2\pi s)^{3/2}}{[\Omega - \phi_\lambda'' - 2\pi s]^{3/2}}$$

It should be noted that the saddle point is a function of parameters ℓ,s and λ. On the other hand since $\Omega = (ct-r)/a$, the location of the saddle point would also be time dependent. For a given observation point (r,ϕ), the arrival time for the creeping wave would be $t \geq (\phi'' + 2\pi s)\, a/c + r/c$ which implies that $(\Omega - \phi'' - 2\pi s) \geq 0$. This indicates that the saddle point falls on the positive side of the imaginary axis in complex η-plane.

Using the conformal transformation

$$w^2 = f(\eta_0) - f(\eta), \tag{116}$$

The integration on η in Eq. (103) can be approximated as:

$$\int_{-\infty}^{+\infty} \frac{K_{\gamma_\ell}(\eta)}{\sqrt{\eta}}\, e^{if(\eta)}\, d\eta \sim -2 \int_{-\infty}^{+\infty} \left[\frac{K_{\gamma_\ell}(\eta)}{\sqrt{\eta}}\right]_{\eta=\eta(w)} e^{i[f(\eta_0)-w^2]} \left(\frac{d\eta}{dw}\right) dw$$

$$= -2\, e^{if(\eta_0)} \int_{-\infty}^{+\infty} F_{\gamma_\ell}(\eta)\, e^{-iw^2}\, dw \tag{117}$$

where

$$F_{\gamma_\ell}(\eta) = \frac{K_{\gamma_\ell}(\eta)}{\sqrt{\eta}}\, \frac{d\eta}{dw} .$$

Expanding $F_{\gamma_\ell}(\eta)$ in Taylor's series about $\eta=\eta_0(w=0)$, then

$$F_{\gamma_\ell}(\eta) = F_{\gamma_\ell}(\eta_0) + \left[\frac{dF_{\gamma_\ell}(\eta)}{d\eta}\right]_{\eta_0} (\eta - \eta_0) + \ldots$$

$$= \frac{K_{\gamma_\ell}(\eta)}{\sqrt{\eta_0}} \left(\frac{d\eta}{dw}\right)_{\eta_0} + \frac{d}{d\eta}\left[\frac{K_{\gamma_\ell}(\eta)}{\sqrt{\eta}}\, \frac{d\eta}{dw}\right] (\eta - \eta_0) + \ldots \tag{118}$$

From Eq. (116) expanding $f(\eta)$ in Taylor's series about η_o

$$w^2 = f(\eta_o) - [f(\eta_o) + f'(\eta_o)(\eta - \eta_o) + \frac{1}{2!} f''(\eta_o)(\eta - \eta_o)^2 + \ldots]$$

$$= [\frac{1}{2!} f''(\eta_o)(\eta - \eta_o)^2 + \frac{1}{3!} f'''(\eta_o)(\eta - \eta_o)^3 + \ldots] \qquad (119)$$

Differentiating Eq. (116) with respect to w

$$2w \frac{dw}{d\eta} = - f'(\eta) \text{ or } \frac{d\eta}{dw} = - \frac{2w}{f'(\eta)} \qquad (120)$$

and substituting for w in terms of η we finally find

$$\underset{w\to 0}{\text{Lim}}(\frac{d\eta}{dw}) = \underset{\eta\to\eta_o}{\text{Lim}} - \frac{2}{f'(\eta)} [- \frac{1}{2!} f''(\eta_o)(\eta-\eta_o)^2 - \frac{f'''(\eta_o)}{3!} (\eta-\eta_o)^3 + \ldots]^{1/2}$$

or

$$= -2\sqrt{-\frac{f''(\eta_o)}{2}} \lim_{\eta\to\eta_o} \frac{(\eta-\eta_o)}{f'(\eta)} = - \sqrt{-2f''(\eta_o)} \left(\frac{1}{f''(\eta_o)} \right)$$

or

$$\underset{\eta\to\eta o}{\text{Lim}}(\frac{d\eta}{dw}) = - \sqrt{\frac{-2}{f''(\eta_o)}} \qquad (121)$$

Using Eqs. (117), (118) and (121), the first term of the asymptotic series approximation could be obtained as follows:

$$\int_{-\infty}^{+\infty} \frac{K_{\gamma_2}(\eta)}{\sqrt{\eta}} e^{if(\eta)} d\eta \sim -2\, e^{if(\eta_o)} \frac{K_{\gamma_2}(\eta)}{\sqrt{\eta_o}} [- \sqrt{\frac{-2}{f''(\eta_o)}}] \int_o^\infty e^{-iw^2} dw$$

$$= \sqrt{\frac{2\pi i}{f''(\eta_o)}} \frac{K_{\gamma_2}(\eta)}{\sqrt{\eta_o}} e^{if(\eta_o)}, \qquad (122)$$

AD-A131 653 ACOUSTIC PULSE SCATTERING FROM IMPEDANCE COVERED CYLINDERS(U) PENNSYLVANIA STATE UNIV UNIVERSITY PARK APPLIED RESEARCH LAB A KHAVARAN AUG 83 2/2

UNCLASSIFIED ARL/PSU/TM-83-100 N00024-79-C-6043 F/G 20/1 NL

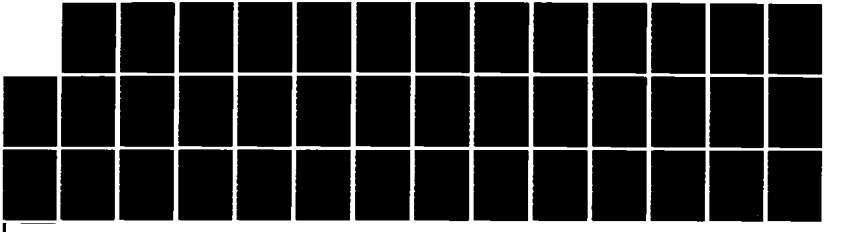

END

FILMED

DTIC

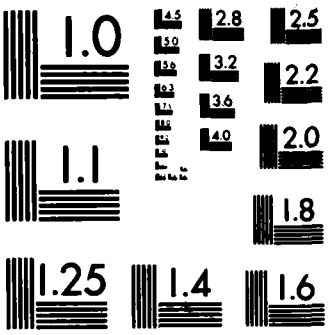

MICROCOPY RESOLUTION TEST CHART
NATIONAL BUREAU OF STANDARDS-1963-A

Thus the creeping waves in Eq. (103) are evaluated by:

$$p^c(r,t,\phi) \sim \sum_{\lambda=\pm} \sum_{s=0}^{\infty} \sum_{\ell=0}^{\infty} \sqrt{\frac{2}{\pi \frac{r}{a}}}\, e^{-i\pi/4} \left[\frac{K_{\gamma_\ell}(\eta_0)}{\sqrt{\eta_0}} \sqrt{\frac{2\pi i}{f''(\eta_0)}}\, e^{if(\eta_0)}\right] \tag{123}$$

The terms $if(\eta_0)$ and $\sqrt{2\pi i/f''(\eta_0)}$ which are needed in Eq. (123) can be obtained by using Eqs. (114) and (115)

$$if(\eta_0) = -2\left(\frac{u_{\ell,\infty}}{3}\right)^{3/2} \frac{(\phi_\lambda'' + 2\pi s)^{3/2}}{[\Omega - (\phi_\lambda'' + 2\pi s)]^{1/2}} \tag{124}$$

and

$$\sqrt{\frac{2\pi i}{f''(\eta_0)}} = 3\sqrt{\pi}\, \frac{[u_{\ell,\infty}(\phi_\lambda'' + 2\pi s)]^{3/4}}{[3(\Omega - \phi_\lambda'' - 2\pi s)]^{5/4}}$$

Finally Eq. (123), representing the creeping wave contribution to pulse scattering can be rewritten as

$$p^c(r,t,\phi) \sim \sqrt{\frac{2}{\pi \frac{r}{a}}} \sum_{\lambda=\pm} \sum_{s=0}^{\infty} P_{\lambda s}(r,t,\phi) H(t-t_{\lambda s}) \tag{126}$$

where

$$P_{\lambda s}(r,t,\phi) = \sum_{\ell} \sqrt{\frac{2\pi i}{f''(\eta_0)}}\, e^{-i\pi/4} \frac{K_{\gamma_\ell}(\eta_0)}{\sqrt{\eta_0}}\, e^{if(\eta_0)} \tag{127-a}$$

The unit step function $H(t-t_{\lambda s})$ represents the arrival of the creeping wave corresponding to known values of λ and s

$$t_{\lambda s} = (\phi_\lambda'' + 2\pi s)\left(\frac{a}{c}\right) + \frac{r}{c} \tag{127-b}$$

The pulse response as expressed by Eq. (126) can be substituted in Duhamel's integral to find the scattered pressure due to creeping waves

only for any incident plane wave. Letting the time signature of the incident pulse be described by:

$$F_{inc}(t) = \cos(\omega t)[H(t) - H(t-T)] \tag{128}$$

then for $t_{\lambda s} < t < t < t_{\lambda s} + T$, the creeping wave pulses are given by:

$$F^c(r,t,\phi) = \sqrt{\frac{2}{\pi \frac{r}{a}}} \sum_{\lambda = \pm} \sum_{s=0}^{\infty} \int_o^{t-t_{\lambda s}} \cos(\omega\tau) P_{\lambda s}(r,t-\tau,\phi)d\tau$$

$$= \sqrt{\frac{2}{\pi \frac{r}{a}}} \sum_{\lambda = \pm} \sum_{s=0}^{\infty} \int_{t_{\lambda s}}^{t} \cos[\omega(t-\tau)] p_{\lambda s}(r,\tau,\phi)d\tau \tag{129}$$

After a change of variable $x = ct/a$ and substituting for ω in terms of dimensionless parameters $\omega = (\bar{\omega}/\bar{\lambda})(c/a)$ one finds:

$$F^c(r,t,\phi) = \sqrt{\frac{2}{\pi \frac{r}{a}}} \sum_{\lambda} \sum_{s} \int_{ct_{\lambda s}/a}^{ct/a} \cos[(\frac{\bar{\omega}}{\bar{\lambda}})(\frac{ct}{a} - x)] p_{\lambda s}(r,x,\phi) \frac{dx}{c/a}$$

Finally multiplying by the factor $(-P_o\xi/4\pi)$, which was dropped out earlier one obtains the time signature of the creeping wave pulse as:

$$F^c(r,t,\phi) = - \sqrt{\frac{2}{\pi \frac{r}{a}}} \frac{P_o}{4\pi} \sum_{\lambda=\pm} \sum_{s=0}^{\infty} \int_{ct_{\lambda s}/a}^{ct/a} \cos[(\frac{\bar{\omega}}{\bar{\lambda}})(\frac{ct}{a} - x)] p_{\lambda s}(r,x,\phi)dx \tag{130}$$

in terms of the new variable x, $\Omega = x - r/a$. The integral in Eq. (130) can be computer numerically for any non-dimensional time ct/a.

For $t > t_{\lambda s} + T$

$$F^c(r,t,\phi) = - \sqrt{\frac{2}{\pi \frac{r}{a}}} \frac{P_o}{4\pi} \sum_{\lambda = \pm} \sum_{s=0}^{\infty} \int_{\frac{c(t-T)}{a}}^{\frac{ct}{a}} \cos[(\frac{\bar{\omega}}{\bar{\lambda}})(\frac{ct}{a} - x)] p_{\lambda s}(r,x,\phi)dx \tag{131}$$

It should be noted that in computing $p_{\lambda s}(r,t,\phi)$ according to Eq. (127), a summation on index ℓ should be carried out, but the factor $e^{if(n_o)}$ represents an exponential decay with ℓ (see Eq. (124), so considering only the first few values of $u_{\ell,\infty}$ would incorporate the major contribution arising from this summation.

CHAPTER IV

NUMERICAL RESULTS AND CONCLUSIONS

4.1 Introduction

Numerical evaluations of the scattered field for various types of incident plane pulses are presented in this chapter. Creeping waves and geometrically reflected waves are plotted separately. The parameters are varied to explore the dependence of the scattered pressure on the observation angle ϕ and impedance covering Z. All calculations were made for an observer in the far field. The computed time signatures describe the ratio of the amplitude of the scattered pressure to that of the incident pressure, plotted versus non-dimensional time ct/a.

4.2 Impedance Model

Since the scattered field is a function of the impedance coverage as well as the radius of the cylinder, one can plot the pressure at specific values of parameters a_1, c_1 and $\bar{\lambda}$. Another factor which influences the total time signature is the parameter $\bar{\omega}$. Once the impedance function and observation angle are fixed, Eq. (75) is solved numerically for the poles η_n in the lower half of the complex plane. Tables 2 and 3 list some of these poles corresponding to $\bar{\lambda} = .5$ and $\bar{\lambda} = 2.0$, respectively. The numerical solution of Eq. (75) has been done with the help of IMSL zero finder subroutine which works for an analytic function of complex variables.

4.3 Geometrically Reflected Pressure

The impulse response of the geometrically reflected pressure (GRP), as expressed in Eq. (82), is shown in Figure 24. The

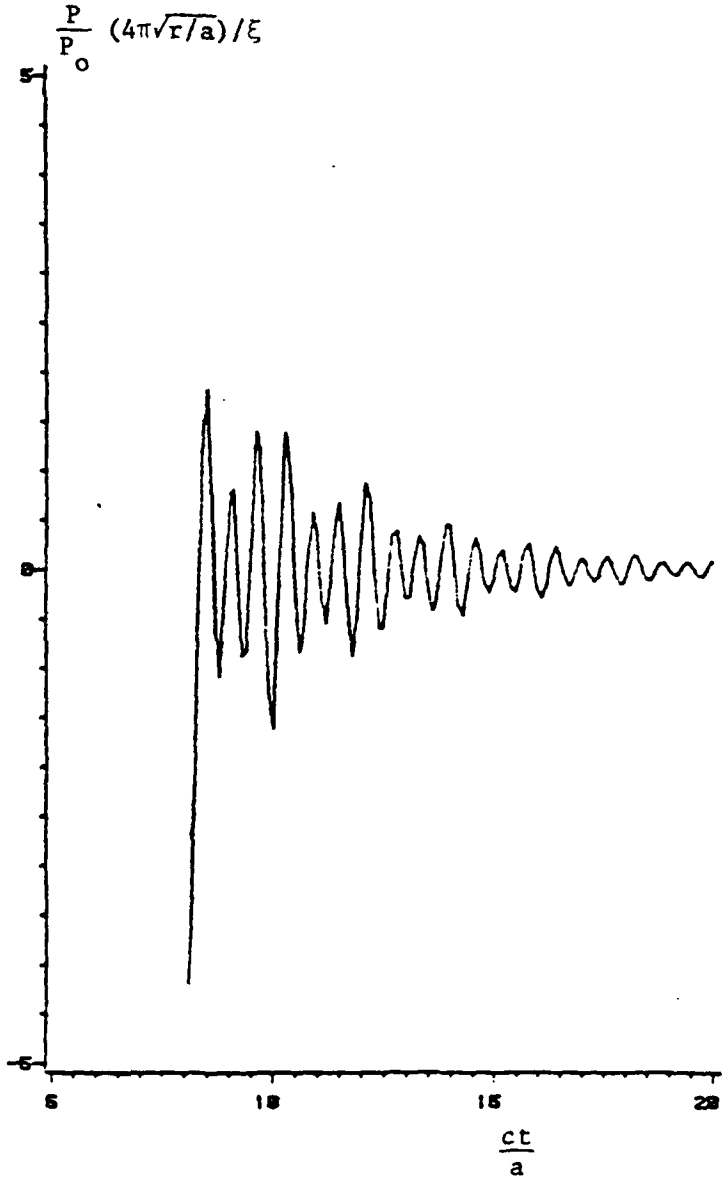

Figure 24. Pulse Response for the Geometrically Reflected Pressure with $\phi = 180°$ and $\bar{\lambda} = 0.5$.

observation radius is set at r/a = 10.0 throughout these calculations. Since time is measured from the arrival of the incident wave at the shadow boundary ($\phi = 90°$), the arrival time for the back scattered GRP would correspond to ct/a = 8.0. Any changes in r/a would simply shift the curve, along the abscissa.

Table 2

The first three roots of

$$H_\gamma^{(1)}(\eta) + i\bar{Z}(\eta)\, H_\gamma'^{(1)}(\eta) = 0, \quad \gamma = \eta\cos\phi/2$$

with

$$\bar{\lambda} = .5, \; a_1 = 2.0 \text{ and } b_1 = 1.1$$

ϕ^o	η_1	η_2	η_3
0	-.3064,-.1406	-1.2195,-.3280	-1.577,-.2063
10	-.3070,-.1410	-1.2192,-.3378	-1.581,-.2035
20	-.3099,-.1424	-1.2175,-.3378	-1.595,-.1921
30	-.3149,-.1462	-1.2142,-.3395	-1.622,-.1734
40	-.3223,-.1513	-1.2091,-.3742	-1.6610,-.1497
50	-.3321,-.1586	-1.2027,-.3742	-1.7147,-.1226
60	-.3445,-.1687	-1.1957,-.3814	-1.7830,-.0937
70	-.3595,-.1826	-1.1890,-.3815	-1.8680,-.0640
80	-.3766,-.2018	-1.1850,-.3709	-1.9740,-.0363
90	-.3944,-.2281	-1.1873,-.3455	-2.2300,-.0001
100	-.4097,-.2631	-1.2019,-.3014	
110	-.4171,-.3057	-1.2390,-.2374	
120	-.4128,-.3498	-1.3116,-.1581	
130	-.3989,-.3883	-1.4290,-.0713	
140	-.3806,-.4180	-1.5500,-.0001	
150	-.3627,-.4391		
160	-.3480,-.4529		
170	-.3382,-.4608		
180	-.3341,-.4639		

Table 3

The first three roots of

$$H_{\gamma}^{(1)}(\eta) + i\bar{Z}(\eta)\, H_{\gamma}^{'(1)}(\eta) = 0, \quad \gamma = \eta\cos\phi/2$$

with

$$\bar{\lambda} = 2.0, \; a_1 = 2.0 \text{ and } b_1 = 1.1$$

ϕ^{o}	η_1	η_2	η_3
0	-.2340,-.1745		
10	-.2342,-.1748		
20	-.2348,-.1763		
30	-.2357,-.1790		-1.3990,-.0000
40	-.2371,-.1827	-.5350,-.0478	-1.4300,-.0000
50	-.2387,-.1875	-.5400,-.0001	-1.4900,-.0001
60	-.2406,-.1903	-.5501,-.0300	-1.5410,-.0005
70	-.2425,-.2004	-.5741,-.0324	-1.6180,-.0094
80	-.2445,-.2076	-.5957,-.0270	-1.7150,-.0260
90	-.2464,-.2158	-.6233,-.0226	-1.8350,-.0607
100	-.2483,-.2244	-.6507,-.0209	-1.9753,-.1314
110	-.2561,-.2333	-.7039,-.0251	-2.0918,-.2806
120	-.2518,-.2423	-.7607,-.0414	-2.0560,-.4126
130	-.2532,-.2510	-.8264,-.0826	-2.001 ,-.3662
140	-.2544,-.2590	-.8779,-.1623	-2.0540,-.1817
150	-.2554,-.2661	-.8804,-.2525	
160	-.2561,-.2717	-.8554,-.3111	
170	-.2565,-.2754	-.8331,-.3407	-3.7821,-.0001
180	-.2567,-.2770	-.8231,-.3512	-3.8990,-.3410

The oscillatory nature of the GRP for an incident plane wave pulse is due to the interference of the geometrically reflected ray and the diffracted rays from the shadow boundaries. A second type of an incident plane wave considered here is a time harmonic pulse train. Figures 25-29 represent the three dimensional plot of the scattered GRP versus time and observation angle varied from 0° to 180°. It can be seen that the peaks at each observation angle correspond to a specific

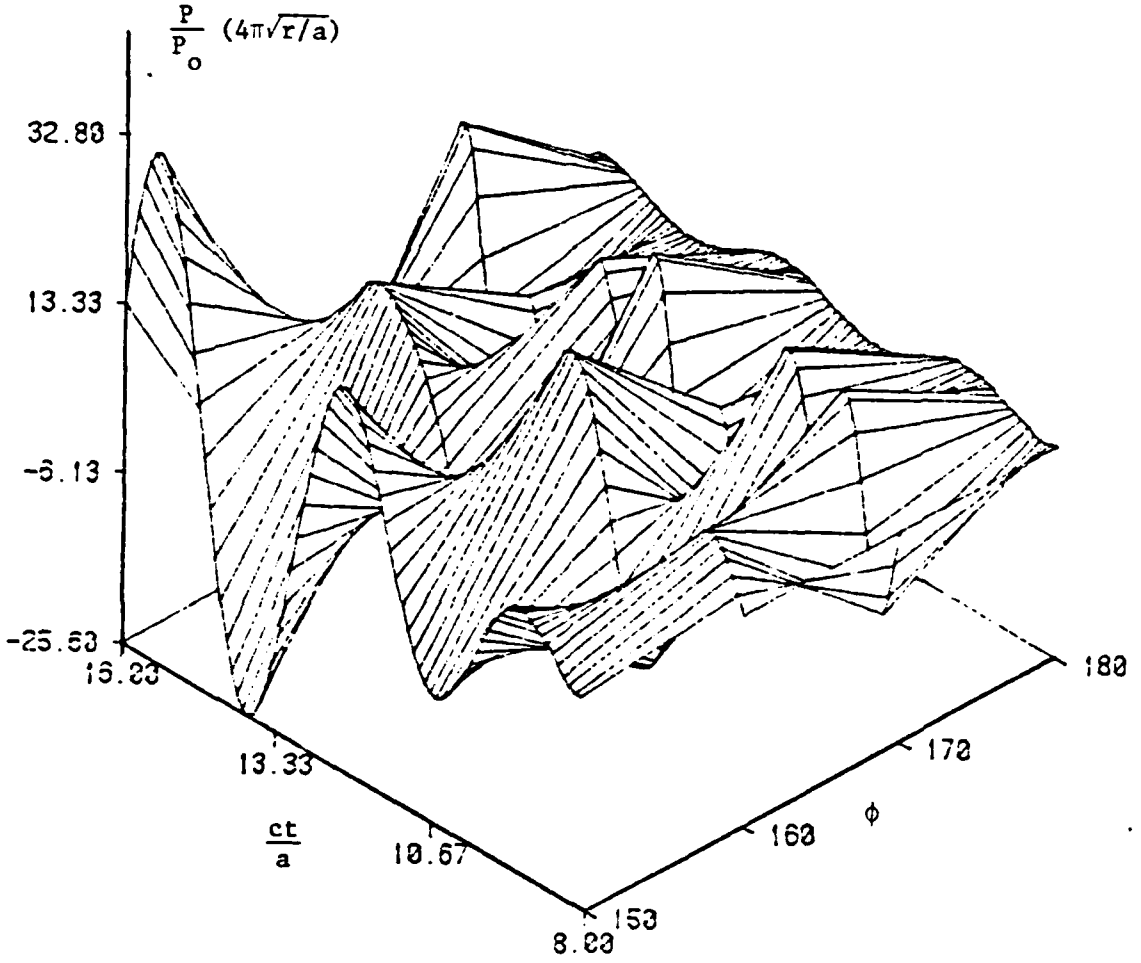

Figure 25. Geometrically Reflected Pressure for a Time Harmonic Pulse Train with $\bar{\lambda}$ = .5, $\bar{\omega}$ = 1.0 and 150° < ϕ < 180°.

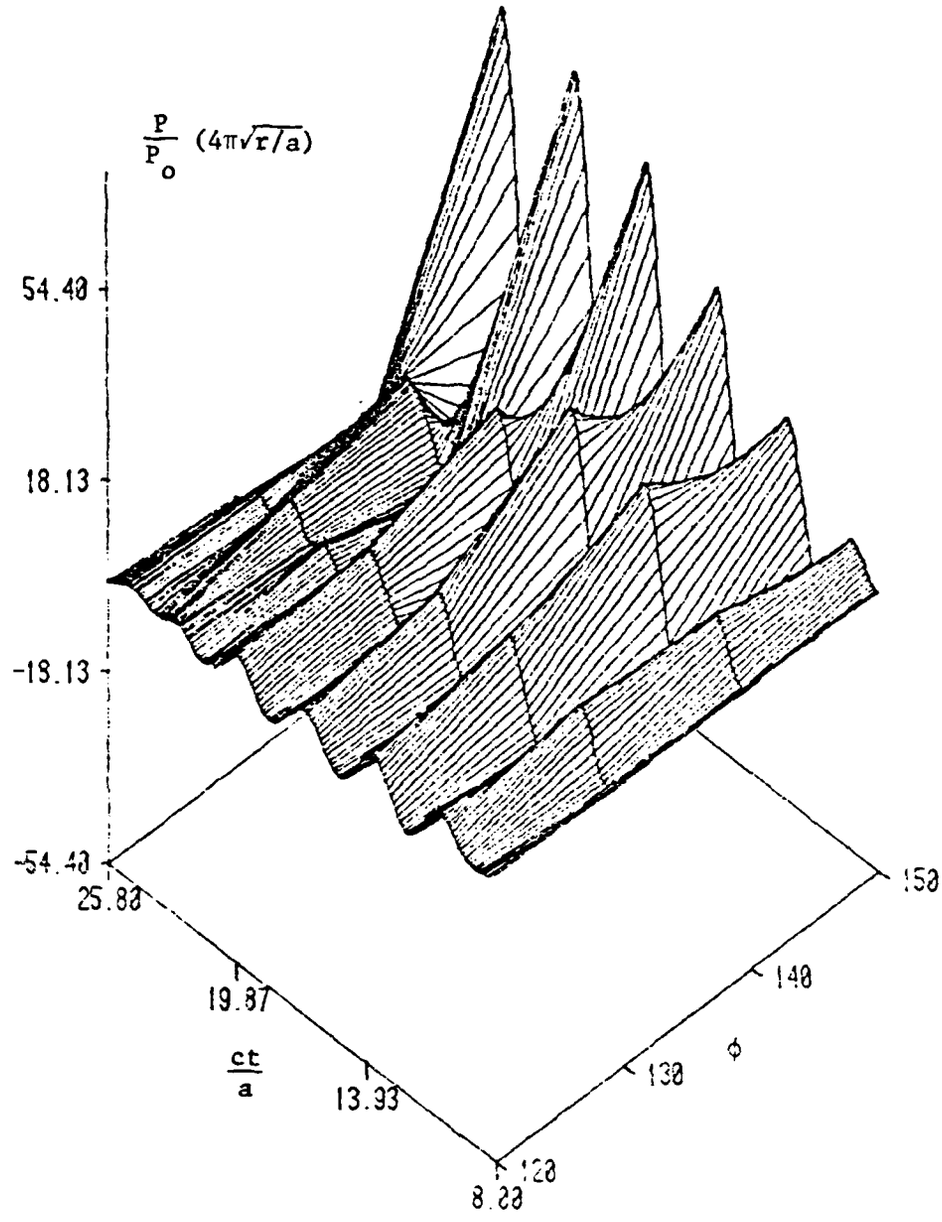

Figure 26. Geometrically Reflected Pressure for a Time Harmonic Pulse Train with $\bar{\tau}$ = .5, $\bar{\omega}$ = 1.0 and 120° < ϕ < 150°.

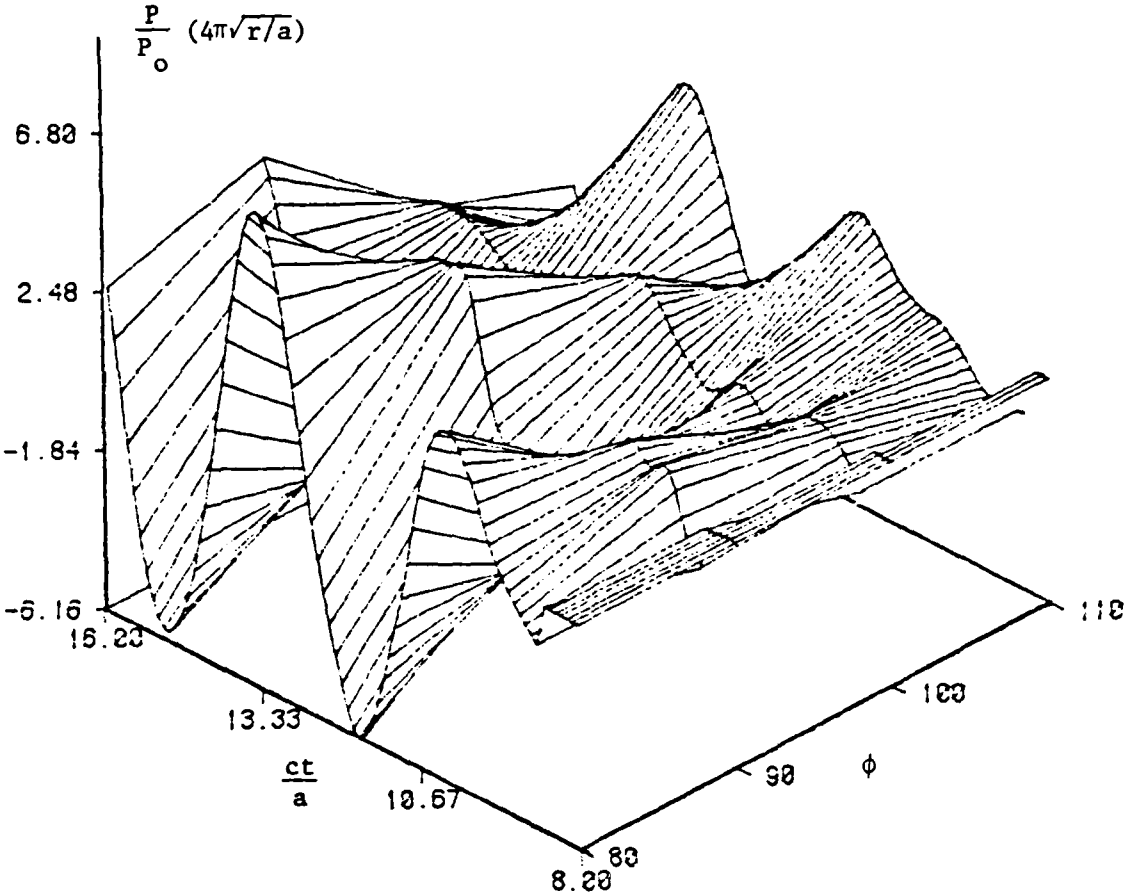

Figure 27. Geometrically Reflected Pressure for a Time Harmonic Pulse Train with $\bar{\lambda}$ = .5, $\bar{\omega}$ = 1.0 and 80° < ϕ < 110°.

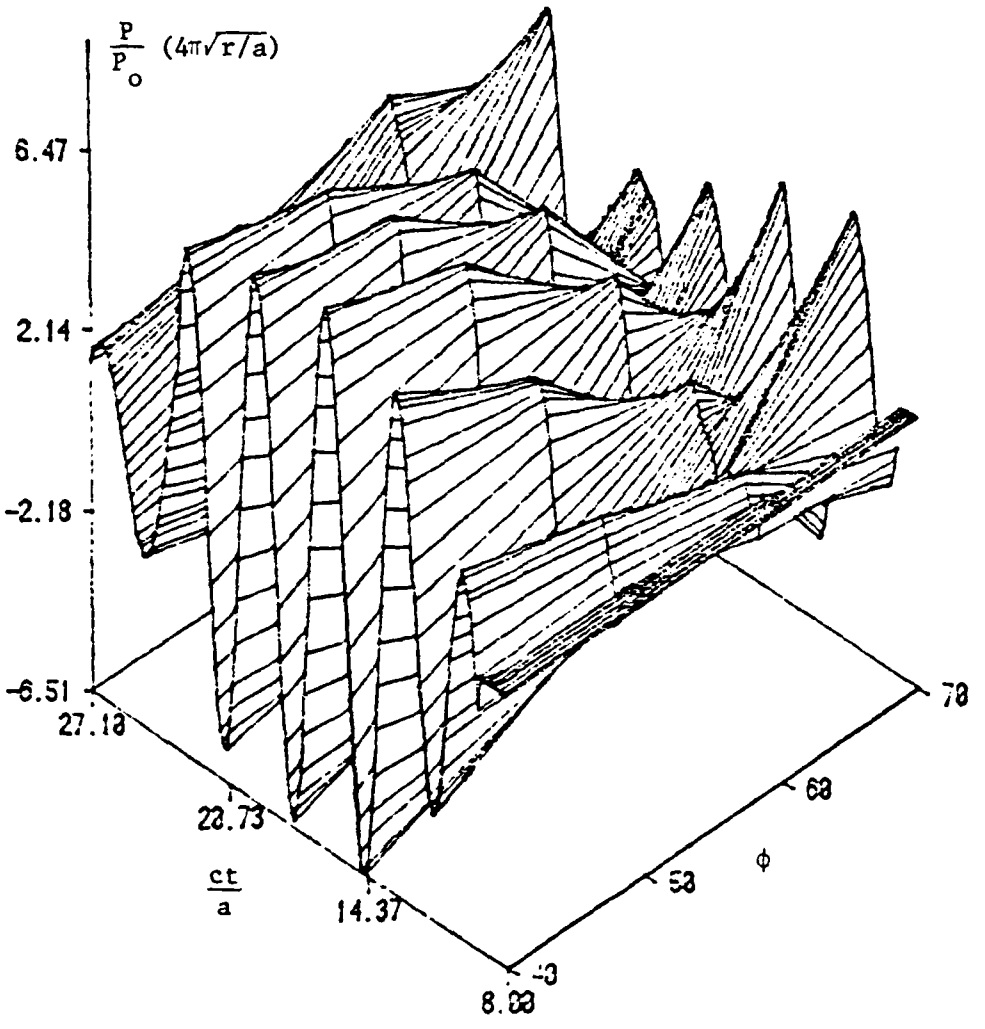

Figure 28. Geometrically Reflected Pressure for a Time Harmonic Pulse Train with $\bar{\lambda} = .5$, $\bar{\omega} = 1.0$ and $40° < \phi < 70°$.

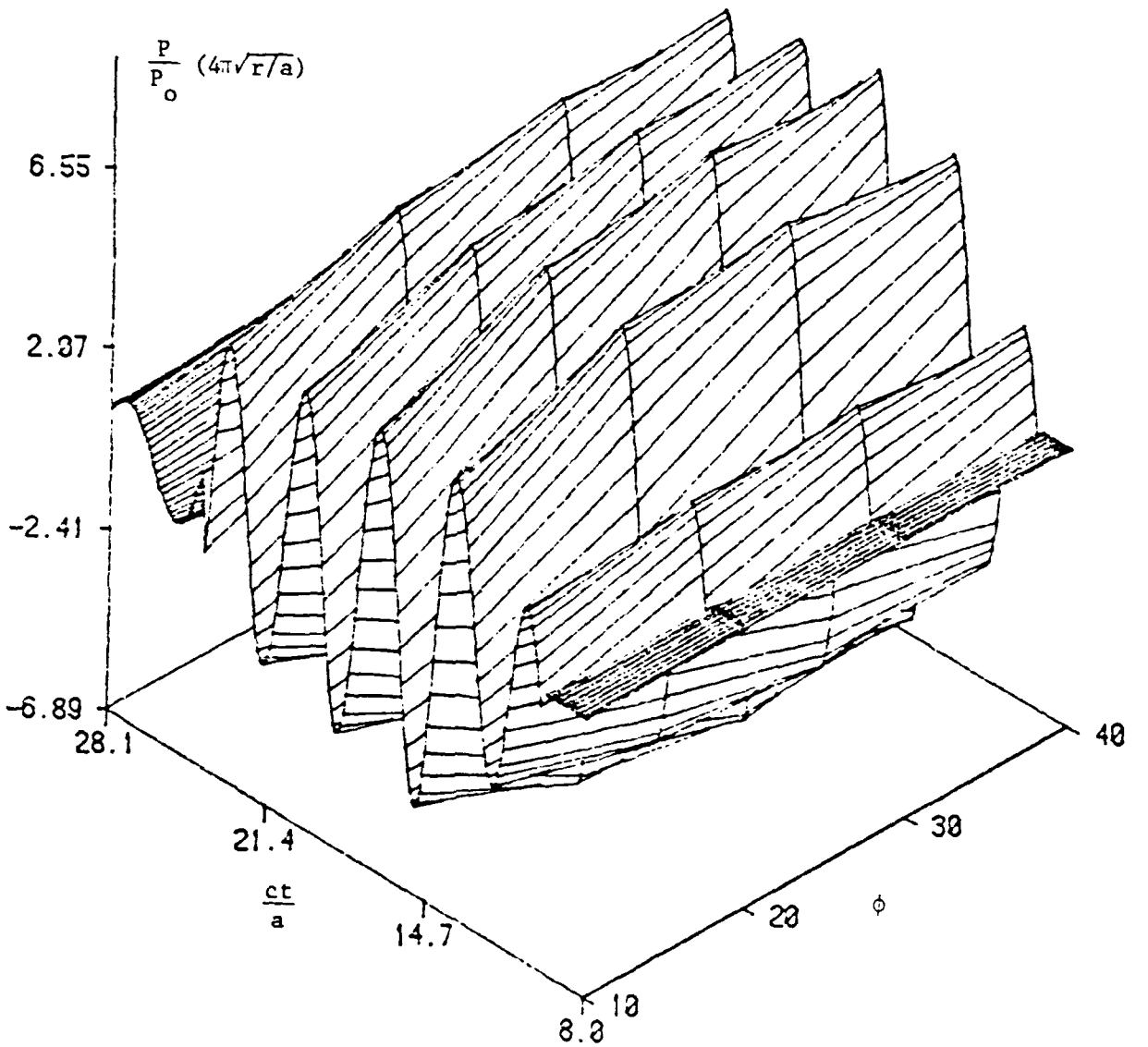

Figure 29. Geometrically Reflected Pressure for a Time Harmonic Pulse Train with $\bar{A} = .5$, $\bar{\omega} = 1.0$ and $10° < \phi < 40°$.

arrival time, which is related to that observation angle. The amplitude of the scattered GRP on the other hand shows a distinct dependency on observation angle. Figure 30 demonstrates a two dimensional plot of the back scattered GRP for the same incident plane wave pulse train. Since the duration of the incident pulse is limited to $0 < \omega t < 8\pi$, the arrival time for the scattered field is described by:

$$(r/a - 2\sin\phi/2) < ct/a < 8\pi(\bar{\lambda}/\bar{\omega}) \ .$$

The GRP after the termination of the pulse would be an exponentially decaying function as demonstrated by negligible amplitudes in Figure 30. Figures 31 and 32 exhibit the significance of the nondimensional frequency of the incident pulse $\bar{\omega}$ on the back scattered GRP. It is observed that unlike an infinite plane boundary, there are little change in the amplitude of the reflected pressure vs.$\bar{\omega}$. Comparison of Figures 30 and 33 shows the backscattered GRP for cylinders with different nondimensional radii $\bar{\lambda}$. The change in $\bar{\lambda}$ from Figure 30 to Figure 33 by a factor of four corresponds to reducing the radius by 1/4.0. Since the ratio of r/a is kept constant, any comparison between Figures 30 and 33 is meaningful only if the observation point is kept fixed in space. This indicates that the time signature as shown in Figure 33 should be multiplied by the factor

$$\sqrt{10/(9\bar{\lambda}_2/\bar{\lambda}_1+1)} = .51$$

so that the geometrically spreading factor is eliminated.

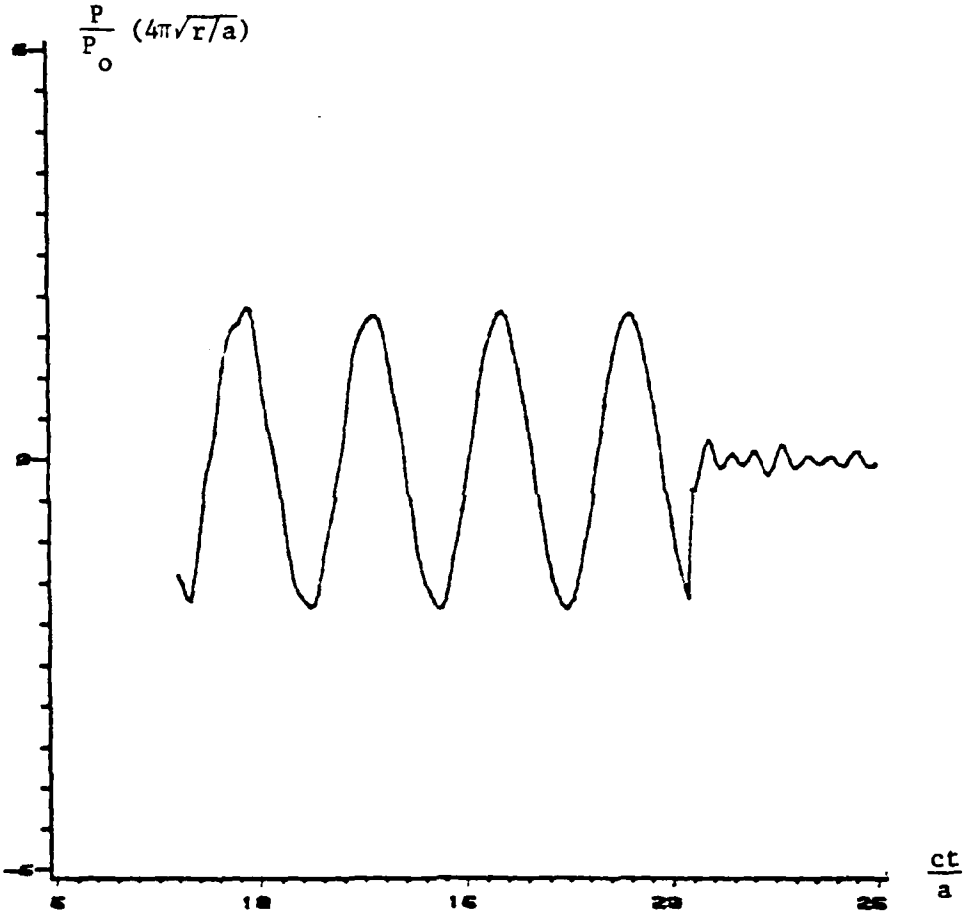

Figure 30. Geometrically Reflected Pressure for a Time Harmonic Pulse Train with $\bar{r}$ = .5, $\bar{\omega}$ = 1.0 and ϕ = 180°.

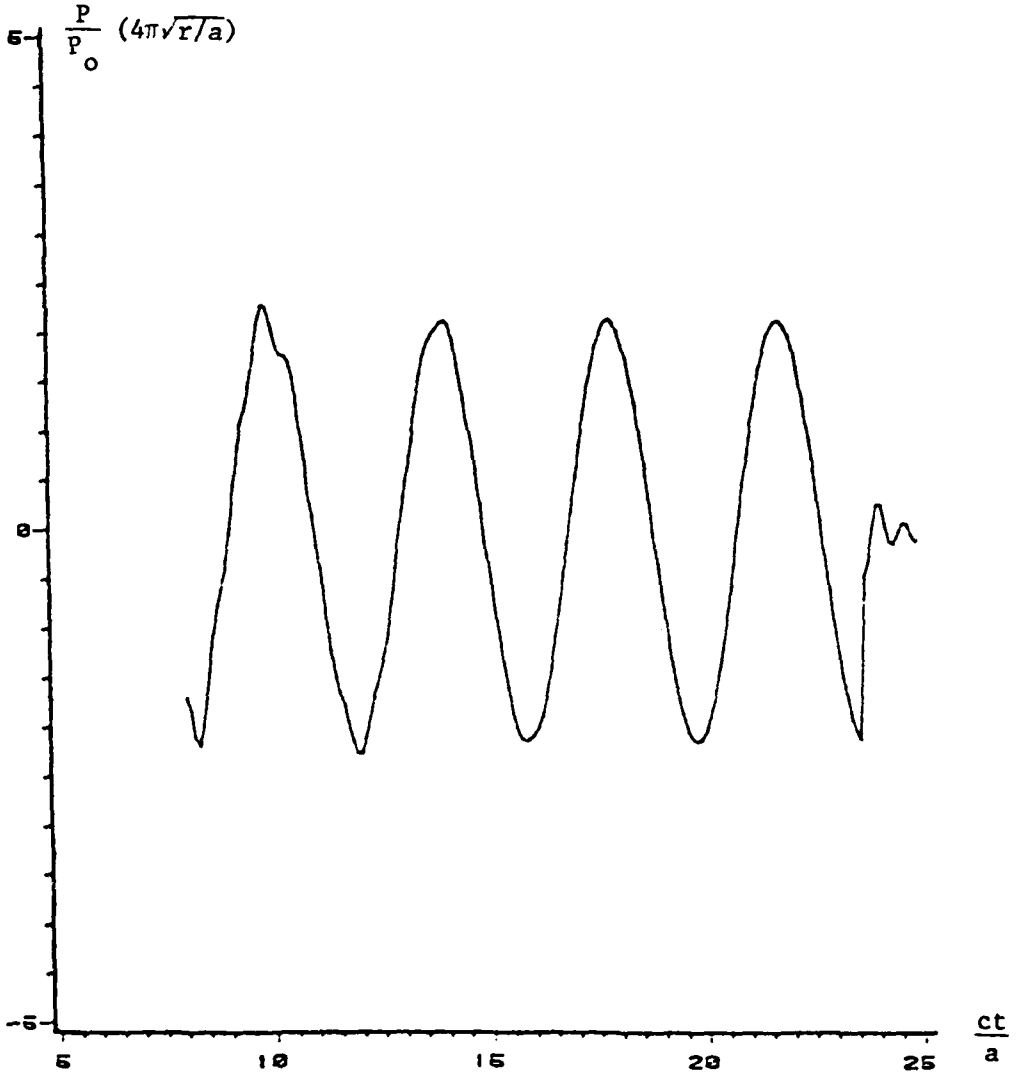

Figure 31. Geometrically Reflected Pressure for a Time Harmonic Pulse Train with $\bar{\lambda}$ = .5, $\bar{\omega}$ = .8 and ϕ = 180°.

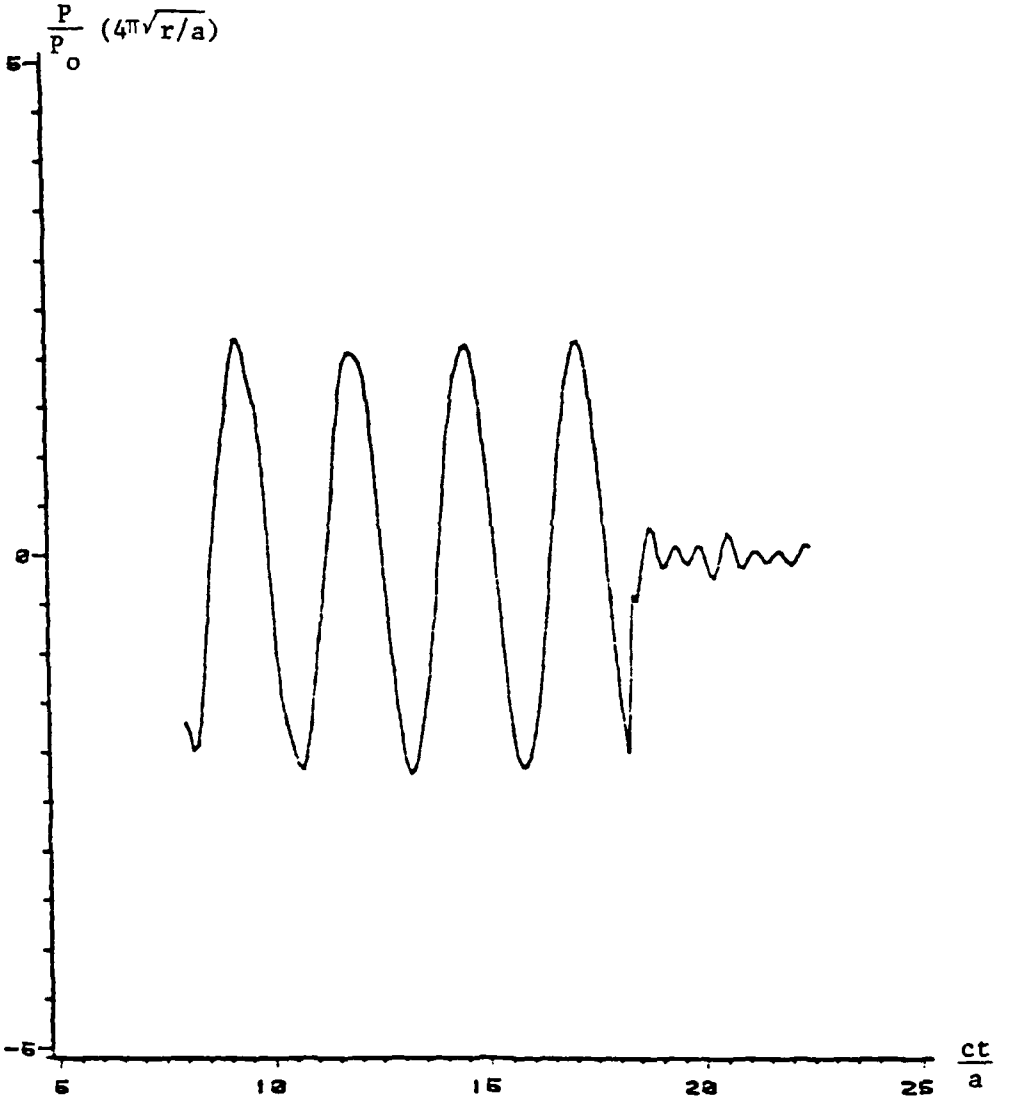

Figure 32. Geometrically Reflected Pressure for a Time Harmonic Pulse Train with $\bar{\lambda}$ = .5, $\bar{\omega}$ = 1.2 and δ = 180°.

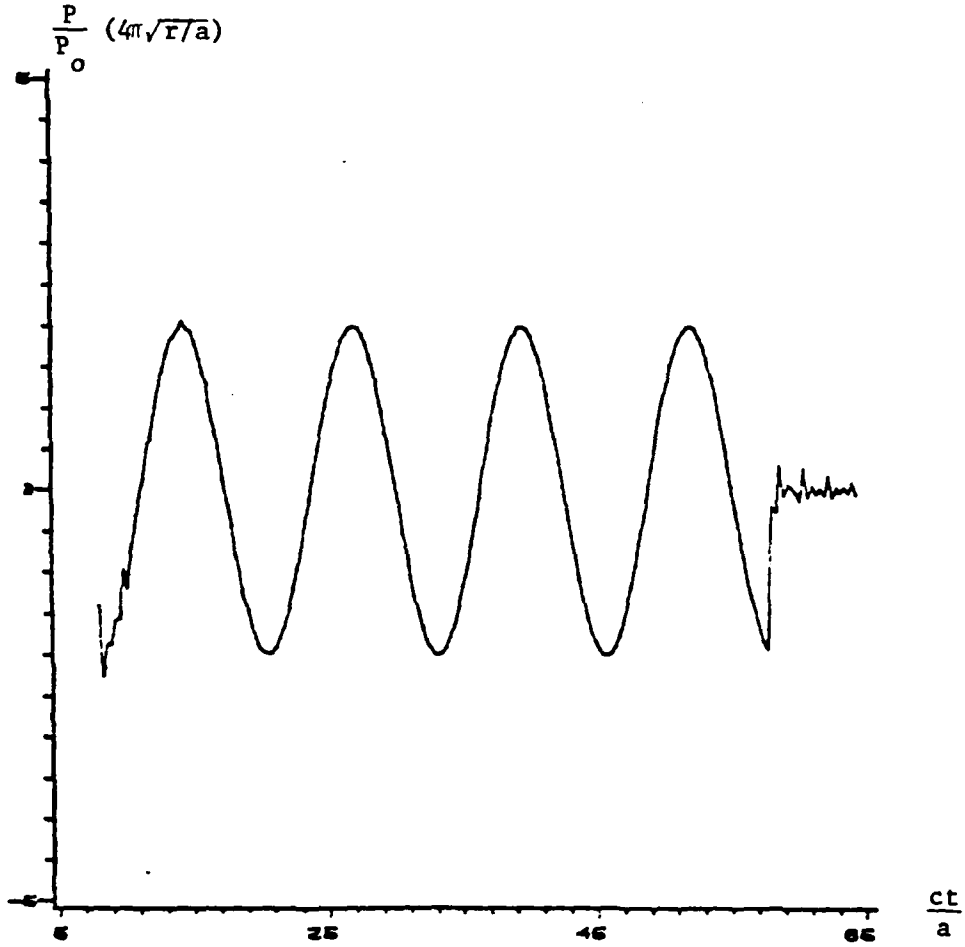

Figure 33. Geometrically Reflected Pressure for a Time Harmonic Pulse Train with $\bar{\tau}$ = 2.0, $\bar{\omega}$ = 1.0 and ϕ = 180°.

Figures 34 and 35 represent the backscattered field for FM plane pulse incidence. Once again these figures do not show a significant variation in the amplitude of the backscattered GRP with changing frequency, a finding which is in agreement with those of Figures 30 and 32.

Finally Figures 36 and 37 show polar plots for the peak amplitude of the GRP time signature as a function of the observation angle for a time harmonic pulse train. The forward scattering is zero as was stated in Eq. (86).

4.4 Creeping Waves

We saw that the fronts of the creeping pulses move with the free-space sound velocity and propagate around the shadow side of the cylinder back to insonified region, and then circle the cylinder an infinite number of times. The exponential factor $e^{if(n_o)}$ in Eqs. (124) and (126) indicates the fast decaying nature of these pulses as they circumnavigate the cylinder's surface. Figure 38, 39 and 40 show the pulse response for the first mode of the circumferential wave (s=0) at ϕ = 180°, 90° and 0° respectively. The discontinuity in Figure 39 corresponds to the two different arrivals of the creeping waves from the two different directions. It should be pointed out that the second modes of the creeping waves (s=1) are so highly attenuated that they show no visible discontinuities, unless plotted separately with a different scale factor. Even for the first creeping wave mode, as they travel from 0° to 180°, the pulses seem to attenuate significantly. The first mode of the creeping waves for a time harmonic pulse train is plotted in Figures 41-44 for different observation angles. All these figures indicate that the amplitude of the creeping wave increases as

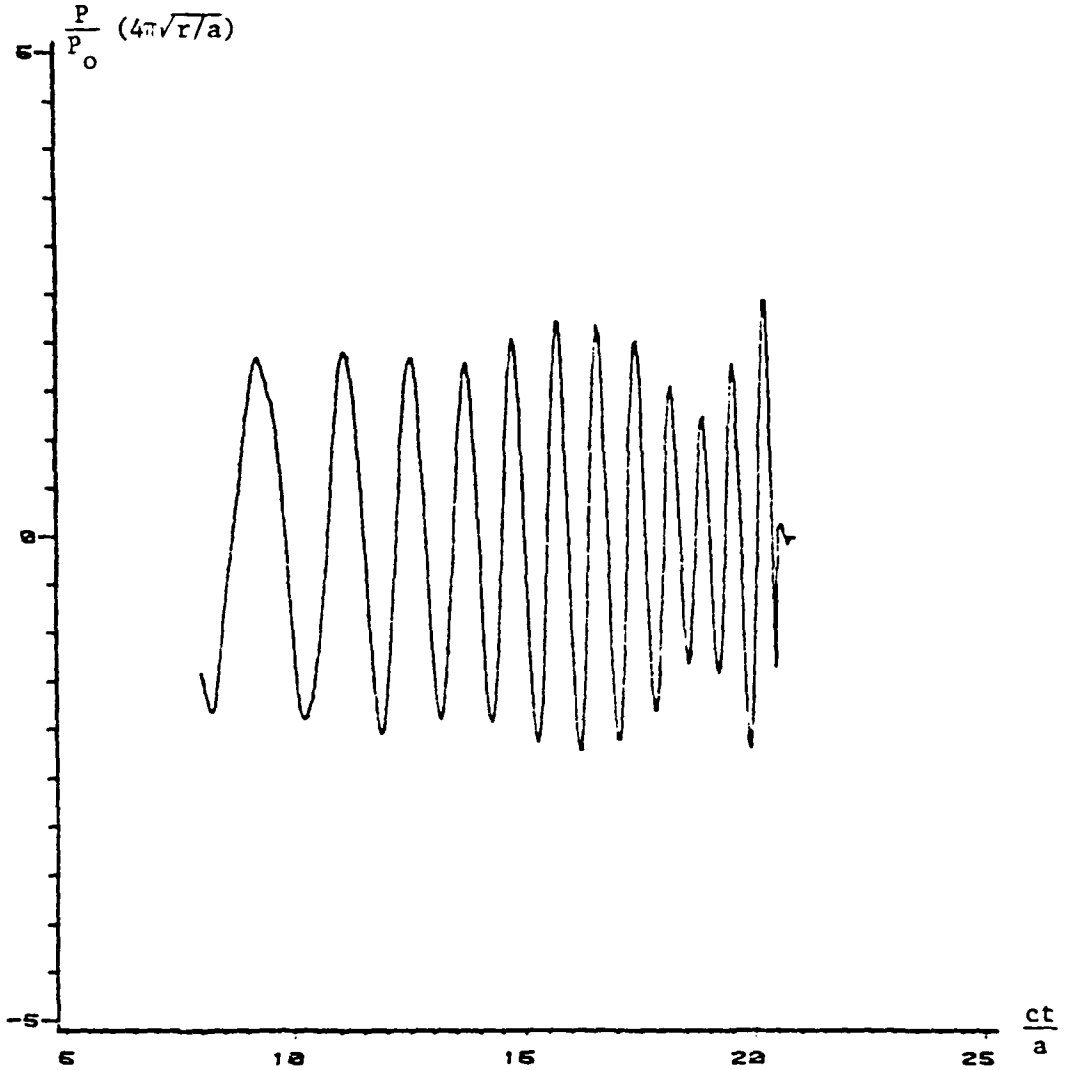

Figure 34. Geometrically Reflected Pressure for an Incident FM Plane Pulse with $\bar{\tau}$ = .5, $\bar{\sigma}$ = 1.0, ϕ = 180° and β = 2.0.

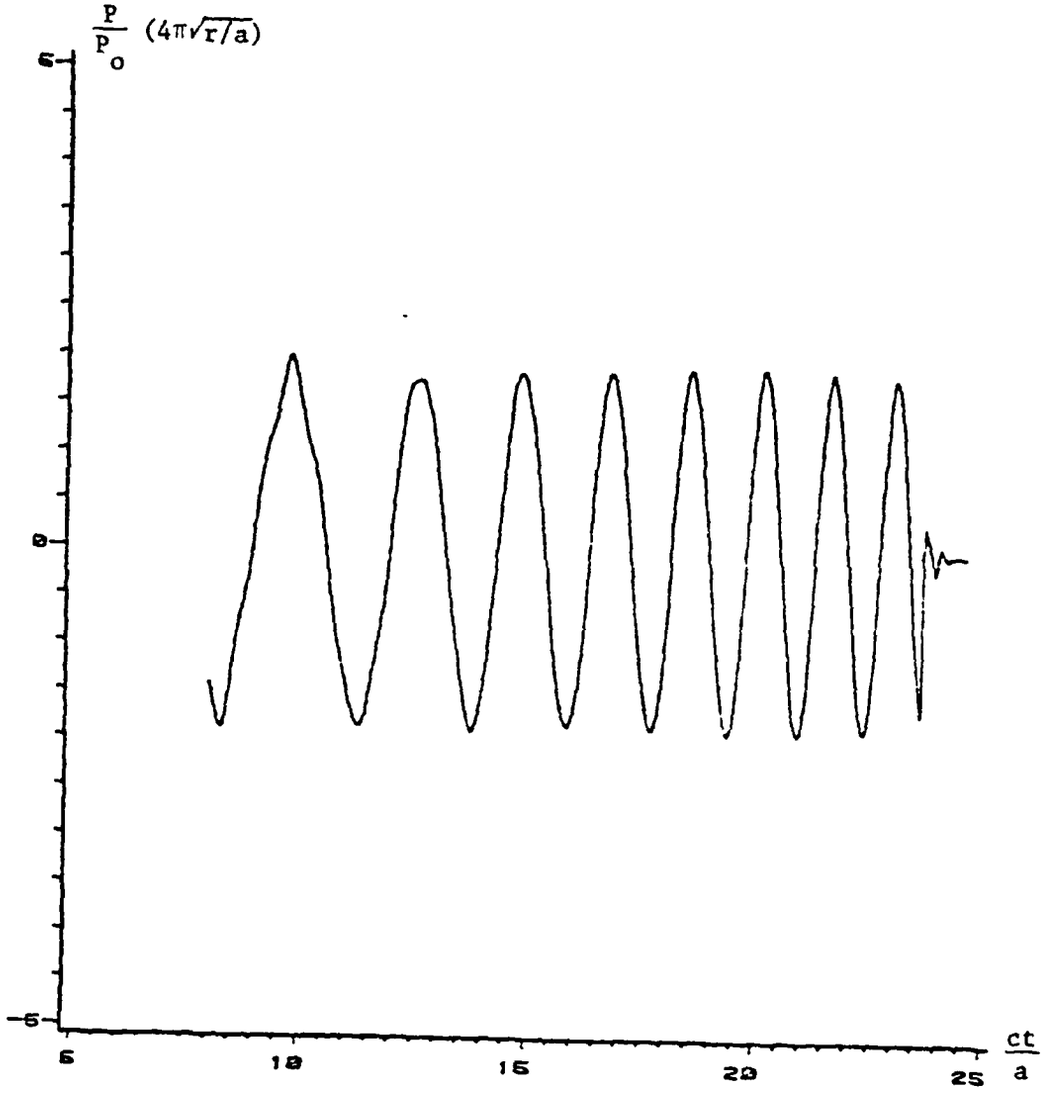

Figure 35. Geometrically Reflected Pressure for an Incident FM Plane Pulse with $\bar{\tau}$ = .5, $\bar{\omega}$ = .8, ϕ = 180° and β = 1.0.

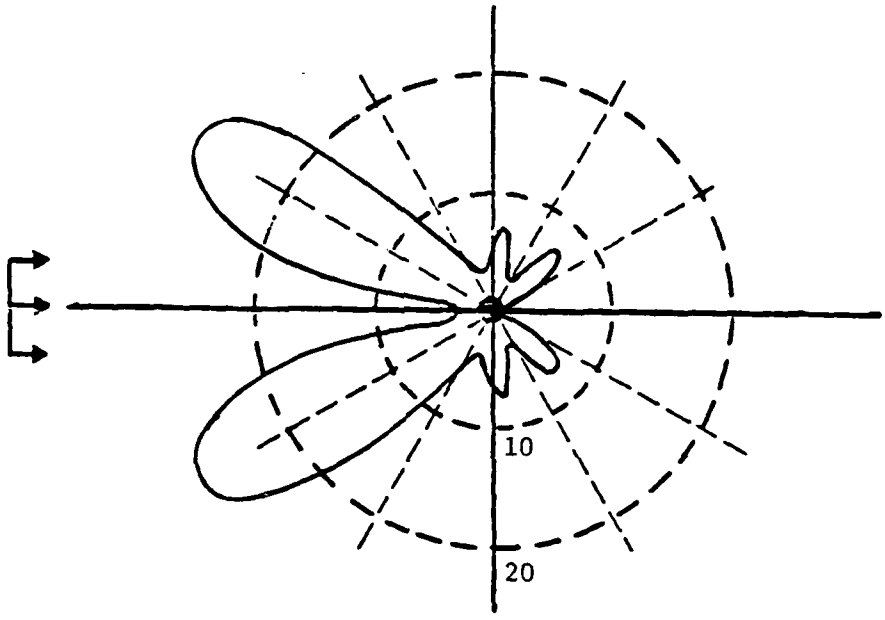

Figure 36. Polar Plot of the Peak Amplitude $\frac{P}{p_o}(4\pi\sqrt{r/a})$ of the Geometrically Reflected Pressure Time Signature for a Time Harmonic Pulse Train with $\bar{\tau} = .5$ and $\bar{\omega} = 1.0$.

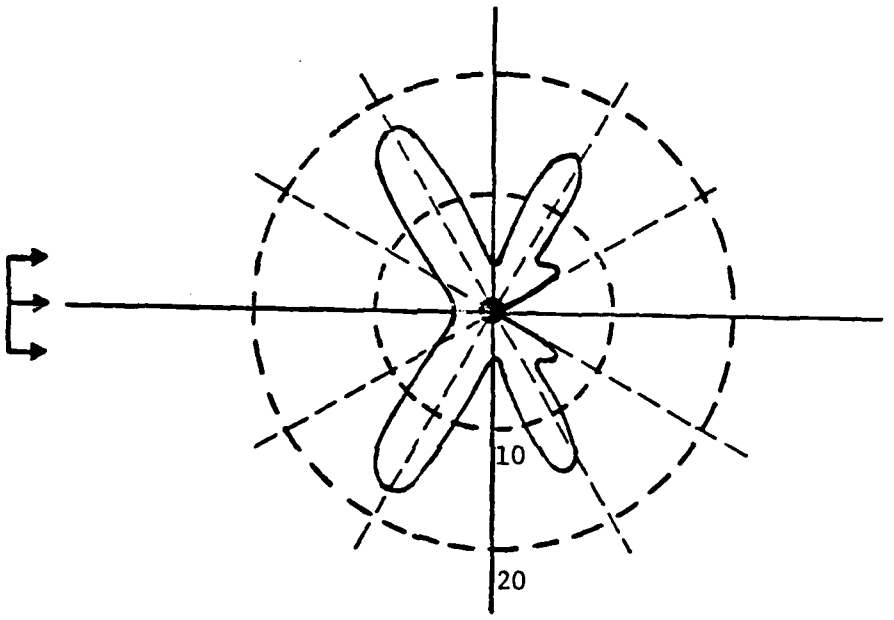

Figure 37. Polar Plot of the Amplitude $\frac{P}{P_o}(4\pi\sqrt{r/a})$ of the Geometrically Reflected Pressure for a Time Harmonic Pulse Train with $\bar{\lambda} = 2.0$ and $\bar{\omega} = 1.0$.

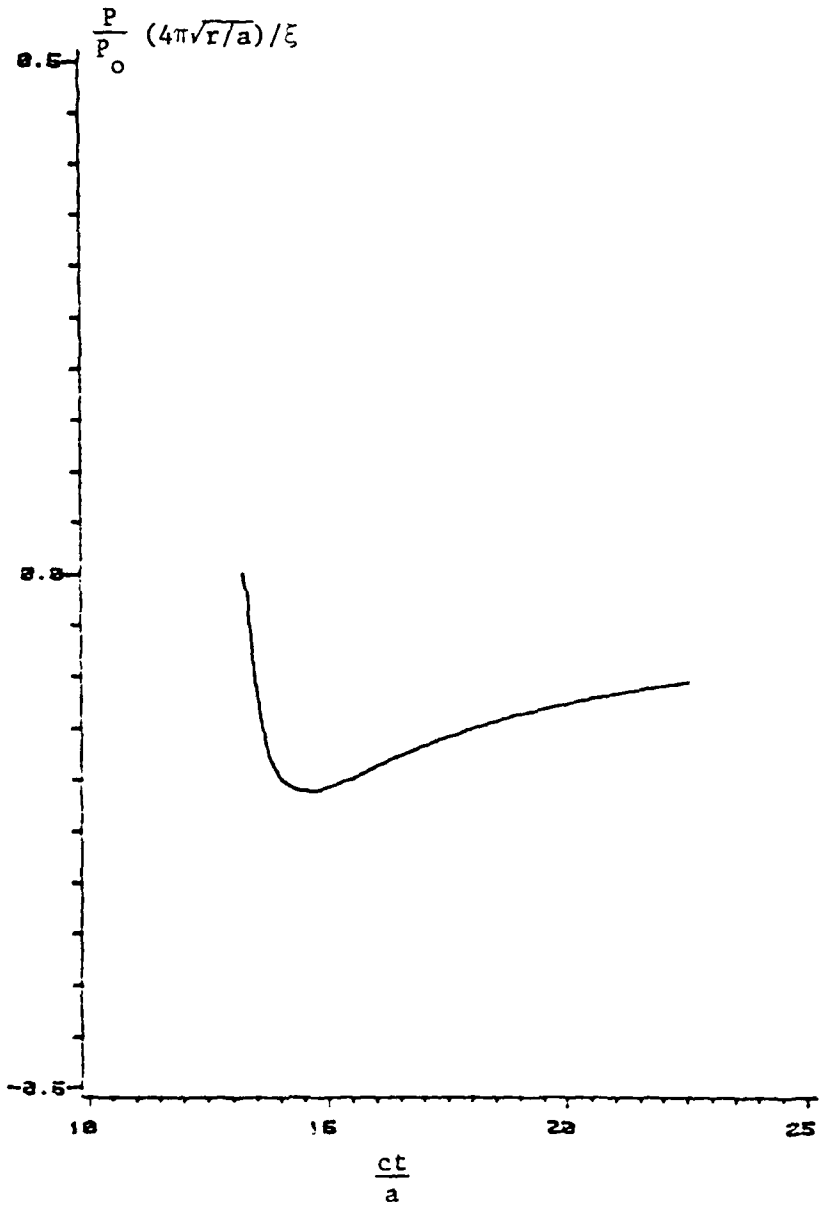

Figure 38. Pulse Response for the First Creeping Wave (s=0) at ϕ = 180°.

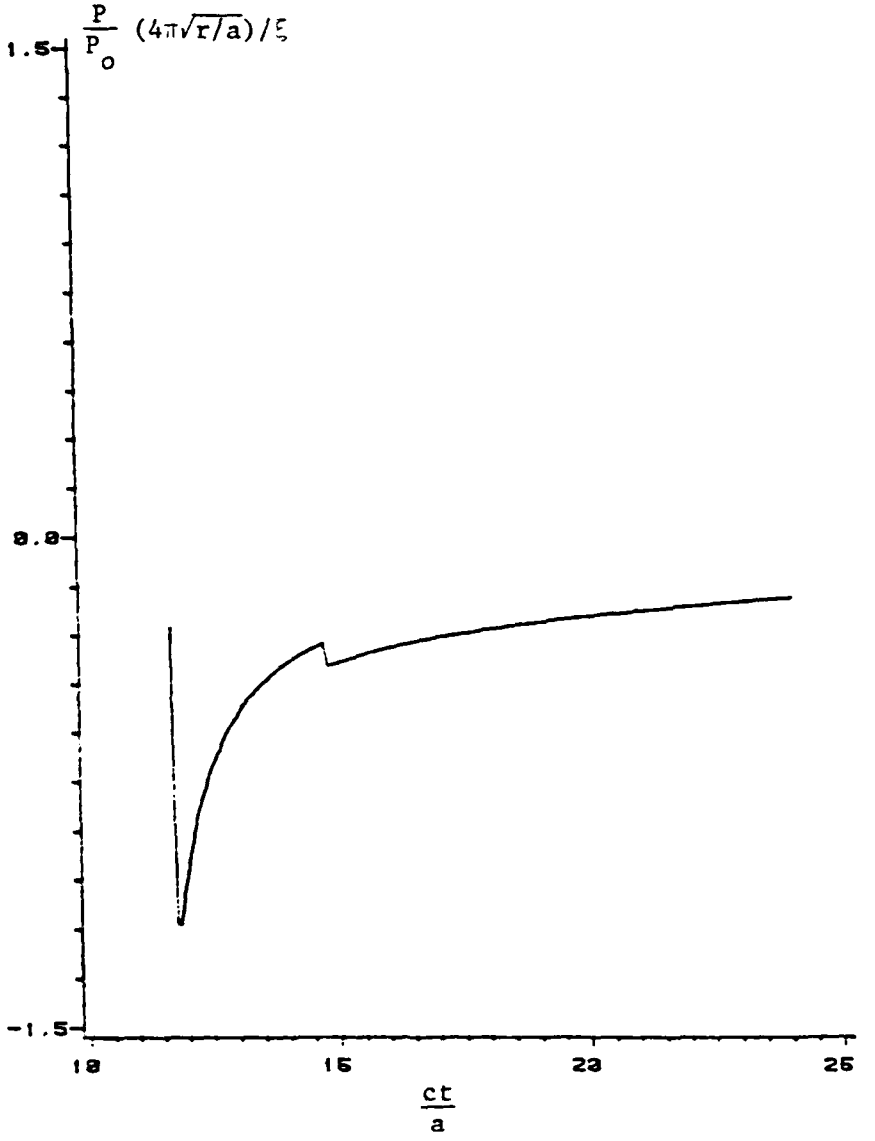

Figure 39. Pulse Response for the First Creeping Wave (s=0) at ϕ = 90°.

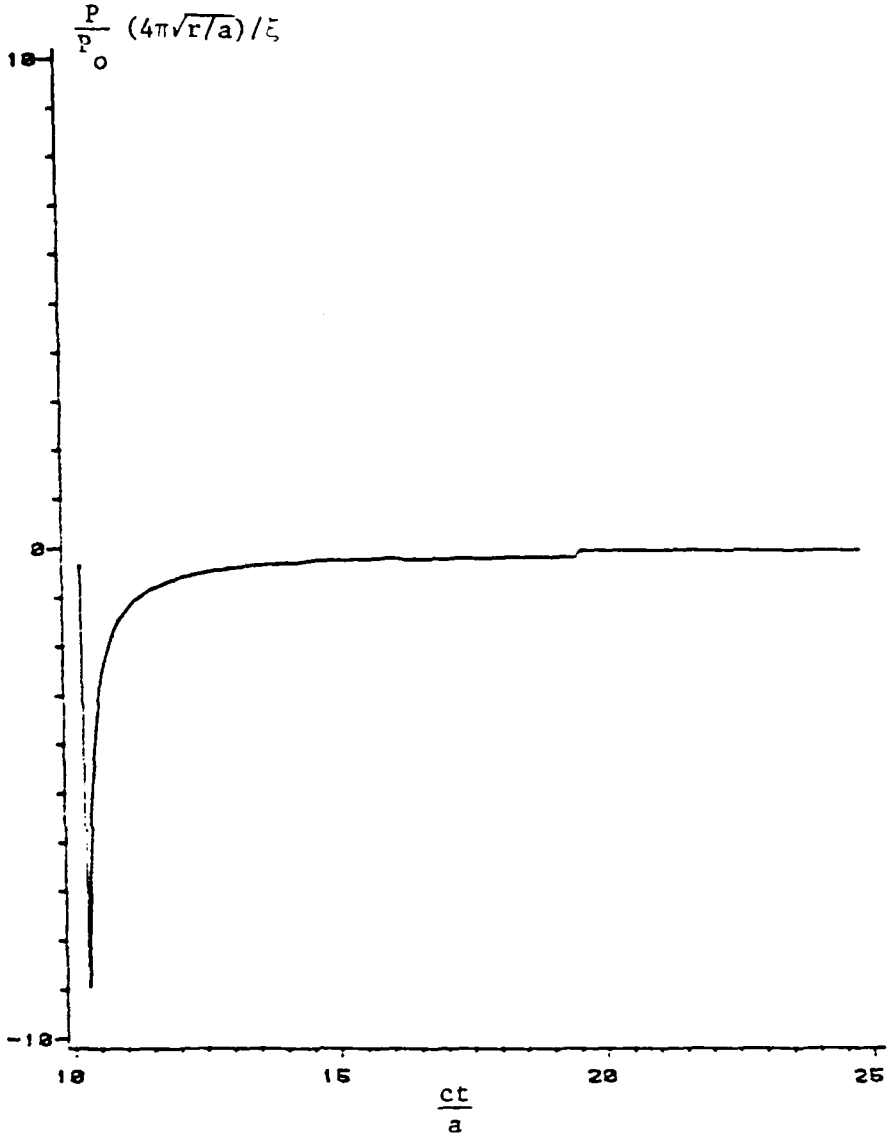

Figure 40. Pulse Response for the First Creeping Wave (s=0) at $\phi = 0°$.

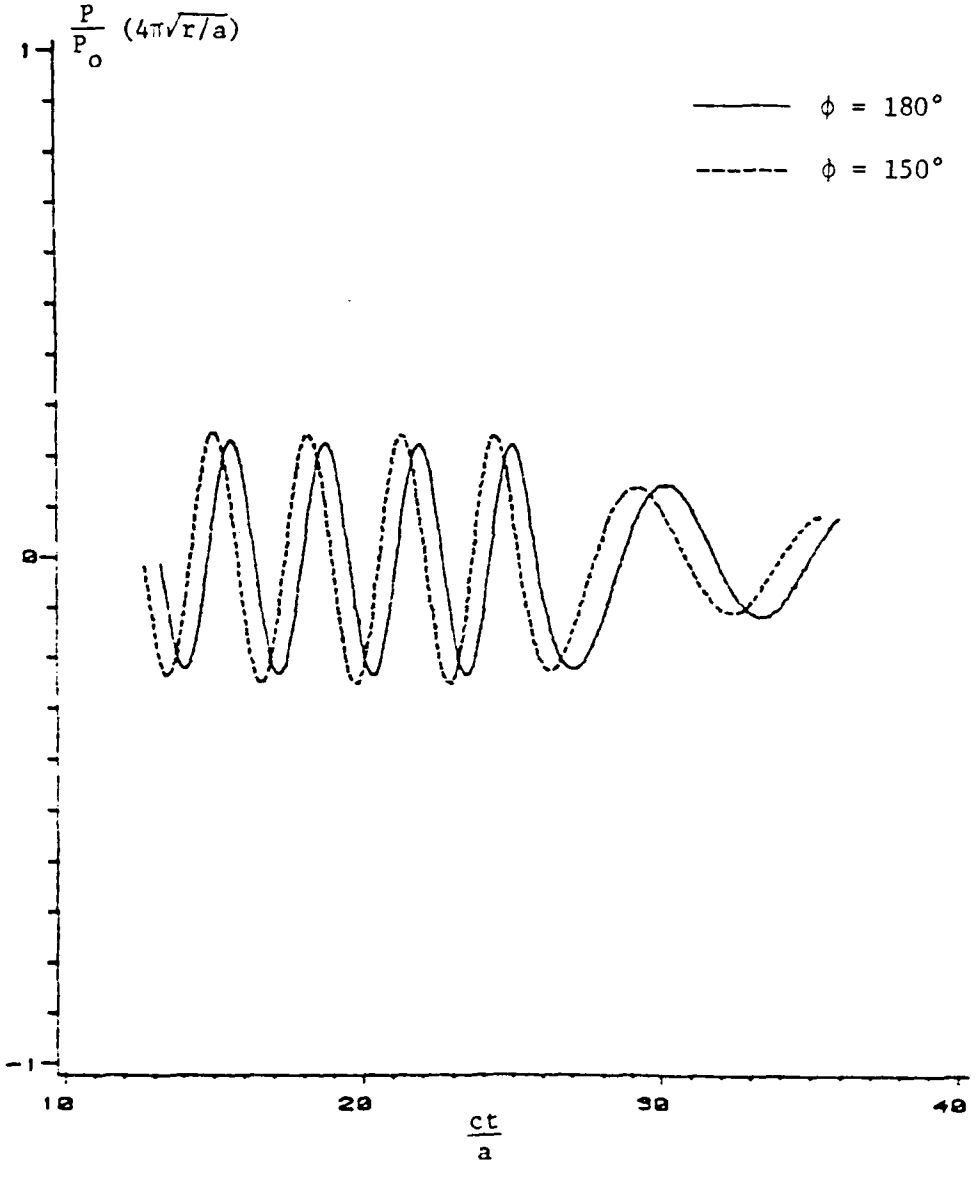

Figure 41. Creeping Waves for a Time Harmonic Pulse Train with $\bar{\tau}$ = .5, s = 0 and $\bar{\omega}$ = 1.0.

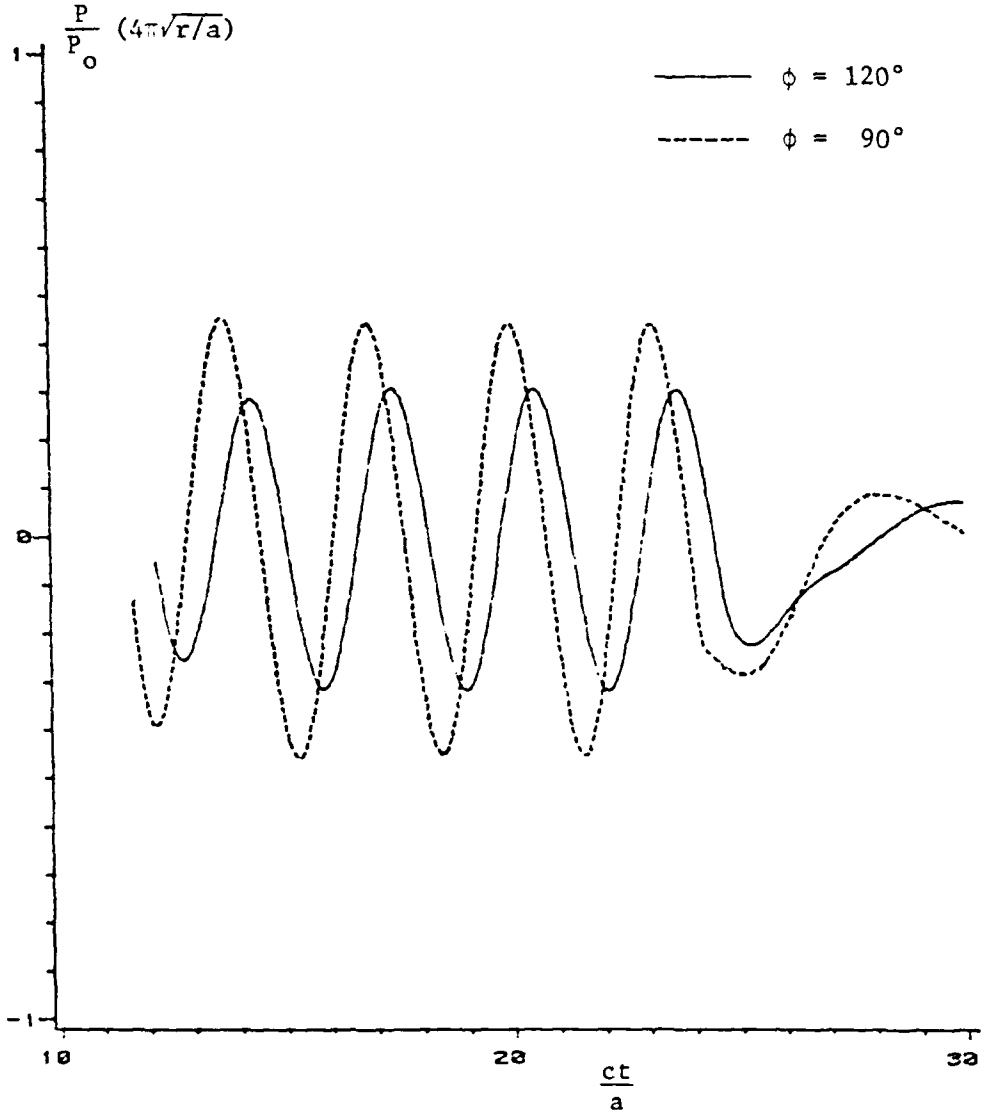

Figure 42. Creeping Waves for a Time Harmonic Pulse Train with $\bar{A}$ = .5, s = 0 and $\bar{\tau}$ = 1.0.

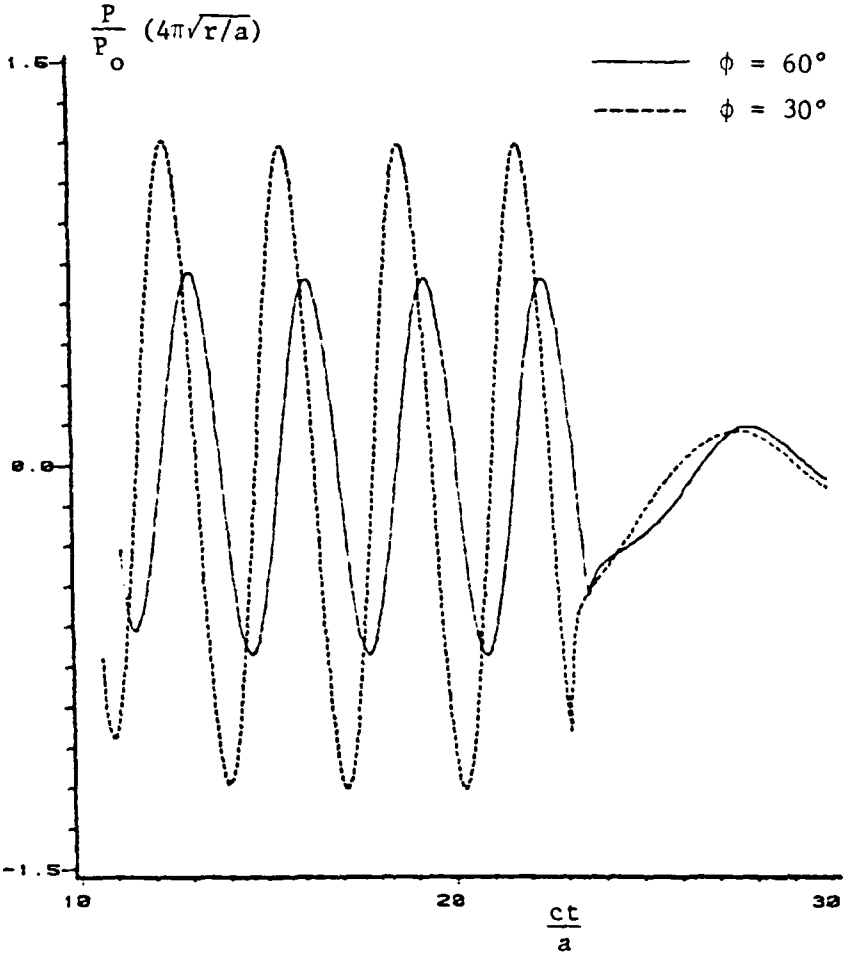

Figure 43. Creeping Waves for a Time Harmonic Pulse Train with $\bar{\lambda}$ = .5, s = 0 and $\bar{\omega}$ = 1.0.

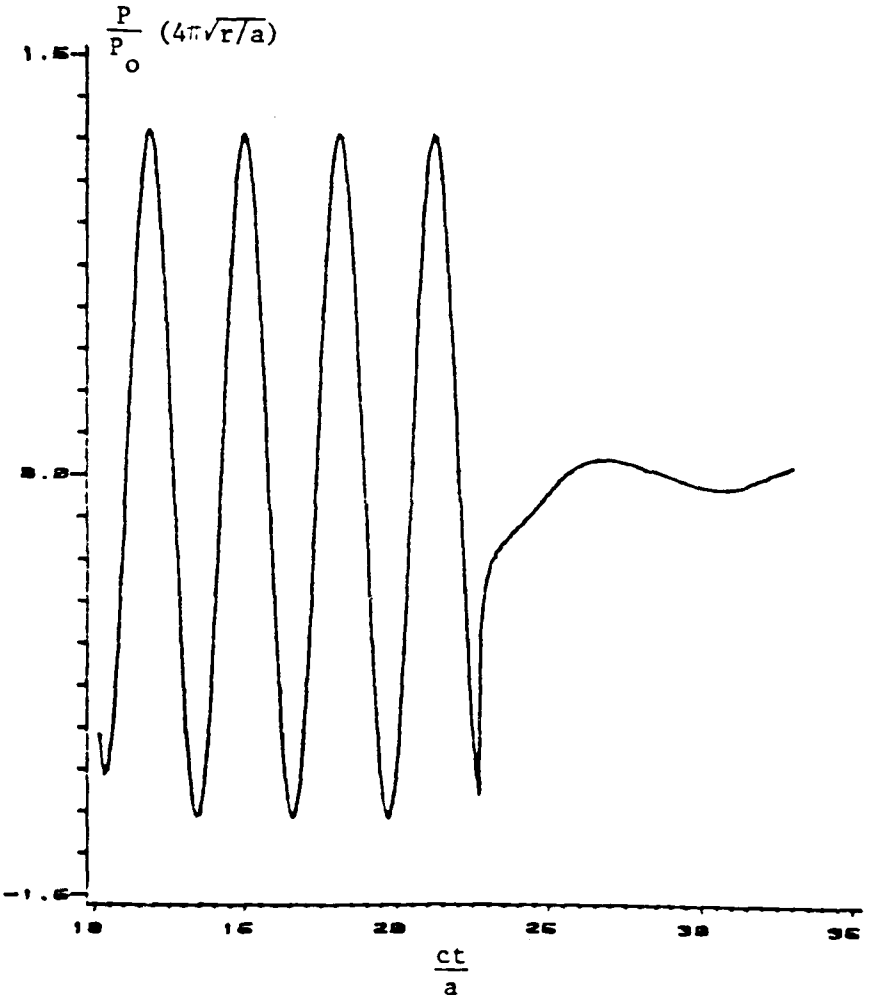

Figure 44. Creeping Waves for a Time Harmonic Pulse Train with $\bar{\tau}$ = .5, s = 0, $\bar{\tau}$ = 1.0 and ϕ = 0°.

the observation angle changes from 180° to 0°, i.e., most of the creeping wave field is concentrated in the shadow zone of the cylinder. Figures 45 and 46 correspond to the second arrival of these waves at 180° and 0°, respectively. The first arrival for the FM pulse train is shown in Figures 47 and 48. The peak amplitude of the creeping waves time signature is plotted in polar coordinates in Figures 49 and 50. Since these figures are plotted for r/a = 10 but for different values of the nondimensional radius of $\bar{\lambda}$, the amplitude distribution as presented in Figure 50 should be multiplied by the factor

$$\sqrt{10/(9\bar{\lambda}_2/\bar{\lambda}_1 + 1)} = 0.51$$

to facilitate comparison in Figures 49 and 50.

4.5 Conclusions

The prediction of the impulse response of an impedance covered cylinder was the main objective of this study. The scattered pressure was obtained for an incident plane wave pulse, a time harmonic pulse train and FM pulses. The computations were carried out for an observer in the far field and at different observation angles. The nondimensional frequency and radius $\bar{\omega}$ and $\bar{\lambda}$ were varied in order to assess the influence of the frequency of the incident wave and the radius of the cylinder on the scattered pressure. The following conclusions can be drawn from the study of the analytic solutions and their numerical evaluation:

a. The directivity of the peaks of the geometrically reflected pressure time signature shifts towards the shadow zone as $\bar{\lambda}$ is increased (or as the radius is decreased) with new diffraction peaks appearing and moving towards the shadow zone.

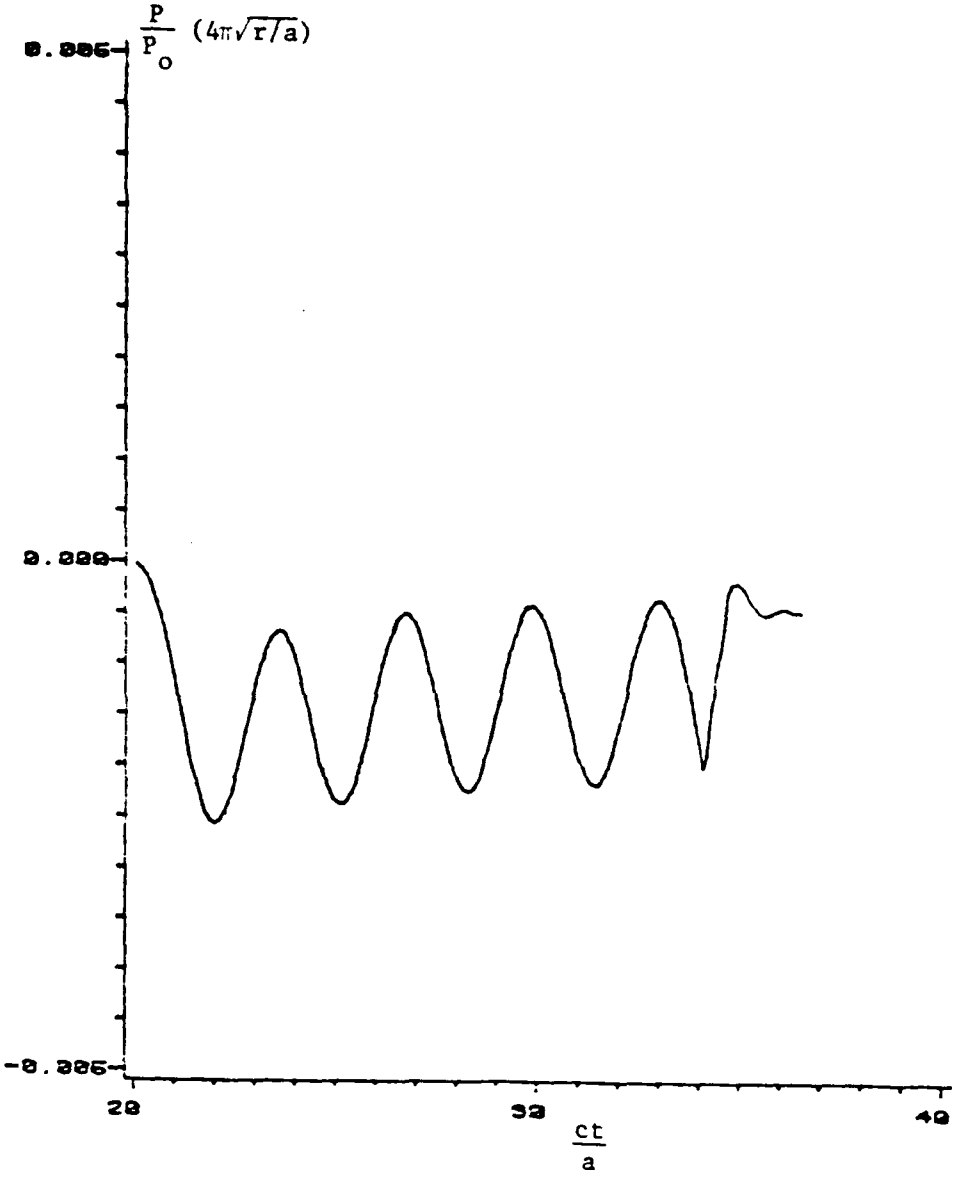

Figure 45. Second Arrival of Creeping Wave for a Time Harmonic Pulse Train with $\bar{\tau}$ = .5, $\bar{\omega}$ = 1.0 and ϕ = 180°.

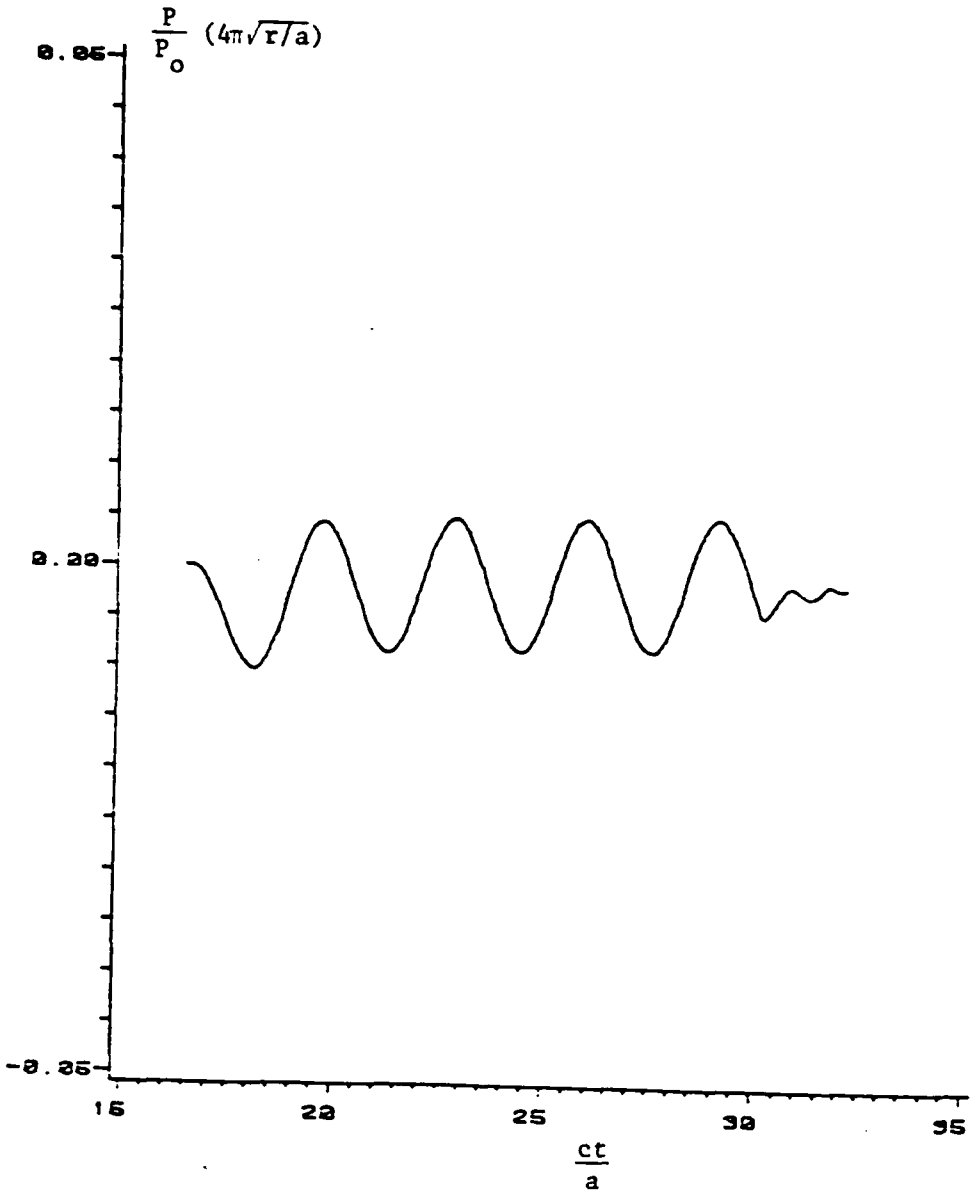

Figure 46. Second Arrival of Creeping Waves for a Time Harmonic Pulse Train with $\bar{\lambda} = .5$, $\bar{\omega} = 1.0$ and $\phi = 0°$.

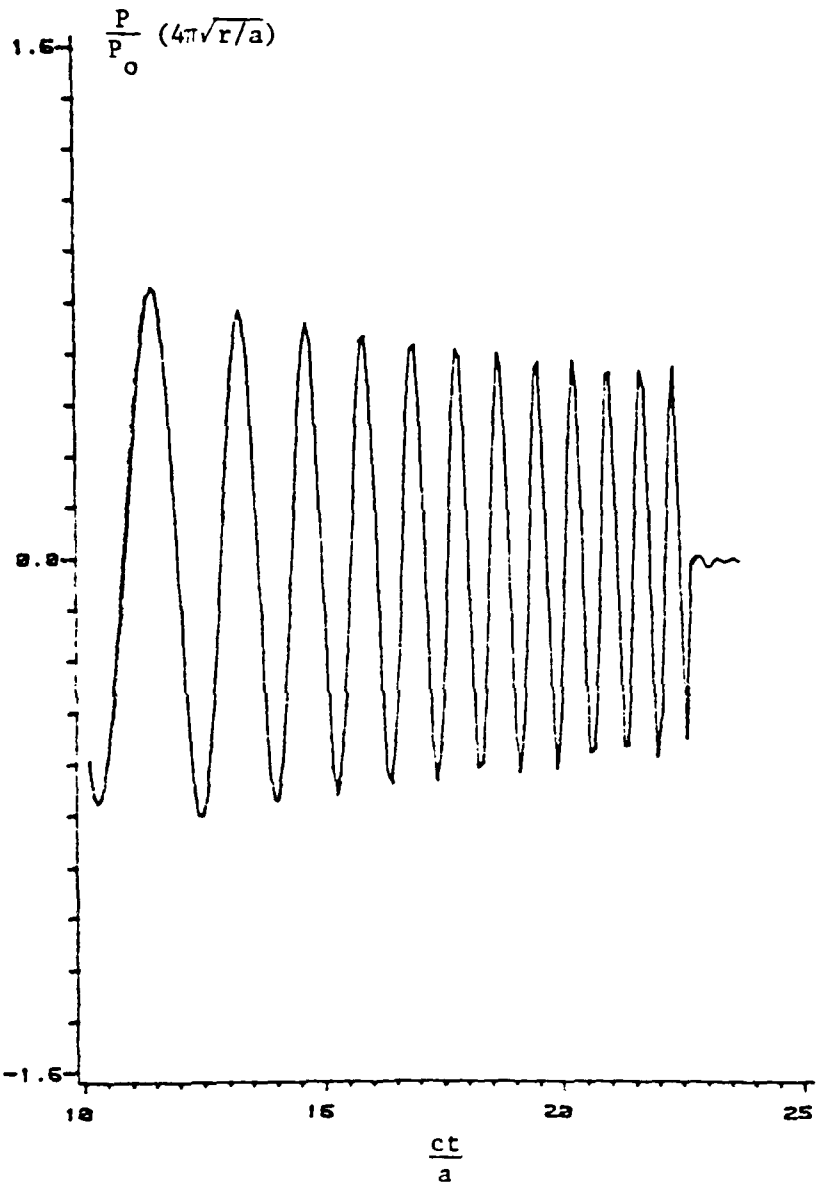

Figure 47. Creeping Waves for an Incident FM Plane Pulse with s = 0, $\bar{\omega}$ = 1, $\bar{\beta}$ = 2 and ϕ = 0°.

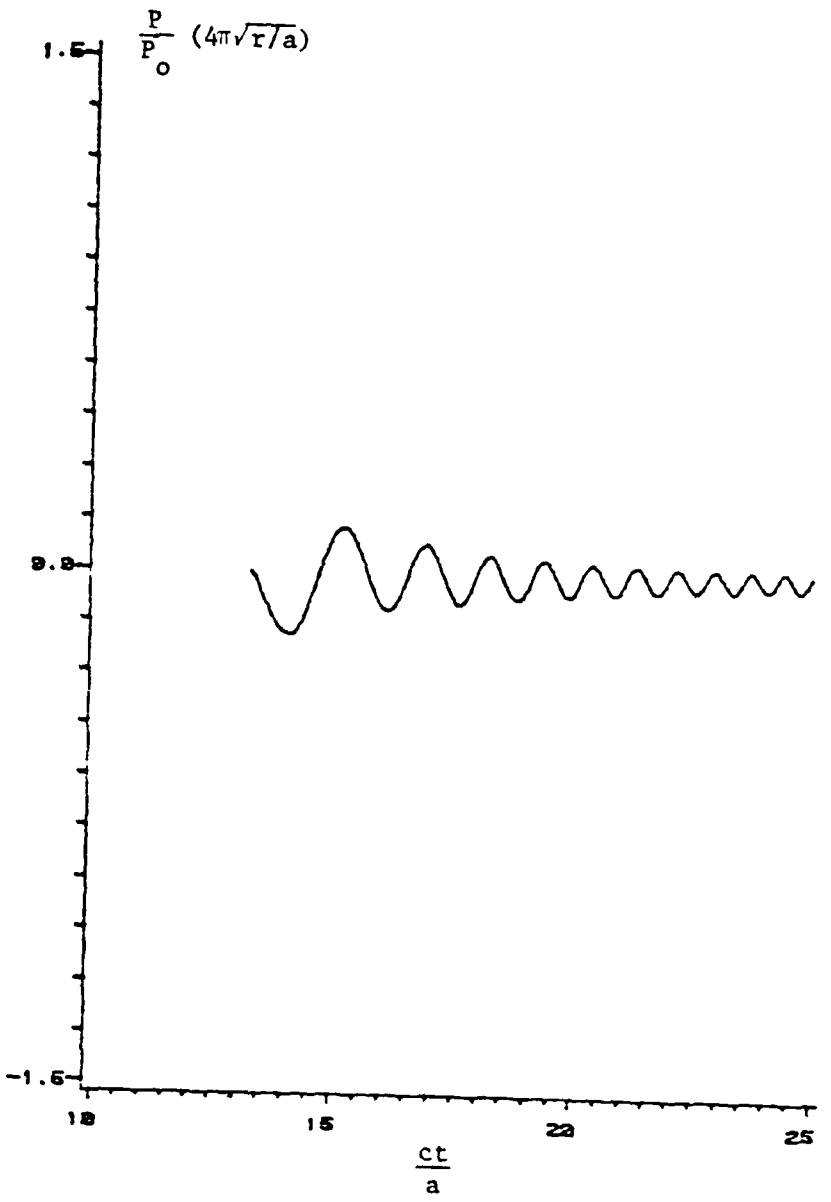

Figure 48. Creeping Waves for an Incident FM Plane Pulse with s = 0, $\bar{\omega}$ = 1, β = 2 and ϕ = 180°.

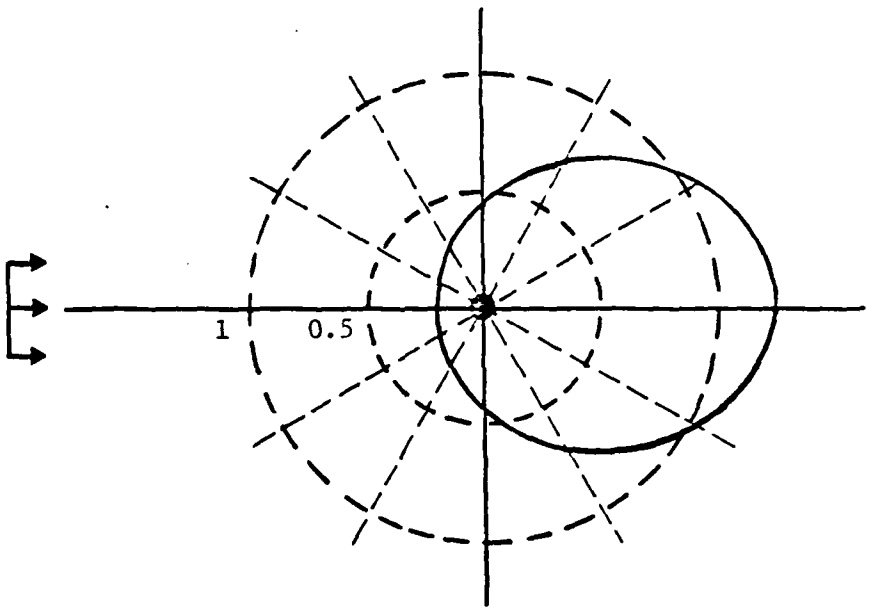

Figure 49. Polar Plot of the Peak Amplitude $\frac{P}{P_o}$ $(4\pi\sqrt{r/a})$ of the Creeping Waves Time Signature for a Time Harmonic Pulse Train with $\overline{\tau}$ = .5 and $\overline{\omega}$ = 1.0.

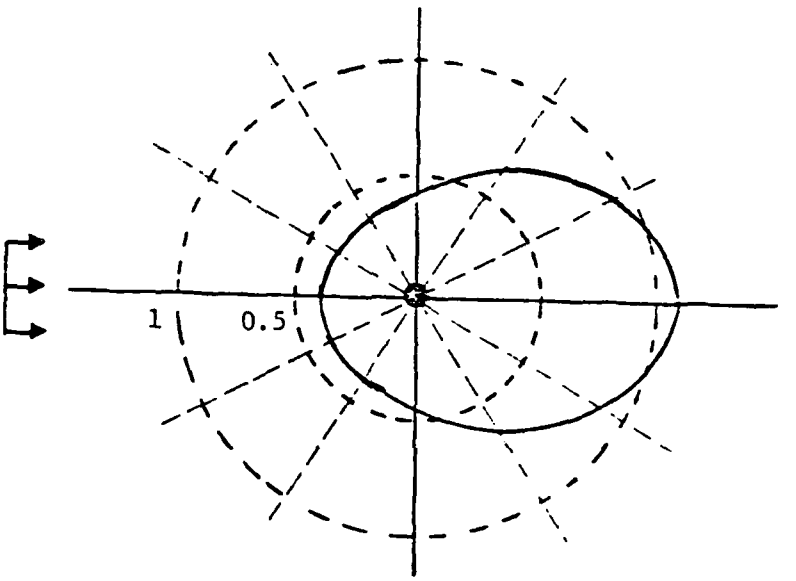

Figure 50. Polar Plot of the Peak Amplitude $\frac{P}{P_o}(4\pi\sqrt{r/a})$ of the Creeping Waves for a Time Harmonic Pulse Train with $\bar{\lambda} = 2.0$ and $\bar{\upsilon} = 1.0$.

b. In contrast to the infinite flat plane boundary, changes in the nondimensional frequency $\bar{\omega}$ do not affect the backscattered field significantly but it changes the directivity of the peaks of the scattered field.

c. The directivity of each peak of the creeping waves is close to being unidirectional.

In the numerical evaluations, the choice of only s = 0 and ℓ = 4 would incorporate the major contribution arising from the infinite series summation.

d. The forward scattering of the circumferential creeping waves could be increased by decreasing the nondimensional radius $\bar{\lambda}$ or increasing a. This agrees with the preceding studies for the scattering from a rigid cylinder.

4.6 Suggested Future Research

The analytical solution of the problem was based on the separation of variables and the Sommerfield-Watson transformation. This technique could be applied to other simple geometries such as spheres and spheroids. The Watson transformation allows decoupling of the geometrically reflected field from the creeping waves which is essential in the understanding of the multiple echoes that return in the case of scattering of a simple plane wave pulse. Other techniques such as the T-Matrix method or finite element method could be applied to solve for the total scattered field. The impedance model, further, can be extended to multi-degree of freedom oscillators, thus creating new resonance frequencies for the impedance boundary.

REFERENCES

1. Bertram R. Levy and Joseph B. Keller, "Diffraction by a Smooth Object," Communications on pure and applied mathematics, Vol. 12, 159-209 (1959).

2. J.B. Keller and Albert Blank, "Diffraction and Reflection of Pulses by Wedges and Corners," Communications on pure and applied mathematics, Vol. 4, No. 1, 75-94 (1951).

3. M. Friedman and R. Shaw, "Diffraction of pulses by cylindrical obstacles of arbitrary cross-section," J. Appl. Mech. 29, 40-47 (1962).

4. R. Hickling, "Analysis of Echoes from a Hallow Metallic Sphere in Water," J. Acoust. Soc. Am. 36, 1124-1137 (1964).

5. R. Hickling, R.W. Means, "Scattering of Frequency Modulated Pulses by Spherical Elastic Shells in Water," J. Acoust. Soc. Am. 44, 1246-1252 (1968).

6. R.P. Shaw, "Diffraction of Acoustic Pulses by Obstacles of Arbitrary Shape with a Robin Boundary Condition," J. Acoust. Soc. Am. 41, 855-859 (1967).

7. H. Überall, R.D. Doolittle and J.V. McNicholas, "Use of Sound Pulses for a Study of Circumferential Waves," J. Acoust. Soc. Am. 39, 564-578 (1966).

8. W. Franz and K. Deppermann, "Theorie der Beugung am Zylinder unter Berücksichtigung der Kriechwelle," Ann. Phys. 10, 361-373 (1952).

9. F.G. Friedlander, Sound Pulses, Cambridge Univ. Press, London, 1958).

10. R.D. Doolittle, H. Überall and P. Ügincius, "Sound Scattering by Elastic Cylinders," J. Acoust. Soc. Am. 43, 1-14 (1968).

11. O.D. Grace and R.R. Goodman, "Sound Scattering by Cylinders of Finite Conductivity," J. Acoust. Soc. Am. 39, 173-174 (1966).

12. W. Franz and P. Beckmann, "Antennas Propagation," IRE Trans., Ap-4, 203-208 (1956).

13. P. Ügincius, H. Überall, "Creeping-wave Analysis of Acoustic Scattering by Elastic Cylindrical Shells," J. Acoust. Soc. Am. 43, 1025-1035 (1968).

14. L.M. Brekhowvskikh, Waves in Layered Media, Academic Press, NY (1960).

15. J.J. Bowman, T.B.A. Senior, P.L.E. Uslenghi, Electromagnetic and Acoustic Scattering by Simple Shapes, John Wiley & Sons, Inc., New York, 1969.

16. K.F. Graff, Wave motion in elastic solids, Ohio State University Press, 1975.

17. P.M. Morse and K. UnoIngard, Theoretical Acoustics, McGraw-Hill Book Co., New York (1968).

18. M. Abramowitz and I.A. Stegun, Handbook of Mathematical Functions, Dover Publications, Inc., New York (1972).

19. H. Bremmer, Terrestrial Radio Waves, Elsevier Publication Co., New York (1949).

20. E. Skudrzyk, Simple and Complex Vibratory Systems, The Pennsylvania University Press, University Park (1968).

21. I.S. Gradshteyn and I.M. Ryzhik, Table of Integrals, Series and Products, Academic Press, New York (1965).

DISTRIBUTION LIST FOR TM 83-100

Commander (NSEA 0342)
Naval Sea Systems Command
Department of the Navy
Washington, DC 20362 — Copies 1 and 2

Commander (NSEA 9961)
Naval Sea Systems Command
Department of the Navy
Washington, DC 20362 — Copies 3 and 4

Defense Technical Information Center
5010 Duke Street
Cameron Station
Alexandria, VA 22314 — Copies 5 through 10

END

FILMED

9-83

DTIC